

The logo consists of the word "FLEXe" in a bold, sans-serif font, with a small superscripted "e". It is contained within a white rectangular box with a thin orange border. This box is positioned above a larger, irregular orange shape that resembles a speech bubble or a cloud, which contains the text "Future Energy System".

FLEX^e

Future Energy
System

RESEARCH REPORT

Tuomas Rauhala, Seppo Vehviläinen, Mikko
Lehtonen, Pekka Koponen, Pertti Pakonen, Lasse
Peltonen, Mika Lötjönen, Antti Rautiainen, Sami
Repo, Pertti Järventausta

Distributed resources as fast frequency reserve



Solution Architect for Global
Bioeconomy & Cleantech Opportunities



CLIC INNOVATION OY
ETELÄRANTA 10
P.O. BOX 10
FI-00131 HELSINKI,
FINLAND
CLICINNOVATION.FI



CLIC Innovation Research report

Tuomas Rauhala, Seppo Vehviläinen, Mikko Lehtonen, Pekka Koponen, Pertti Pakonen, Lasse Peltonen, Mika Lötjönen, Antti Rautiainen, Sami Repo, Pertti Järventausta

Distributed resources as fast frequency reserve





Name of the report: Distributed resources as fast frequency reserve

Key words: distributed fast reserves, frequency measurement, load disconnection, frequency restoration,

Summary

In this report, feasibility of small distributed demand response resources as fast frequency reserves was assessed. The research focused especially on smart meter based implementation issues. The present smart meters in Finland do not enable fast frequency reserve implementation, but one has to consider the following generation of meters. A compact power system simulation model based on the structure and data provided by Finnish transmission system operator (TSO) Fingrid Oyj was developed in the project for PSCAD and RTDS (real time digital simulator) transient simulation software, and was applied to analysis of frequency measurement techniques and effect of different disconnection switching patterns of distributed fast reserves on power system performance. Various frequency measurement techniques presented in literature were studied and compared by simulations and with real measurement devices in real time digital simulator (RTDS) laboratory environment. Robust frequency measurement method was developed in the project and implemented in a prototype smart meter by MX Electrix Oy. The measurement performance of the smart meter was verified in the RTDS environment and compared with PMU and the simulated measurement techniques. The impact of different fault types and locations in the power system were varied (e.g. remaining voltage, fault inception angle) on frequency measurement located at the customer connection point in the distribution network was studied in the above comparison of frequency measurement techniques. Large scale use of small distributed resources as fast frequency reserves was assessed in system performance studies by varying amount of reserve loads and their response time (i.e. fast and very fast) with different rotational kinetic reserves of power generation participating in frequency control. The system performance studies showed that the distributed resources could work well as fast disturbance reserves.





CONTENTS

1 INTRODUCTION.....	1-8
2 OVERVIEW ABOUT DISTRIBUTED RESOURCES AS FAST FREQUENCY RESERVE	2-11
2.1 PRINCIPLES	2-11
2.2 POSSIBILITIES	2-13
2.3 POTENTIAL	2-13
2.4 RISKS.....	2-14
3 FUNCTIONAL REQUIREMENTS FOR SMART METERS IN PROVISION OF FAST FREQUENCY RESERVE SERVICES	3-14
3.1 LITERATURE ON FREQUENCY MEASUREMENT METHODS AND THEIR REQUIREMENTS	3-14
3.2 KNOWN SHORTCOMINGS OF CERTAIN POPULAR FREQUENCY MEASUREMENT METHODS.....	3-15
3.3 MEASUREMENT NEEDS IN THE NORDIC SYNCHRONOUS AREA	3-16
3.3.1 <i>Load-frequency control</i>	3-16
3.3.2 <i>Frequency quality monitoring</i>	3-16
3.4 DEFINITION OF REQUIREMENTS	3-17
3.4.1 <i>Reliability</i>	3-17
3.4.2 <i>Frequency range 45 – 65 Hz</i>	3-17
3.4.3 <i>Accuracy</i>	3-17
3.4.4 <i>Immunity to disturbances</i>	3-18
3.4.5 <i>Response speed</i>	3-19
3.4.6 <i>Rate of change of frequency</i>	3-20
3.5 DEVELOPMENT OF SMART KWH-METERS TO MEET THE FUNCTIONAL REQUIREMENTS	3-21
3.5.1 <i>Adaptive observer of the rotating voltage phasors</i>	3-21
3.5.2 <i>Development of the method to improve immunity to disturbances</i>	3-22
3.5.3 <i>Development of the method to improve accuracy</i>	3-22
3.5.4 <i>Tuning the frequency measurement method by simulations</i> ..	3-22
3.5.5 <i>Implementation in the new smart power quality monitoring kWh-meter</i>	3-24
3.6 TESTING OF SMART KWH-METER WITH RESPECT TO THE FUNCTIONAL REQUIREMENTS	3-24
3.6.1 <i>Test setup</i>	3-24
3.6.2 <i>Accuracy</i>	3-25
3.6.3 <i>Noise of the measurement circuits</i>	3-25
3.6.4 <i>Immunity to disturbances</i>	3-25
3.6.5 <i>Response speed</i>	3-31
4 APPLICATION OF SMART KWH-METER CONNECTED LOADS AS FAST FREQUENCY RESERVES: ROBUSTNESS AND QUALITY REQUIREMENTS FOR FREQUENCY ESTIMATION ALGORITHMS.....	4-34
4.1 TYPICAL SYSTEM EVENTS AFFECTING THE QUALITY OF ESTIMATE.....	4-34





4.2	ESTIMATION OF ERROR BETWEEN ESTIMATE AND ACTUAL SYSTEM FREQUENCY	4-35
4.3	QUALITY ASSESSMENT BASED ON SYSTEM STUDY RESULTS	4-35
4.4	DIFFERENT FREQUENCY ESTIMATION TECHNIQUES	4-35
4.4.1	<i>Zero crossing</i>	4-35
4.4.2	<i>DFT based</i>	4-36
4.4.3	<i>PLL based</i>	4-36
4.4.4	<i>Commercial product PMU</i>	4-37
4.4.5	<i>Commercial product ELV</i>	4-37
4.5	POWER SYSTEM MODEL FOR ANALYSIS OF FAST FREQUENCY RESERVES	4-37
4.6	MODELLING SMART METER CONNECTED LOADS	4-38
4.7	STUDY CASES	4-39
4.8	STUDY RESULTS	4-39
4.8.1	<i>Three-phase-to ground faults</i>	4-39
4.8.2	<i>Characteristic parameters</i>	4-44
4.8.3	<i>Performance enhancement by adding delay before releasing load switching</i>	4-48
4.9	RESULTS OF ANALYSIS OF FREQUENCY ESTIMATION TECHNIQUES	4-51

5 STRUCTURE OF THE STUDY AND SIMULATION MODELS FOR ANALYSIS OF IMPACT ON TECHNICAL PERFORMANCE OF TRANSMISSION NETWORK.....5-53

5.1	INTRODUCTION.....	5-53
5.2	SYSTEM STUDY NEED AND POSSIBLE APPROACHES	5-53
5.3	AMR METER CONNECTED LOADS AS FAST FREQUENCY RESERVES	5-53
5.3.1	<i>Concept for using AMR meter connected load as fast frequency reserves</i>	5-54
5.3.2	<i>Risks related to the concept</i>	5-54
5.4	POWER SYSTEM MODEL FOR ANALYSIS OF FAST FREQUENCY RESERVES	5-54
5.5	MODELLING SMART KWH-METER CONNECTED LOADS	5-56
5.6	PARAMETERIZATION OF THE LOAD	5-57
5.7	RESULTS OF PRODUCTION LOSS WITH THE DIFFERENT DISCONNECTION SWITCHING SCHEMES	5-61
5.8	SIMULATION PRINCIPLE OF PRODUCTION LOSS WITH DIFFERENT AMOUNT OF DISTRIBUTED FAST RESERVES AND ROTATIONAL RESERVES	5-62
5.8.1	<i>110 GWs, fast reserve control based on PLL srf method – production loss 1300 MW</i>	5-63
5.8.2	<i>110 GWs, fast reserve control based on PLL srf method – production loss 300 MW</i>	5-64
5.9	RESULTS OF PRODUCTION LOSS WITH DIFFERENT AMOUNT OF DISTRIBUTED FAST RESERVES AND ROTATIONAL RESERVES	5-64
5.9.1	<i>Reference case – 110 GWs, 1300 MW, no fast reserves</i>	5-64
5.9.2	<i>110 GWs, 1300 MW, 150 MW / 50 MW</i>	5-66
5.9.3	<i>110 GWs, 1300 MW, 50 MW / 150 MW</i>	5-68
5.9.4	<i>110 GWs, 750 MW, 450 MW / 150 MW</i>	5-70
5.9.5	<i>110 GWs, 750 MW, 150 MW / 450 MW</i>	5-72





5.9.6	110 GWs, 450 MW, 750 MW / 250 MW.....	5-75
5.9.7	110 GWs, 450 MW, 250 MW / 750 MW.....	5-77
5.9.8	Reference case - 110 GWs, 300 MW, no fast reserves	5-80
5.9.9	110 GWs, 300 MW, 450 MW / 150 MW.....	5-82
5.9.10	110 GWs, 300 MW, 150 MW / 450 MW.....	5-83
5.9.11	110 GWs, 300 MW, 750 MW / 250 MW.....	5-85
5.9.12	110 GWs, 300 MW, 250 MW / 750 MW.....	5-88
5.9.13	Summarizing graphs of 300 MW production loss.....	5-90
5.10	RESULTS OF ANALYSIS OF IMPACT ON TECHNICAL PERFORMANCE OF TRANSMISSION NETWORK).....	5-91
6	CONCLUSIONS AND CONTRIBUTIONS.....	92
7	REFERENCES.....	93





1 Introduction

In an electric power system, the balance between power consumption and production has to be continuously maintained. Alternating current (AC) synchronous power systems have an inherent interconnection between the frequency of the network voltage and the balance between power production and consumption. When production is less than the consumption, the frequency decreases, and when production is higher than the consumption, the frequency increases. This behavior stems from the inertia of rotating machines and the inertia emulation by some power electronic interfaces. Therefore, the grid frequency is used as a control quantity when maintaining the balance between production and consumption. Power system's frequency control keeps the grid frequency near to its nominal value.

In the future it is probable that maintaining the power balance and thus keeping the frequency within reasonable limits becomes more challenging. Throughout Europe, intermittent power production such as wind and solar power is expected to further increase significantly. These types of production plants supply power in accordance with wind and solar conditions and typically are not adjusted from power system's frequency management point-of-view. Due to the fact that increasing amount of new production will be connected via power electronic converter to the grid, the inertia in the power system is decreasing, and the variations and oscillations in the frequency are increasing [NAG 2015]. Therefore, new and appropriate frequency control resources would be highly welcomed by the TSOs (Transmission System Operators).

The grid frequency is kept within allowable limits using frequency reserves. Frequency reserves can be divided into two different types by the way of control: automatically and manually activated. Frequency reserves can be divided into two types also by their purpose: frequency containment reserves (FCR) and frequency restoration reserves (FRR). In the Nordic/North-European synchronous area there are three types of automatic frequency reserves: frequency containment reserves for normal operation (FCR-N), frequency containment reserves for disturbances (FCR-D) and automatic frequency restoration reserve (FRR-A). Manual frequency restoration reserve (FRR-M) is the manual reserve type owned by the TSO, but resources from balancing power market (BPM) are used very often as a manual frequency control. All resource owners can bid their capacity in the annual or hourly reserve markets. FCR-N and FCR-D operate based directly on local frequency measurements. FRR-A, FCR-M and BMP are controlled centrally by communication and/or by requesting a control action from the resource owner.

The required operating times of power plants operating as FCR-N and FCR-D are 3 minutes and 5–30 seconds, respectively [Fingrid 2016]. Relay controlled loads are expected to react "immediately" [Fingrid 2016] when certain criteria are fulfilled. In addition to the reserve types mentioned above, new types of reserves could be introduced to the system. This report concentrates mostly to very fast reserves with operating times of 1–5 s. This kind of reserve is called





“fast frequency reserve” in this report. Traditionally, only large industrial loads or HVDC (high voltage direct current) systems have been available for such conceptual reserve use, and the concept has been typically implemented as load shedding schemes to be activated only under exceptional emergency conditions. Different sources of frequency reserves available at the moment or identified as potential sources of frequency reserves in near future are identified in Table 1. The table describes different characteristics of conventional power plants, intermittent power production, industrial and distributed loads, HVDC links and novel resource types such as batteries and microgrids.

Today the frequency reserves are mostly realized by large production units and loads, but especially over the past few years, also the use of smaller distributed resources in frequency control has been under interest of TSOs, industry and academics. See [Donnelly 2012], [Beil 2016] and [SmartNet 2016], for example. The use of distributed resources is very different paradigm from the traditional one where only large units are used, and requires open-minded thinking and new business models. The scope of the work of this report is on analysis of the use of small distributed resources, also flexible loads, in fast frequency reserve.

The targets of the work of this report are the following.

- 1) To present and assess general feasibility of different possibilities for implementation and management of fast frequency reserve using controllable loads.
- 2) Develop and test smart kWh-meter features required to obtain robust frequency measurement technique for application of smart kWh-meter connected loads as fast frequency reserve.
- 3) Analyze the impact of different concepts to implement DR based fast frequency reserve on transmission network performance.
- 4) Present and discuss the use of information available from smart kWh-metering for monitoring, validation and verification of reserve capacity.



Table 1. Estimate of the status in Finland concerning characteristics of different types of possible fast frequency reserve resources from Finnish power system point-of-view.

	Sync. generation - hydro	Synch. generation - rest	Loads - industrial	Loads - distributed	Wind	PV	HVDC	Batteries	Combinations (microgrids)
Response speed (reserve perspective)	fast	slow	very fast / fast	very fast / fast	very fast (with twist)	very fast	very fast	very fast	very fast/fast
Capable for up regulation	yes	yes	yes	yes	yes	basically	yes	yes	yes
Capable for down regulation	yes	yes	not really	possibly	yes	yes	yes	yes	yes
Maturity as frequency reserve (technology)	Established	Established	Established	RnD	Established	Concept known	Established	Concept known	Concept known
Maturity as frequency reserve (availability of market)	Established	Established	Established	Established	Established	Established	Established	Established	Established
Maturity as frequency reserve (dedicated technical requirements)	Established	Established	Established	RnD	RnD	RnD	Available (AFC)	Available (AFC)	RnD
Maturity as frequency reserve (business model)	Established	Established	Established	RnD	RnD	RnD	RnD	RnD	RnD
Factors affecting availability	Availability of required controls / schemes	Availability of required controls / schemes, availability of energy	Availability of required controls / schemes, availability of energy	Operational condition at the other end of system	Availability of required controls / schemes	Availability of required controls / schemes, availability of energy			
Inherent features affecting performance	Electro-mechanical dynamics	Electro-mechanical dynamics	Depends on load characteristics	Depends on load characteristics	Availability of energy	Availability of energy	Power system characteristics at the different ends of link	Not much, type of battery perhaps	Depend on characteristics of production, loads and storages



2 Overview about distributed resources as fast frequency reserve

In the following, basic principles, possibilities, potential and risks of the use of distributed resources as fast frequency reserve are described and analyzed.

2.1 Principles

The possibility to use distributed resources is affected by various factors that have been arising along with developments on various fields of electrical engineering. With the digital controls and reduced price of electronics fast processing the electrical measurement has become possible at the same time when electric components and electronic has becomes available in price range allowing their extensive use in domestic applications.

In context of fast frequency reserves these developments allow both rapid analysis of system frequency as well as implementation of algorithms, logic and interfaces required to regulated or control of the power consumed of produced by the distributed resource. The time frame for the whole process starting from identification of significant frequency deviation to the time to reach the requested change in the power output of the distributed resource may be even shorter than 500 milliseconds.

Such response times would allow not only the use of distributed resources as part of the traditional fast frequency reserve required to act within time frame starting from few seconds up to some tens of seconds, but rapid response would also allow their use in similar manner that has been introduced for wind power as "inertial reserve". This concept is illustrated in Figure 1.

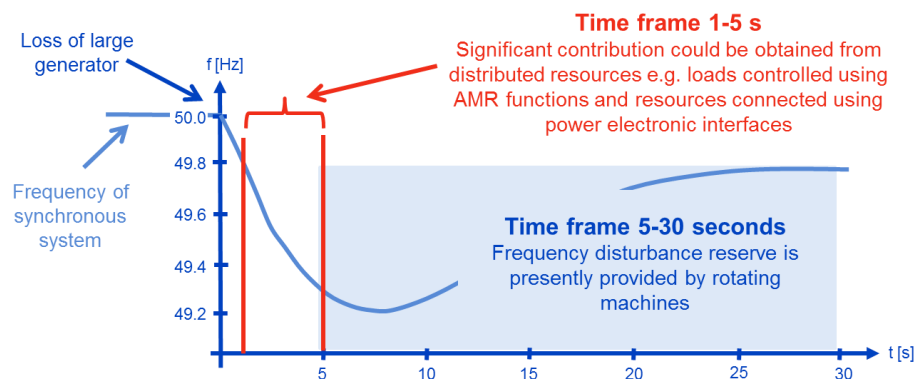


Figure 1. The time frames for fast frequency reserves that distributed resources could offer.

In principle there is large variety of concepts based on which the large scale use of distributed resources as fast frequency reserves can be implemented. It can be considered that these concepts can be described based on certain key



technical areas which can be implemented in few various manners. Depending on implementation of each of the technical area, the concept will have different drawbacks and benefits.

In the scope of this work, the different concepts to implement large scale use of fast frequency reserves using distributed resources consists the technical areas presented in Figure 2. Each of these areas can be considered to allow few different approaches to implement the technical feature. The relevant in the scope of this work are highlighted using blue in Figure 2 below:

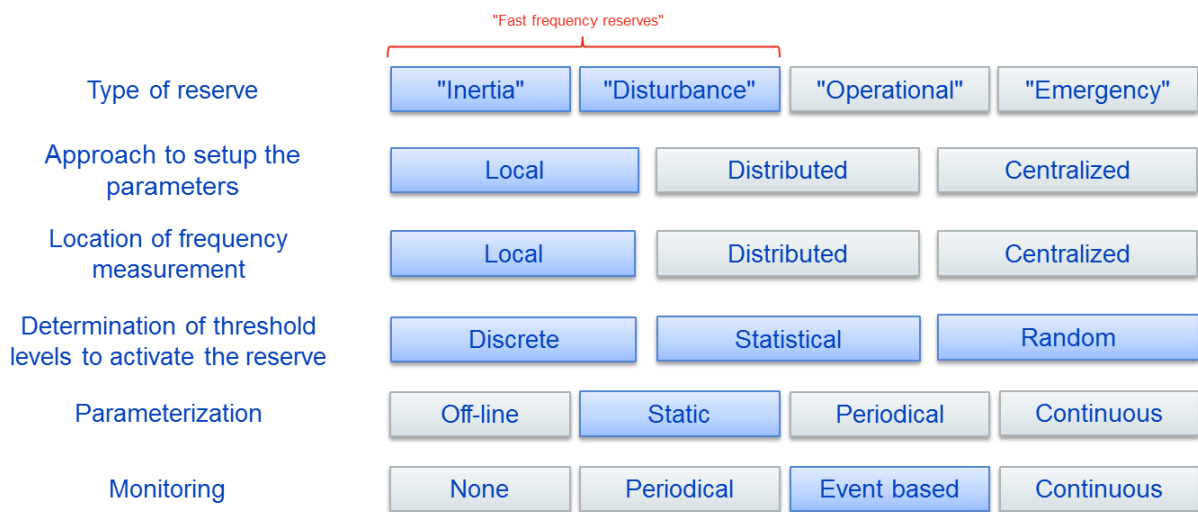


Figure 2. The technical areas of different concepts to implement large scale use of fast frequency reserves using distributed resources.

With reference to Figure 2, there are many ways to realize distributed resources as “fast frequency reserves”. One dimension is the amount of decentralization of measurement and control. The control is often local and could be based on local on-site frequency measurement. That enables simple low cost implementation of very fast and reliable responses and a robust system. Very reliable and fast data communication is still expensive and relatively vulnerable to attacks. High penetrations of distributed frequency control cannot be completely autonomous. There is still a need for communication between the distributed resources and the system operator for coordination and validation purposes. However, it does not need to be as fast and reliable as in the case of centralized measurements. The distribution of the location of the responses needs to be coordinated depending on grid constraints and location of the potential sources of the main disturbances and these may vary with time. It must also be possible to verify the delivery of the local response. Real time measurement of the responses is often required but model based estimation and forecasting of the aggregated responses is more useful and less costly than extremely reliable data communication for real time measurements. Where real time measurements are affordable they can complement the estimation.

As the inertia in power systems is decreasing, the relatively slow response speed of the existing power plant based frequency controlled reserves is causing somewhat inadequate control stability that causes oscillation at a





resonant frequency. To a certain extent this is solved by updating the control response requirements of the resources. A more complete solution is to establish a new market for faster frequency control than what the existing frequency controlled resources are capable of providing. Such a market for very fast frequency control is called inertia market. Distributed frequency controlled resources can provide such very fast frequency control at low cost, if the market participation requirements are reasonable designed

2.2 Possibilities

With appropriate business models, distributed resources may become a cost effective reserve solution. This could be realized especially if the same assets could be applied also for other types of demand response applications when not allocated as fast frequency reserved, which could further enhance the operation of the power system. Due to the wide diversity in the nature, distributed resources offer a new type of resource with different and inherently even better characteristics than the large units thus extending the reserve portfolio. Possible improvements include a more flexible frequency response (the pattern of the response could be designed and adjusted) and geographical diversity bringing perhaps a smoother response which might be desirable in some networks.

2.3 Potential

If considering only the total capacity, the potential of small sized electric loads is quite significant reaching easily amount of > 1000 MW [Järventausta 2015]. However, as largest domestic loads in Finland are mostly heating related, the availability depends very much on the outdoor temperature. This means that during the summer there would be only a very little heating load available, and mostly it would be water heating. Thus the flexibility of cooling and ventilation loads needs to be used too, although in the Nordic countries there are not as much cooling load as, for example, in the countries in southern Europe. Also there are unknown but presumably non-negligible potential in medium size loads in agriculture, service, small scale industry sectors.

The potential of distributed resources as fast frequency reserves can be considered inherently significant only due to the fact that domestic and small industrial loads present significant share of the total power system load throughout the year. Although the share of different load types of the total system load varies seasonally, weekly, daily and hourly, the patterns of variation may be very different which enhances the availability of the resources but there are also some distributed resources with nearly constant availability. Additionally, the amount of distributed resources with potential capability to serve both as load and generation, such as EVs (electrical vehicles) and micro grids, are increasing constantly and they may have very different power balance patterns as compared with domestic loads.





2.4 Risks

While the wide variety of distributed resources can be considered a great opportunity, the main challenge of their application as fast frequency reserves can be considered to be related to the same issue. The management of reserve power fleet consisting even hundreds of thousands unit that may or may not be allocated as frequency reserve at certain moment presents a major technology, standardization and infrastructure challenge. Especially in case the distributed resources would and should consist of very different types of load, generators and storages, only modeling, forecasting and allocating of the resources may become a complex task. Aggregated behavior of a large number of autonomous small resources is well predictable, unless there is a common point fault mode. Complexity involves also risks e.g. in form of example modeling/forecast errors. Additionally, the development of the required standards and platforms would require very systematic approach.

The risks could be tackled by careful market and system design. Considering the acceptance of resources for reserves, there are two issues of very high priority: controllability and verifiability. TSOs want to know in advance that the resource (each of the resources individually or resources as a whole in an aggregated manner) would be controllable as contracted with the resource owner/operator. After and/or during a disturbance TSO has to ensure that the reserves were/are being controlled in the way as agreed. From the TSO point-of-view, it is not so important how these steps are taken care of, but the outcome of the procedures is essential. If a service provider (SP) (or aggregator) driven model is considered, the SP has to model and make resource forecasts, and allocate reasonable amount of resources for relevant points of time and location. The business model could be such that it would encourage the SP to minimize the risk of modeling, forecasting and allocation.

3 Functional requirements for smart meters in provision of fast frequency reserve services

3.1 Literature on frequency measurement methods and their requirements

Frequency measurement is a much needed and studied subject. Thus, many methods and variants have been reported in the literature. [Reza 2015] alone gives 28 literature references to different methods for measuring the fundamental frequency of power systems, such as DFT (Discrete Fourier transform), KF (Kalman filter), ZCD (Zero Crossing Detection), PLL (phase-locked loop), FLL (frequency-locked loop), FIR (Finite Impulse Response) filter and NTA (Newton type algorithm). Also the comparison by [Karimi-Ghartemani 2004] refers to many popular methods.

Already [Terzija 1994] and later [Rheza 2012] noticed that in order to have excellent and consistent performance over a sufficiently wide frequency range it is necessary that the frequency estimator is adaptive. In [Terzija 1994] the





adaptive method is Newton-type. [Rheza 2012] used a PLL with a Kalman-filter. [Rheza 2015] developed another Newton-type adaptive method and compared it with the method of [Terzija 1994]. The newer method had smaller demand for calculation capacity and it was less sensitive to voltage dips, swells, DC-component and harmonics.

The literature on the methods mentioned above discusses also requirements, because without them comparisons of the methods would be rather vague. The requirements mentioned include tolerance to voltage dips and swells, DC-component, harmonics, and phase angle jumps and consistently fast and stable responses well over the whole frequency range than can be needed in the worst case.

For a non-power systems related but detailed explanation and comparison of some advanced zero crossing methods and DFT methods for frequency and phase angle estimation, see [Liao 2011]. There the zero crossing method is sequential to keep latencies and data computation load low. It also compares the results to a hybrid PLL method described in [Ni 2011], in which the PLL is not very advanced and suffers from inconsistent convergence behavior in the unlocked state. A good adaptation mechanism would likely have solved the problem with the PLL.

3.2 Known shortcomings of certain popular frequency measurement methods

In order to know which requirements to define, it is useful to consider what weaknesses and tests for the frequency measurement methods are known. The following shortcomings are mentioned by [Karimi-Ghartemani 2004]:

- Zero crossing methods are not capable of fast frequency estimation and their performance is sensitive to switching transients.
- DFT is highly sensitive to distortions.
- A DFT related phasor rotation based method requires long measurement time window for small frequency deviations.
- Kalman-filter is dependent on the model used for the signal and is sensitive to initial conditions and internal parameters of the model
- Demodulation methods and ANN methods are sensitive to noise.
- A three-phase phase-locked loop is a fast and robust frequency estimation method for balanced three phase systems, but it is prone to error due to unbalanced conditions. Also sensitivity to harmonics was reported.

They mention almost all of the following performance sensitivity tests reported in the literature:

- white noise
- harmonics
- DC component
- periodic notches
- dips and swells





- amplitude jumps
- phase angle jumps
- step variations in frequency
- ramp variations in frequency
- oscillatory variations in frequency
- variations in sampling frequency (that is based on the internal frequency reference of the meter).

The above overview considers what is possible. It is also useful to know the requirements for the distributed frequency control applications. Such requirements have been reported for the control response. For example, according to them faster than 250 ms - 500 ms control responses, from measurement to the change of controlled power of the flexible resource, are not really needed in large power systems. Measurement delays are only one component of such control response dynamics. Thus having faster measurements will also leave more time for the other parts of the control circuit. There is a need for studies on more detailed requirements of distributed frequency control.

3.3 Measurement needs in the Nordic Synchronous Area

Load-frequency control and frequency quality monitoring are the most obvious and important needs to measure and estimate the fundamental frequency locally.

3.3.1 Load-frequency control

The minimal requirements for load-frequency control are defined in the document [ENTSO-E 2013]

It defines for each synchronous area the default values of the frequency quality target parameters (Article 19) and frequency quality evaluation criteria (Article 21). For these purposes, it requires that frequency measurement accuracy is 1 mHz or better. Article 32 mentions the total inertia and the synthetic inertia of the synchronous area as one of the criteria that the TSOs shall at least take into account when defining the process responsibility structure for frequency control. It is not explained how the inertia and the synthetic inertia shall be estimated and distinguished.

3.3.2 Frequency quality monitoring

The challenges regarding frequency quality and its measurements are discussed in the reports [Kuisti 2015] and [Zhou 2011].

The current Nordic target value of 10000 min/year outside normal operation corresponds to the standard deviation of 42 mHz. In the Nordic Synchronous area it is required that 50% of FCR-D is activated in 5 s and the rest in 30 s, and FCR-N in 2-3 min. In a forced outage of a large production unit in 2013 the time to the minimum instantaneous frequency was about 10 s and the recover was





oscillating. This indicates that there is a need for somewhat faster responding control resources than what now exist.

3.4 Definition of requirements

3.4.1 Reliability

Large number of distributed small resources together can form a very reliable frequency reserve resource, if there are no significant common mode failure modes. Local frequency measurement can be a source of common mode errors, if it is unreliable regarding extra or missing voltage zero points, for example. Thus the frequency measurement method shall be reliable with respect to voltage distortion etc. It is not enough that the measurement method is reliable. Common mode failure modes can also appear by vulnerability of the distributed FCR control system to cyber security attacks, software errors and hardware failures. FCR control is mainly autonomous and based on local measurements. It is very necessary but also relatively easy to design and analyze FCR for adequate reliability.

3.4.2 Frequency range 45 – 65 Hz

Normal frequency range in AC power systems is within 2.5 Hz from the fundamental frequency of the electricity network. The fundamental frequency can be 50 Hz or 60 Hz depending on the country. For meeting the range 47.5 Hz to 52.5 Hz together with the other requirements, it is necessary to use an adaptive frequency measurement method. For good adaptive methods, the frequency range can be very wide. Thus we can safely require that the frequency range shall be 45 – 65 Hz without causing any additional difficulties to the implementation.

3.4.3 Accuracy

Accuracy of individual meters is normally not critical in distributed control applications. When on-off type control is applied modest accuracy can even be beneficial. Sometimes certain inaccuracy is artificially added to make the aggregated responses smoother. Some overlap of the response distribution regarding the frequency ranges of the different frequency control services may be acceptable or even beneficial.

More problematic is the case that a large number of meters has the same systematic error. Thus the accuracy requirements should likely focus on the reduction of systematic frequency estimation errors.

Maximum inaccuracy should be better than 10 mHz, when response settlement time is 100 ms or less and there are no disturbances. For monitoring the frequency quality the accuracy is more important than response speed; there the requirement is 1 mHz. Then the response time is not critical and the needed accuracy can be achieved by low pass filtering the measurements that are used for control. It is important to distinguish the different accuracy requirements of the different purposes.





The disturbance immunity requirements are discussed in the following.

3.4.4 Immunity to disturbances

Increasing the response speed increases the sensitivity to disturbances. This also worsens the accuracy. The immunity to disturbances is the main challenge when fast responding measurements are needed. Distributed frequency reserve resources are in distribution networks where the voltage is more distorted than in the transmission networks. A significant mitigating fact is that the disturbances in different distribution networks are typically mostly rather local and thus their impacts on the responses do not mutually correlate.

3.4.4.1 Voltage dips and swells

The impact of voltage dips and swells on the measured frequency estimate depends on the depth, timing and asymmetry of the dips and swells. For example, the size and direction of the frequency errors due to a dip depend on which point in the voltage waveform the dip starts and ends. Three-phase frequency measurement methods tend to be less sensitive to symmetric dips than to unbalanced ones. Thus worst case maximum sensitivity requirements should be specified.

In distribution networks there are more dips and swells than in the transmission networks. The transmission system dips and swells are typically also seen in the distribution networks. Nevertheless, most dips and swells are local to the distribution network. Usually the biggest concerns for distributed frequency control are the dips that originate from the transmission system, because they appear in all the distribution networks thus affecting all the controlled resources.

The speed of the measurement or the settlement time has a strong impact on the sensitivity to disturbances. The faster the measurement the more sensitive it is.

For a one-phase dip of 50% remaining voltage and a frequency measurement settlement time 100 ms, the instantaneous frequency measurement error should be smaller than 0.1 Hz and the error should almost completely settle out in the measurement settlement time.

3.4.4.2 Phase angle jumps

Fast methods for frequency measurement are by necessity sensitive to phase angle jumps. The sensitivity tends to be roughly similar to voltage dip sensitivity. Models that estimate the maximum rate of change of frequency can be, to a certain extent, used to reduce the sensitivity to phase angle jumps and other rapid disturbances. Complete removal of the sensitivity is in principle impossible.

Some frequency measurement methods are clearly more sensitive to phase angle jumps than step changes in voltage amplitude. Based on initial simulation test, that is not the case with the method discussed in chapter 5 below. Thus the voltage dip sensitivity requirement may be adequate for limiting the sensitivity





to phase angle jumps. Tests are needed for finding out the validity of this assumption and the severity of the sensitivity.

3.4.4.3 DC-component

In some frequency measurement methods and their implementations DC-component may increase errors, such as some bias and oscillation at fundamental frequency or its multiple. Thus testing the impact of DC-component on the measurement accuracy is needed. Voltage DC-component levels that can occur in distribution networks in normal operating conditions should not cause deviations from the other requirements.

3.4.4.4 Waveform distortion

The method should not be significantly sensitive to voltage waveform distortion that can appear in distribution networks in normal operating conditions. For example, extra or missing zero crossings should not have any noticeable impact on the accuracy. Frequency measurement methods based on counting zero crossings are completely unsuitable. Such power quality measurement methods that use the whole information in the voltage waveform are typically rather insensitive to voltage distortion. Increased distortion level only slowly reduces the accuracy.

Recommended tests:

- How much noise will increase by adding certain amount of white noise voltage distortion to the measured voltage.
- Do additional or missing zero crossings due to distortion and transients cause any noticeable measurement errors.
- Sensitivity to 3rd and 5th harmonic components. The accuracy requirement should not be compromised due to levels of harmonics that can typically occur in the distribution networks.

3.4.4.5 Voltage unbalance

The voltage unbalance that can occur in distribution grids in normal operating conditions shall not cause errors to exceed the accuracy requirement. Then method described in chapter 3 estimates the frequency using voltage measurements of all the three phases. Compared to single-phase frequency measurement this gives faster response and smaller sensitivity to voltage unbalance and distortion. Verifying this with laboratory tests is recommended.

3.4.5 Response speed

Response speed is critical for distributed frequency controlled resources. Most challenges of the frequency control of power systems stem from response delays and latencies that are not small enough as compared to the inertia time constant of the system. Applying a control engineering rule of thumb one can





deduce that resources that give the responses that are about 10 times as fast than the inertia time constant of the system or even faster, always make the frequency control of the system easier and not more difficult. Thus, a control loop with a response time of 500 ms should be adequate in most cases and response time below 250 ms practically always improve the system. In addition, simulation studies of large power systems have resulted to similar conclusions, see [Donnelly 2012] and [Ma 2013].

Many demand response resources are typically much faster than ramping of thermal and hydropower plants [Ma 2013]. Anyhow, metering, local communication and the actuating device all have some delays and latencies. Thus for frequency estimation and the communication the response speed requirement it is good to be much shorter than for the whole control loop. About 100 ms may be a reasonable target. The requirement is not stiff, because the local communication latencies may be reduced to some tens of milliseconds and the electronic network interfaces of many small devices and appliances are also very fast, responding even faster than 100 ms.

3.4.6 Rate of change of frequency

Numeric differentiation of the frequency estimate is often used to get the rate of change of frequency. It results in a noisy estimate of the rate of change and often requires further filtering stages. The increased noise, latency and sensitivity mean that for the control purposes the benefits of such use of the estimate of the rate of change of frequency are small.

In some frequency measurement implementations, the accuracy and speed of the rate of change of frequency estimation are in practice defined by the accuracy and response speed of the frequency measurement. This requires that the method includes a good model on the possible dynamics of the fundamental frequency and of the noise sources. Depending on the method and implementation it is also possible to add information on the maximum possible rate of change later, but the performance may be sacrificed compared to doing it already in the frequency measurement method.

For normal control purposes the benefits of derivative term of PD control tend to be small and often out weighted by the increasing sensitivity to the changes in the dynamics of the controlled system. In this case this means changes in the inertia of the power system. There are more robust control methods, such as model reference control, for delay compensation.

In the frequency control of power systems, the rate of change of frequency is used to detect the start of important events such as large disturbances in the power balance of the system. That is needed, when the control resources are very large and used in an on-off type, or are used in a way that emulates such behavior. For the use of very fast and small distributed resources it is not necessary to separately detect events, because smooth gradual control responses can be easily applied.





The frequency measurement and estimation methods often have, for their internal purposes, estimates for the rate of change of frequency. They are especially useful for reducing the sensitivity to disturbances. These estimates of the rate of change may be differently filtered.

Estimates for the rate of change of frequency may be needed for other than control purposes. Each purpose may have different requirements that may conflict with the requirements of some other application. For example, they have been used for estimating the inertia of the power system. That approach is very inaccurate and sensitive to disturbances. Better approaches for estimating the inertia, such as adaptive state estimators, are available in control theory. Also protection systems include measurements of the frequency rate of change. It may be necessary in order to the protection system to be able to react in time. Also there the measurement sensitivity to disturbances may be an important issue.

It is useful to define requirements for the frequency rate of change. Then the most suitable models and filters for meeting the requirements can be designed. The requirements should not depend on the application that uses the frequency rate of change. Each application should do its own further filtering. The emphasis for the requirements of the generic estimate should be on fast responses and accuracy should be secondary to speed. Then each application can filter the estimate according to its own needs.

The specification of the quantitative requirements for the rate of change cannot be defined right now so it is now left to future work.

3.5 Development of smart kWh-meters to meet the functional requirements

3.5.1 Adaptive observer of the rotating voltage phasors

The starting point of the development was a smart power quality monitoring kWh-meter described in [Koponen 2001] and [Koponen 2002] and the concept in [Koponen 1994]. It uses observers of rotating phasors for the measurement of several power quality quantities. Because of a sparse sampling rate these measurements were only possible by making the observers to adapt fast and accurately to the variations in the fundamental frequency. The needed adaptive observer of the rotating voltage phasors of the fundamental frequency component had been designed and proven to be asymptotically hyperstable by using the theory of model reference adaptive systems explained by [Landau 1979]. The method can be tuned to be as fast as accuracy requirements and immunity to disturbances allow, because the stability region is theoretically proven. The method can adapt autonomously to a much wider frequency range than required. The method is described in [Koponen 1996]. The frequency estimate is common to all the three phase voltages. As can be expected, in simulations such a three phase implementation was found superior to one phase





implementations regarding the response speed and disturbance sensitivity. New hardware with a substantially increased sampling rate was being developed and the method design was updated accordingly. The gains of the new adaptive observer were tuned for fast and accurate frequency estimation performance.

3.5.2 Development of the method to improve immunity to disturbances

The disturbance immunity of the method was improved by adding and tuning some filters including a model of the highest possible rate of change of frequency in the measured system. The model will be applied on every sampling instant of the calculation to achieve maximum suppression of the disturbances.

3.5.3 Development of the method to improve accuracy

In the simulations of the method the maximum errors of frequency estimates have been about 2 mHz. These errors are mainly slowly varying or systematic comprising a bias and oscillation on known frequency. Thus they could be mostly removed rather easily. So the errors of the method itself likely are not the main concern. Thus more important may be the analysis of the errors stemming from the distortion of the measured voltage and the amplitude and timing errors of the AD-transformers. The design and testing of the hardware is important.

3.5.4 Tuning the frequency measurement method by simulations

Software simulations of the method were used to find out how to tune and develop the frequency measurement method to meet the requirements in a best possible way. Mainly the three-phase implementation was simulated, because it was clearly superior to one phase implementations regarding response settlement time and disturbance sensitivity. The simulations included responses to amplitude, frequency, DC-component and phase angle jumps in the measured voltages. Figure 3 shows how in the simulation the frequency estimate responds to a 50% step in amplitude at time 1.5s, a 2 Hz step in frequency at time 1.9s and a 90 degree phase angle jump at time 3.0s.



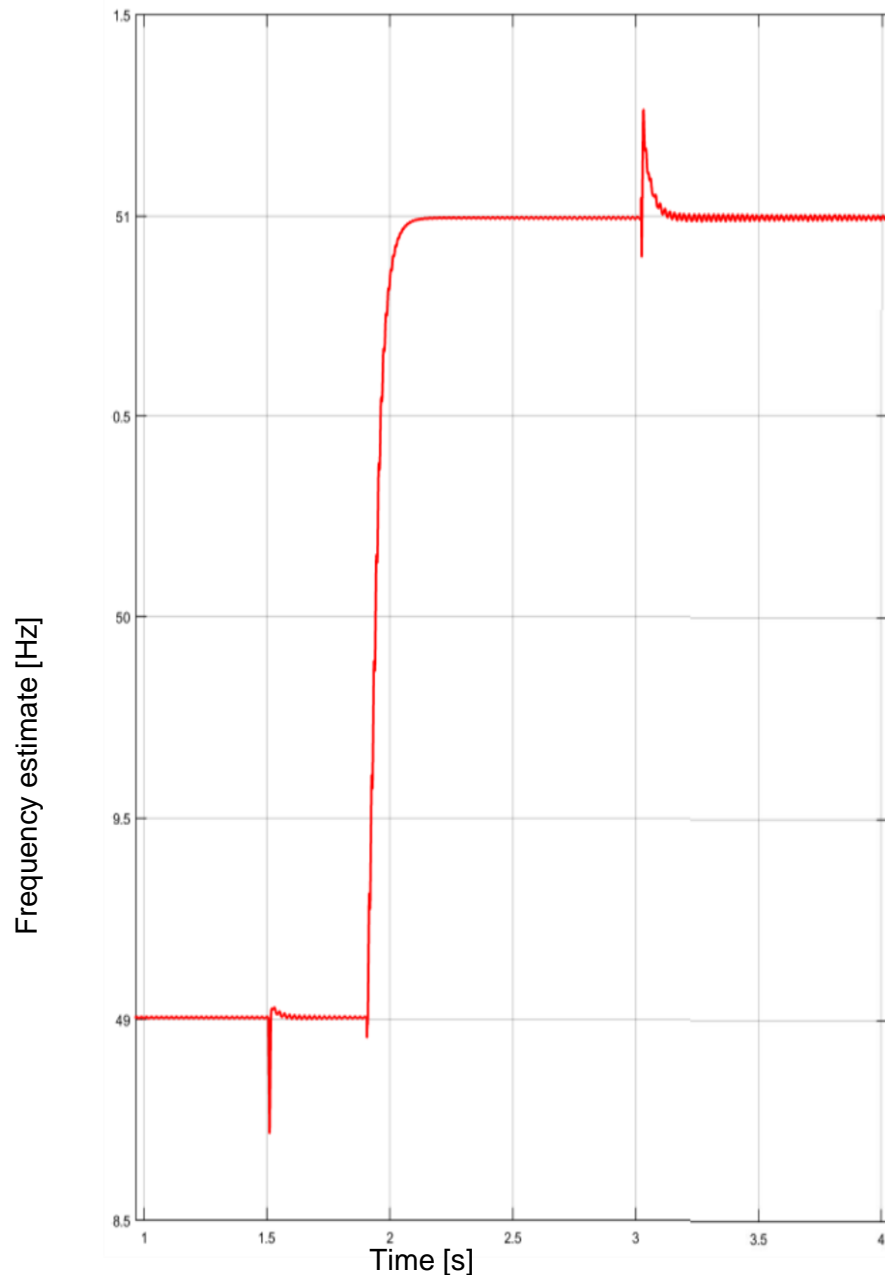


Figure 3. The estimated frequency

It was also verified with simulations that the method works without any problems nor retuning everywhere at the least in the frequency range 45 Hz to 65 Hz. Simulations suggest that the range is actually much wider but that was not systematically tested.

As new increasingly accurate knowledge of the requirements accumulates, it can be used to further improve the tuning. In order to achieve best possible performance, the tuning could be changed according to the type and amount of noise in the measured voltage and to the dynamics of the particular power system. During the comparisons with other meters, the tuning must not change.





3.5.5 Implementation in the new smart power quality monitoring kWh-meter

The method was implemented in the new hardware. The implementation was verified by comparing with the software simulations. The meter was ready for laboratory testing of the conformance with functional requirements and related comparisons with a reference meter. These tests are described in the following chapter. The total latency due to the measurement, estimation and communication hardware is designed to be smaller than one fundamental frequency cycle (20 ms).

3.6 Testing of smart kWh-meter with respect to the functional requirements

The performance of the new implementation of smart kWh-meter was studied by real-time simulations in the RTDS environment. The measurement results produced by the smart kWh-meter (later referred as ELV3) were compared to those produced by ABB RES 521 Phasor Measurement Unit (PMU) and in some measurements those produced by Dranetz PX-5 power quality analyzer.

3.6.1 Test setup

The test setup is presented in Figure 4. To enable comparison of the responses of the smart kWh-meter, PMU and Dranetz PX-5 in time domain RTDS produced synchronization signal (a TTL level pulse) which was amplified by Omicron CMS-156 and applied to all the measurement units.

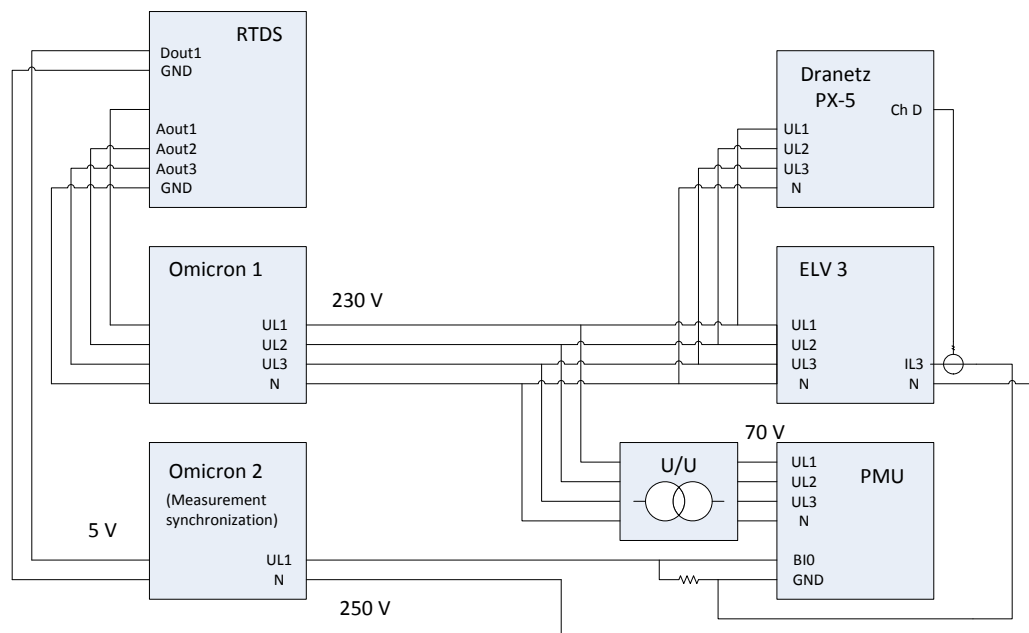


Figure 4. Test setup in RTDS simulations.





The PMU setup used in the tests presented in this report is described below:

- Manufacturer and type: ABB RES 521 Ver 1.0
- Production date: 2005-08-12
- Software version 1p0r12
- IEEE 1344 transfer filter selection: 0
 - Description: No filter for IEEE 1344 transfer
 - Total Group delay at $f_0 = 50$ Hz: 12.5 ms
 - Comment: Only the limited filtering in the “phasor3I/U” blocks. Not good for aliasing suppression.

The IEEE 1344 transfer filter 0 was selected to provide as rapid and unfiltered response as possible for the performance comparisons.

3.6.2 Accuracy

The differences in the measurement results of the smart kWh-meter (ELV 3) and the PMU relevant from the viewpoint of this report are reported in Chapter 3.6.4 “Immunity to disturbances”, where both static and dynamic accuracy are dealt with.

3.6.3 Noise of the measurement circuits

Noise accumulating to the measured voltage or current signal along the signal path of the measurement hardware impairs the accuracy of the measurement. The impairment becomes a problem especially when measuring small signal levels such as small distortion in voltage or current. The performance of the smart kWh-meter (ELV 3) in measuring harmonic distortion at various voltage levels was compared with Dranetz PX-5. The results indicate that the hardware of the ELV 3 gives less noise to the measurement than the hardware of the Dranetz PX-5.

3.6.4 Immunity to disturbances

3.6.4.1 Voltage dips and swells

The effect of voltage dips and swells on the frequency estimate of the smart kWh-meter (ELV 3) and PMU was studied by applying voltage dips and swells with various remaining voltages to phase voltage L1, L2 and L3. The results indicate that the frequency estimate provided by the smart kWh-meter was less sensitive to voltage dips and swells than the estimate provided by the PMU. The difference was largest at large dips and swells. More detailed results and analysis of the responses of the smart kWh-meter and the PMU to voltage dips and swells are presented in Chapters 3.6.5 and 4.

3.6.4.2 Phase angle jumps

The effect of phase angle jumps on the frequency estimate of the smart kWh-meter (ELV 3) and PMU were studied by applying both positive and negative phase angle jumps with a magnitude of 5.0, 2.0, 1.0, 0.5, 0.2 and 0.1 degrees. As indicated in Figure 5 and Figure 6 the frequency estimates of the PMU and





ELV 3 show reasonably similar responses to small phase angle jumps. The smart kWh-meter is less sensitive to large phase angle jumps. The difference in the steady state frequency estimates is due to the fact that ELV 3 is synchronized to its local quartz oscillator, while the PMU is synchronized to GPS clock.

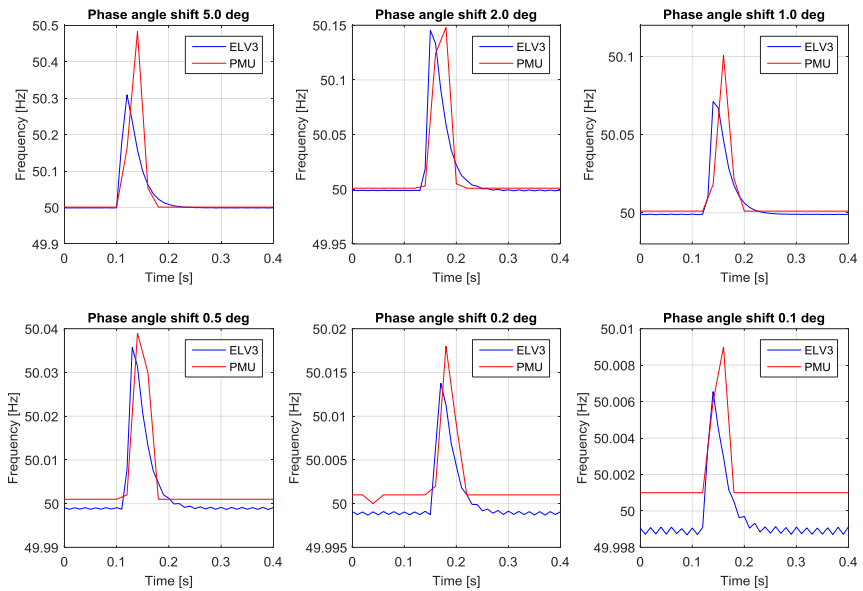


Figure 5. Response of the smart kWh-meter (ELV3) and PMU frequency estimates to positive phase angle jumps.

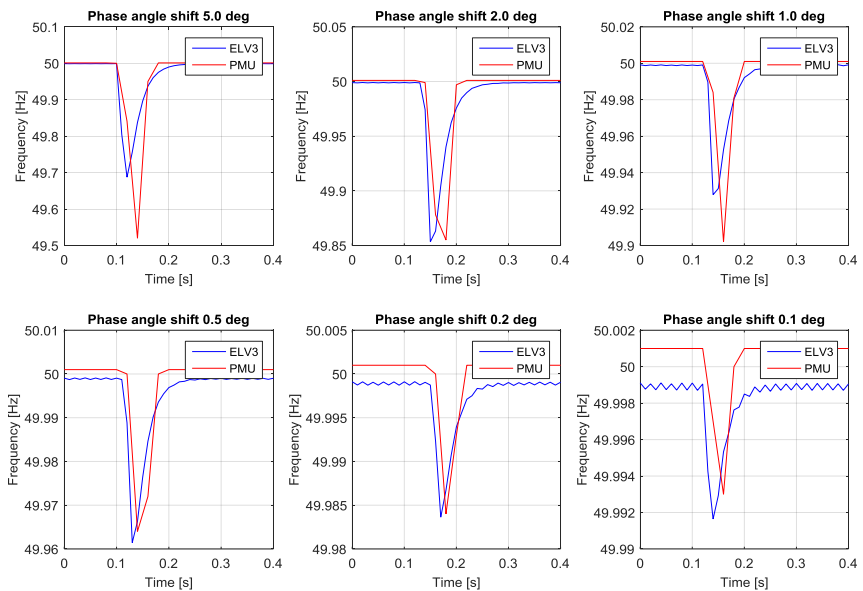


Figure 6. Response of the smart kWh-meter (ELV3) and PMU frequency estimates to negative phase angle jumps.

In this test, the measurement units were not synchronised and therefore, the results only indicate the magnitude of the change in the frequency estimate, not





the delay of the response. Results of synchronized tests are presented in Chapter 3.6.5.

3.6.4.3 White noise

The effect of white measurement noise on the frequency estimate was studied by summing white noise to the 230 V phase voltage L1, L2 and finally all three phases in ten steps so that the resulting total distortion of the phase voltage(s) was 0 %, 0.17 %, 0.35 %, 1.05 %, 1.75 %, 3.5 %, 6.9 %, 10.0 %, 12.8 % and 15.7 %. As indicated in Figure 7 as a result of added white noise in a single phase the variance of the smart kWh meter and the PMU measurement behave approximately similarly, but in case of white noise applied in all three phases the variance of smart kWh meter is larger than that of PMU.

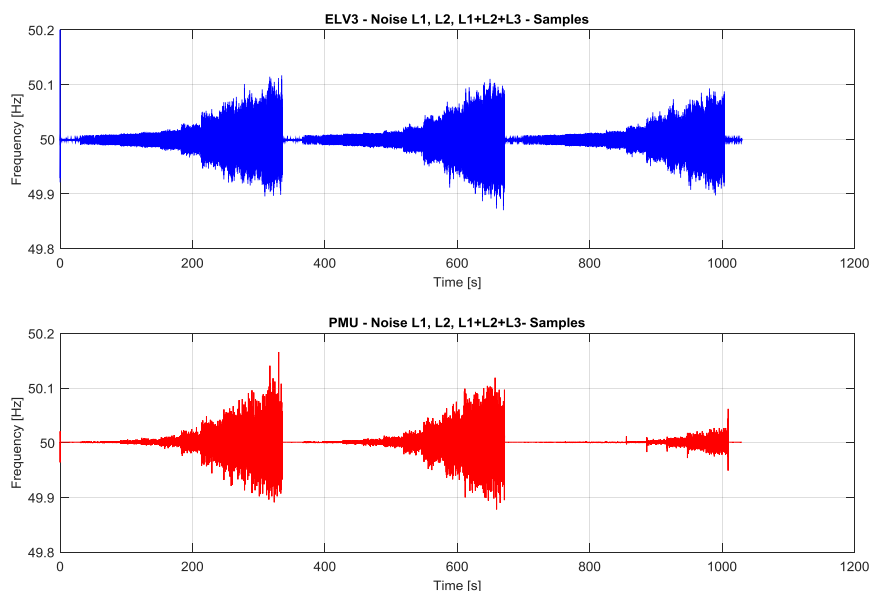


Figure 7. Response of the smart kWh-meter (ELV3) and PMU frequency estimates to white noise applied to L1, L2 and all three phases.

As illustrated in Figure 8 the 5s moving average of the frequency estimate of the smart kWh-meter is much more sensitive to added white noise. This implies that there may be some need and a possibility to significantly improve the white noise immunity of the smart kWh-meter.



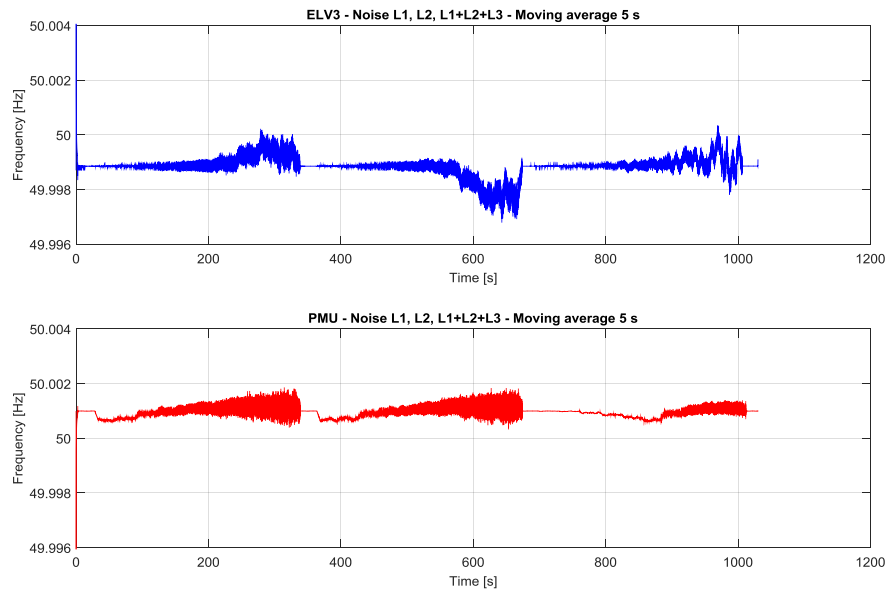


Figure 8. Response of the smart kWh-meter (ELV3) and PMU frequency estimates to white noise applied to L1, L2 and all three phases (5 s moving average).

Complete removal of this sensitivity may be very challenging, because the phenomenon likely results to some extent from the relatively sparse sampling rate. If the sensitivity is not reduced the frequency estimate of the smart kWh-meter may be significantly affected in the presence of strong nonharmonic distortion. 16% voltage distortion, which was almost fully non harmonic, caused an error of 0.035 Hz. For comparison, in simulations presented in chapter 5, a disconnection of a large generator from the network caused a voltage dip resulting in a 0.15 Hz negative and 0.2 Hz positive oscillation in the frequency estimate.

3.6.4.4 Harmonic distortion

The effect of harmonic distortion on the frequency estimate was studied by varying the harmonic content of the phase voltages. The test consisted of two simulation sets and the results of the sets are presented in Figure 9 and Figure 10. Both simulation sets consisted of five consecutive runs with 6 different THD levels (approx. 2 %, 5 %, 8 %, 16 %, 32 %) in each. In the first run equal amounts of 3rd, 5th, 7th and 9th harmonic were applied, in the second run only 3rd harmonic was applied, in the third run only 5th harmonic, in the fourth run only 7th harmonic and in the fifth run only 9th harmonic was applied. In the first simulation set the phase angles of each harmonic were set to 0 degrees and in the second simulation set for the 3rd, 5th, 7th and 9th harmonic they were set to 0, 180, 180 and 180 degrees, respectively. This resulted in additional voltage zero crossings in the second simulation set.

The smart kWh-meter sensitivity to high harmonic distortion is similar to but much smaller than the sensitivity to white noise type distortion. This implies that the distortion measurement could be to small extent used to compensate the error caused by distortion. The sensitivity is so small that it most likely has not





any practical significance. The sensitivity will likely be reduced, when a solution to the sensitivity to white noise is found and implemented.

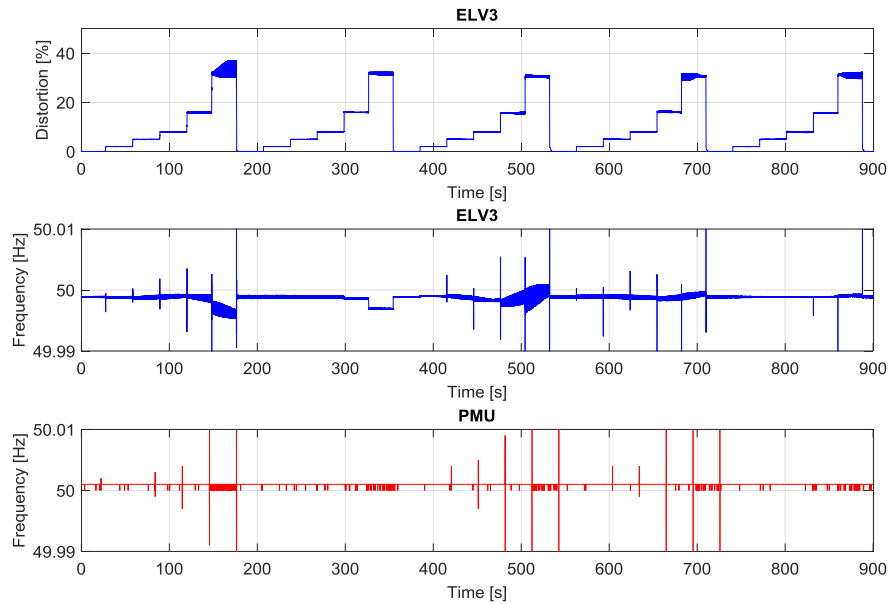


Figure 9. Response of the smart kWh-meter (ELV3) and PMU frequency estimates to harmonic distortion (simulation set 1).

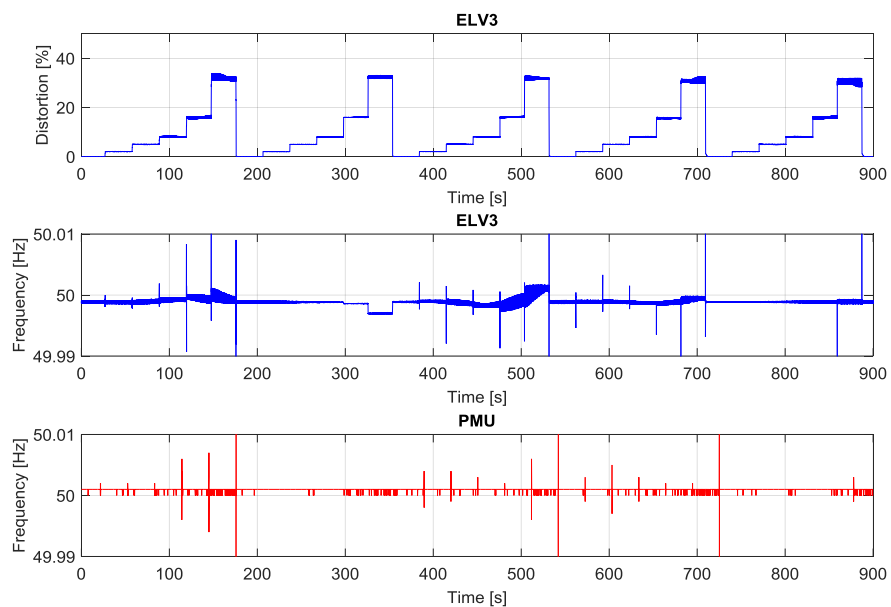


Figure 10. Response of the smart kWh-meter (ELV3) and PMU frequency estimates to harmonic distortion causing additional voltage zero crossings (simulation set 2).

3.6.4.5 Voltage transients

The effect of voltage transients on the frequency estimate was studied by applying a transient to a single phase or all three phases simultaneously. The





transients were generated in the RTDS model by connecting a large capacitance to one or all three phases simultaneously. An example of the transient waveform measured by Dranetz PX-5 is presented in Figure 11. Such transients may occur due to switching of e.g. capacitor banks or various loads and are quite common in low voltage networks.

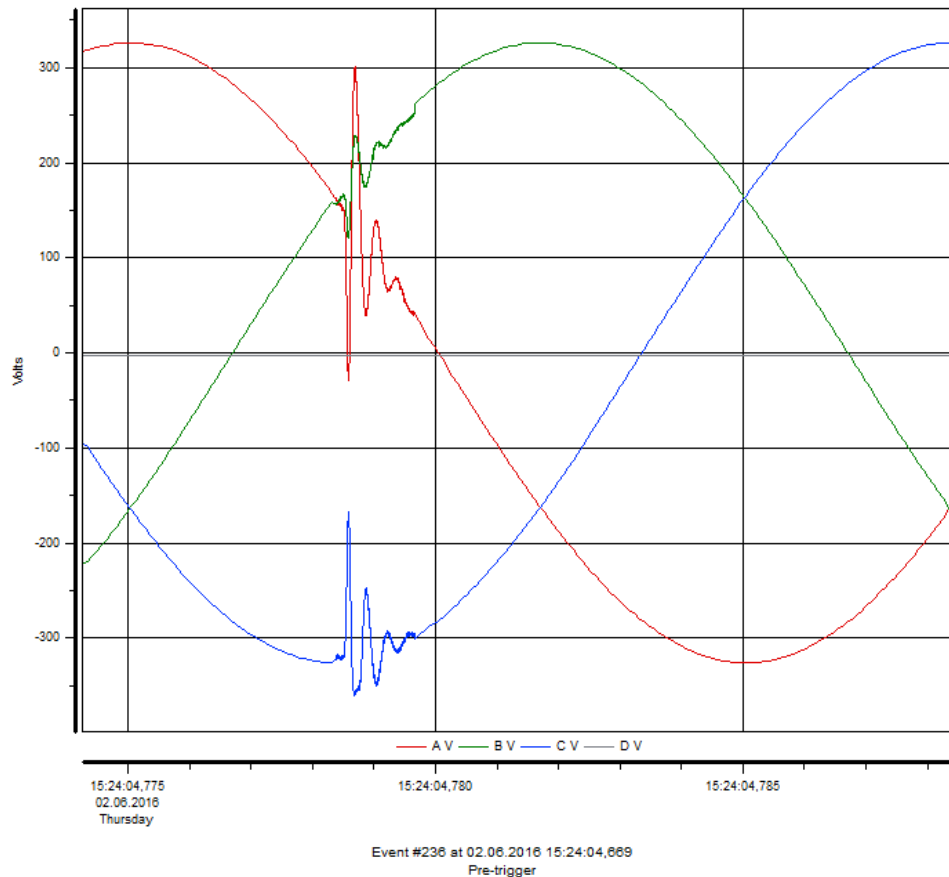


Figure 11. Transient waveform applied into one or all three phases in transient tests.

As illustrated in Figure 12 and Figure 13 the frequency estimated by the smart kWh-meter was occasionally more sensitive than PMU to voltage transients. This can be expected, because the sampling rate is lower. Nevertheless, the sensitivity to transients was not too strong.



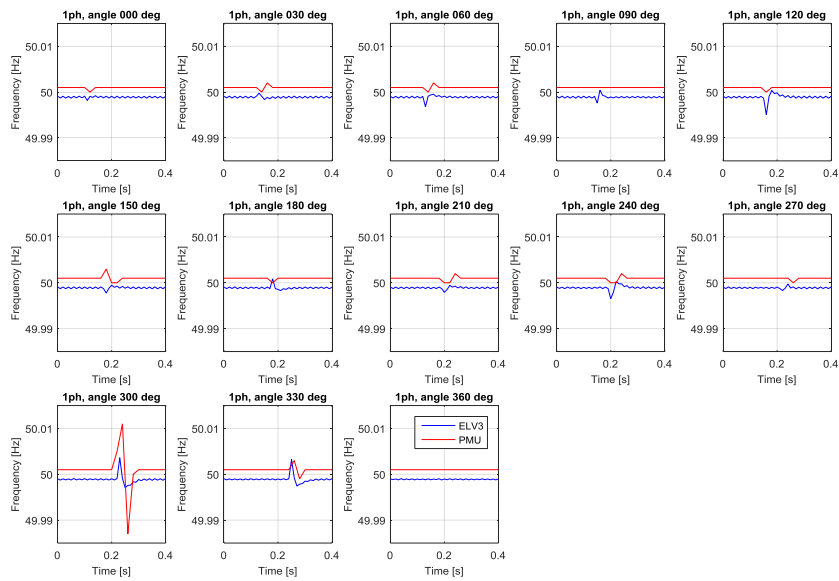


Figure 12. Response of the smart kWh-meter (ELV3) and PMU frequency estimates to transients applied to L1 at different phase angles.

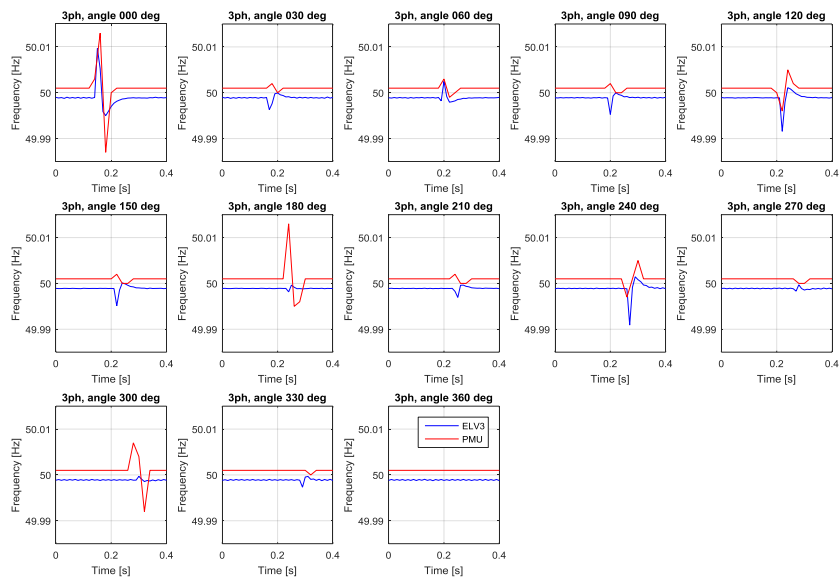


Figure 13. Response of the smart kWh-meter (ELV3) and PMU frequency estimates to transients applied to all three phases at different phase angles.

3.6.5 Response speed

The response speed of the smart kWh-meter (ELV 3) and PMU were studied by applying both positive and negative phase angle jumps with a magnitude of 5.0, 2.0, 1.0, 0.5, 0.2 and 0.1 degrees to the phase voltage and observing the response of the frequency estimates produced by the measuring units. As indicated in Figure 14 and Figure 15 the response of the smart kWh-meter is at least as fast as the response of PMU. Small uncertainty in this respect stems from the fact that the timing of the PMU and the smart-kWh meter with the RTDS





could only be determined with a resolution of 20 ms for PMU and 10 ms for the smart-kWh meter.

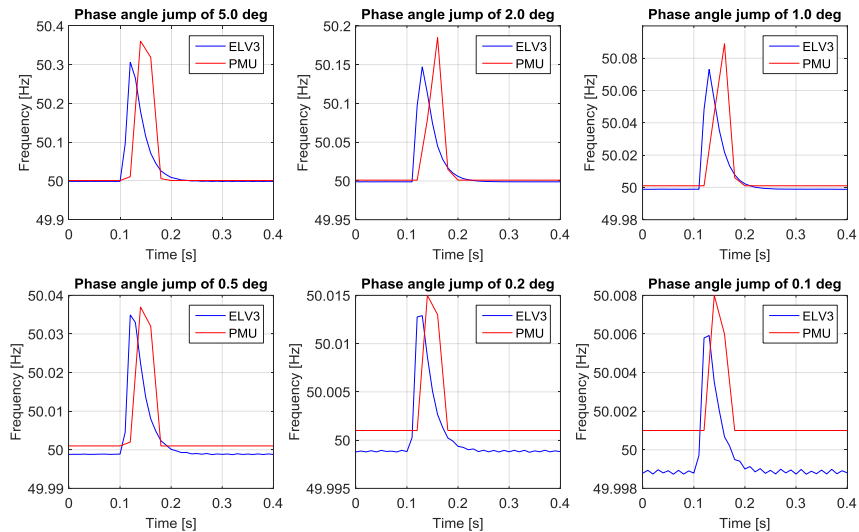


Figure 14. Response speed of the smart kWh-meter (ELV3) and PMU in case of positive phase angle jumps.

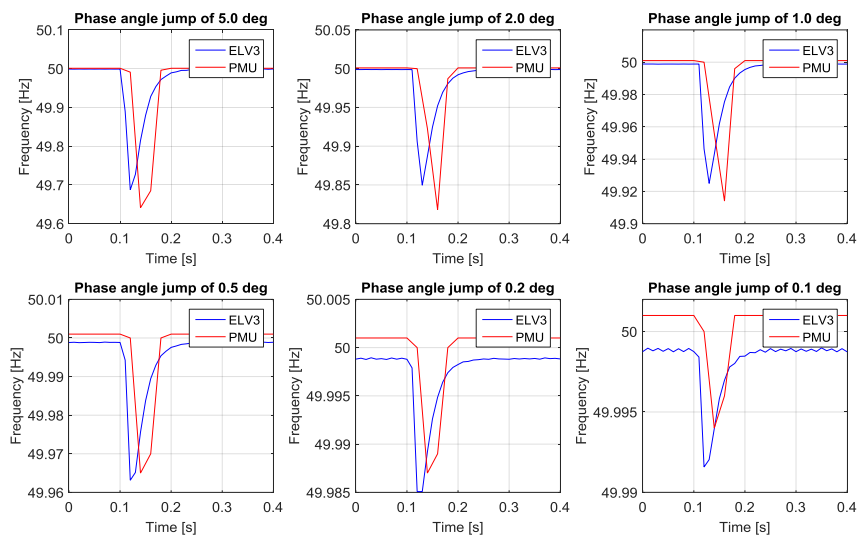


Figure 15. Response speed of the smart kWh-meter (ELV3) and PMU in case of positive phase angle jumps.

The response of the smart kWh-meter (ELV 3) and PMU were studied also in case of voltage dips and rapid stepwise frequency changes. Voltage dips with remaining voltages of 5.5 % U_n , 50 % U_n and 80 % U_n were applied to L1, L2 and L3. As illustrated in Figure 16, ELV 3 is less sensitive to voltage dips than the PMU. Stepwise frequency change was tested with two different amplification settings: ELV 3 slow ($k\alpha = -1000$) and ELV 3 fast ($k\alpha = -5000$). The setting ELV 3 slow ($k\alpha = -1000$) was used in all the other tests presented in this report. The amplification setting has an effect on the response mainly at the final settling of the frequency estimate in the end of the change where the higher





amplification results in a slightly more rapid settling but also some overshoot. It may be concluded that the frequency estimate of ELV3 is less sensitive to voltage dips and the response speed of ELV 3 is comparable to that of the PMU in both the voltage dip tests and the stepwise frequency change tests. Small uncertainty in this respect stems from the fact that the timing between RTDS, ELV 3 and the PMU could not be accurately determined with the test arrangement used in these tests.

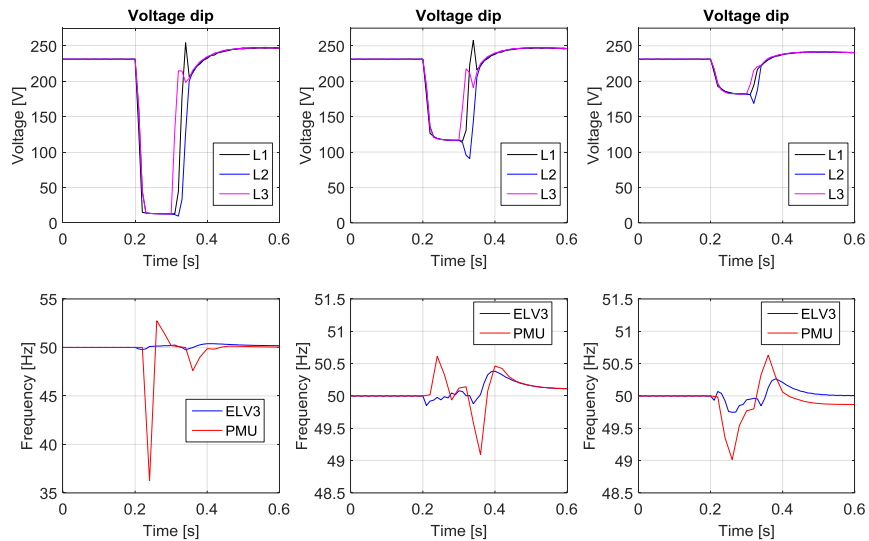


Figure 16. Response of the smart kWh-meter (ELV3) and PMU in case of three different voltage dips.

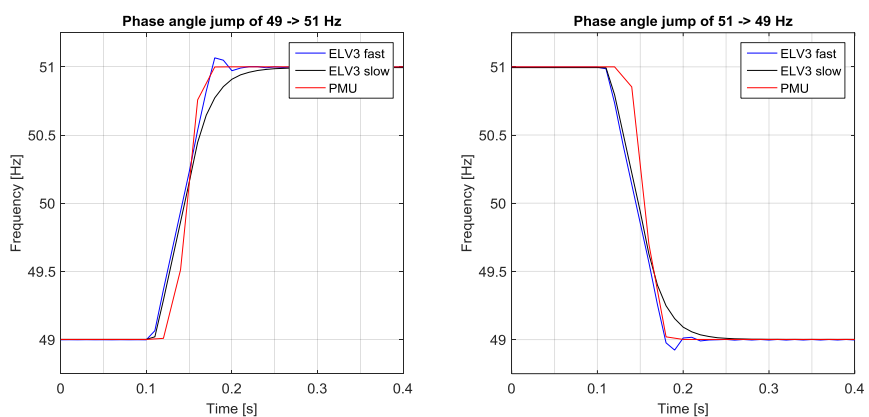


Figure 17. Response speed of the smart kWh-meter (ELV3) and PMU in case of a stepwise frequency change.

The test setup built up during this project would enable also more comprehensive tests dealt with e.g. in [Ghica 2015a, Ghica 2015b] and IEEE Std37.118.1a-2014 in potential follow-up research projects.





4 Application of smart kWh-meter connected loads as fast frequency reserves: robustness and quality requirements for frequency estimation algorithms

4.1 Typical system events affecting the quality of estimate

Robust implementation of frequency estimation algorithms is highly important for applications which require fast response times based on variations in system frequency. For most of the power system applications the frequency estimate is derived based on the local voltage measurement. Depending on implementation of the estimate, rapid changes in the amplitude and/or phase of the voltage, or voltage distortion, the frequency estimate may deviate significantly from the system frequency. Different frequency estimation methods have well known weaknesses which were covered in the chapter 3.

The quality of the frequency estimated is affected by the same factors as voltage sags are during said faults. Said factors are source impedance, voltage sag duration, voltage sag angle, sag magnitude, type of fault, effects of transformer connections, pre-fault voltage, fault impedance and loading conditions [Radhakrishna 2001]. Faults close to substation cause more severe sags than faults further away from the substation [Radhakrishna 2001].

It becomes increasingly challenging analyze the voltage signal due to noise and distortion when voltage reaches close to zero value during fault. Asymmetrical faults are also a challenge due to lack of voltages in faulted phases. Frequency estimates are also affected by distortion from power electronic devices. Power electronic devices can also cause asymmetry in the system on low voltage side. Noise also affects the quality of the measurement. Reducing the noise is mostly important.

Short circuits and faults lead to drop in voltage and phase angle jumps. Magnitude and phase angle jumps during sags are directly related to voltages in faulted phase, or between faulted phases at the Point of Common coupling (PCC) between the load and fault [Radhakrishna 2001]. Active power transfer causes directly proportional angle differences between different nodes. A change in active power in certain node thus also causes a change in phase angle. Phase angle changes affect the voltages and thus affect the frequency estimation. Depending on the angle change there can be either a positive or a negative temporary transient change in frequency.





4.2 Estimation of error between estimate and actual system frequency

Three different frequency estimation methods are compared via estimating errors between the measured values and the frequency from the bigger generator model in the power system model. Five different error estimates are shown:

- Maximum positive frequency error
- Maximum negative frequency error
- Maximum positive area error
- Maximum negative area error
- Average error

Error estimates are divided to three different time windows post fault. First time window starts immediately after the fault and ends at 40 ms. The second time window starts immediately after the first time window and ends at 100 ms. The third and final time window starts at 100 ms and ends at 500 ms post fault.

Maximum positive frequency error (MPE) is the maximum frequency difference between the measured value and the generator frequency. Maximum negative frequency error (MNE) is the maximum negative frequency difference between the measured value and the generator frequency. Maximum positive (MPEA) and negative frequency error area (MNEA) are calculated using trapezoidal summing of errors. Average error (AVE) is the sum of errors divided by sample count.

4.3 Quality assessment based on system study results

Considering the main use case being in the scope of this work, every frequency estimate should stay above the limit of activation set by the TSO during a fault to prevent unnecessary activation of the FCR-D. In the Nordic grid the under-frequency limit is at 49.9 Hz. On the other hand, rate of change of frequency should also stay above a certain limit. In the case of positive frequency estimation error, the reserve activation could potentially be delayed. The opposite holds true for the negative frequency estimation error.

4.4 Different frequency estimation techniques

The frequency estimation techniques compared in this study are described in the following. They comprise methods in the RTDS library and methods in the two commercial products studied. From the RTDS library are 1) the zero crossing method, 2) the discrete Fourier transform (DFT) method and 3) the phase locked loop (PLL) method. The commercial products are 4) PMU and 5) ELV3. These methods are described more in detail in the next sections.

4.4.1 Zero crossing

Zero crossing based estimators usually require noise reduction filters since input signal are seldom ideal sinusoids. Especially this is the case when distribution





network voltages are used as inputs. In this paper zero crossing frequency estimation method from RTDS library is used. The library component has one voltage input. The input voltage is further filtered with a moving average filter over 8 consecutive samples. Sampled voltage is the input of zero crossing frequency estimation. The RTDS-library zero-crossing method output has a sample time of 20 ms.

4.4.2 DFT based

Discrete Fourier transform method in RTDS library has one voltage input. The single phase input voltage is fed to a discrete Fourier transform block. Discrete Fourier transform is defined as in (1)

$$X_k = \sum_{n=0}^{N-1} x_n \cdot e^{-j\frac{2\pi nk}{N}} \quad n = 0, \dots, N-1 \quad (1)$$

DFT is utilized to acquire the fundamental frequency of a single phase voltage signal. The RTDS-library DFT frequency estimation method has a sample time of 20 ms.

DFT based frequency estimation has more inherent latency than the sequential (recursive) estimation methods described in the following. The reasons to the latency are:

- performing the DFT can only be started when its entire input signal is available. DFT also takes much more computation time than sequentially (recursively) calculating a new posteriori estimate from the last measurement and an a priori estimate. Using special DFT-hardware can mitigate or remove this difference.
- the necessary post filtering of the DFT estimate adds some further delay.

4.4.3 PLL based

The PLL has three-phase voltage inputs and a center frequency $\omega_c = 2 \cdot \pi \cdot 50$. Phase locked loop estimator has two outputs angular frequency estimate ω_{PLL} and phase angle estimate θ_{PLL} . The PI-controller of the PLL consists of transfer function with narrow bandwidth. Narrow bandwidth is achieved by adding a pole to the transfer function of the PI-controller.

As can be seen from Figure 18 changes in q-component of the voltage lead to transients in frequency estimate. Phase voltage phase angle jumps and amplitude changes will affect the q-component and thus the frequency estimate. Phase-angle changes occur in a power system when there is a change of active power transfer between two nodes. Voltage transients on a power system level can be due to faults such as sags. A transient in frequency estimate will occur during the events mentioned before.



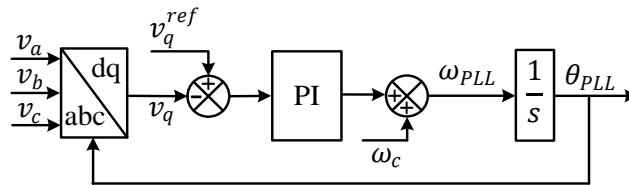


Figure 18. Basic SRF-PLL.

4.4.4 Commercial product PMU

A phase measurement unit (ABB RES 521) is also utilized. The measurement unit output has a sample time of 20 ms. Filtering is also available but is not used in these simulations. Filtering increases latencies or delays, improves accuracy and reduces sensitivity to disturbances. In addition to the PMU unit a commercial product is also utilized.

4.4.5 Commercial product ELV

A smart kWh-meter named ELV is used to measure the frequency. The meter estimates the fundamental frequency of the three phase input voltages. The frequency estimation of the meter is based on the model reference adaptive estimator of the voltage phasors [Koponen 1996] but has been recently improved by increasing the input sample rate, adding some filtering and tuning the estimator gains to simultaneously meet the requirements of both fast frequency measurement and power quality monitoring. The method can be considered as a globally asymptotically stable PLL design. The output from the smart kWh-meter has a sample time of 10 ms. The possibility to retune the estimator performance between speed, accuracy and disturbance sensitivity was not used in these tests, because that would have made performance comparisons impossible.

4.5 Power system model for analysis of fast frequency reserves

Power system model is in Figure 19 and it consists of two generators and their exciter and governor control systems. One of the synchronous generators acts as a rotating reserve the other one generates fixed power. Loads and generators are interconnected via MV/HV transformers with no saturation. Exciter model for both generators is IEEE ST2A.



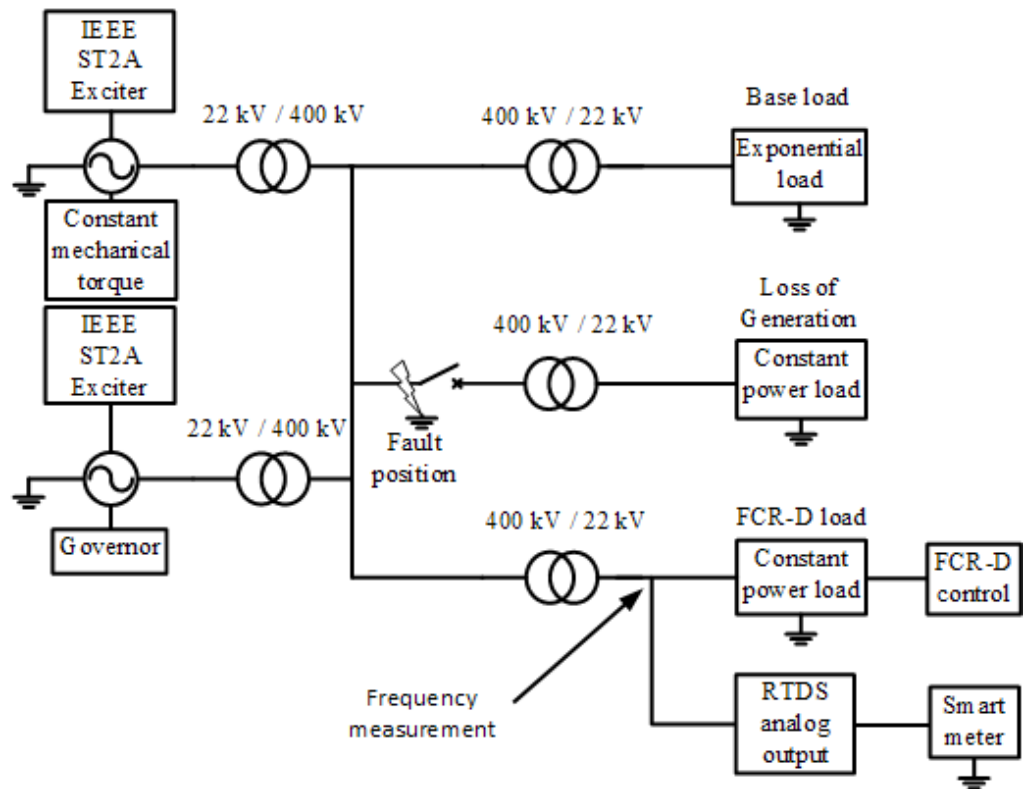


Figure 19. Power system model.

The power system base load model is based on exponential load model in [Chiang 2007]. Power system loads are modelled as voltage-dependent and frequency dependent active power loads. The load model can be expressed as in (2)

$$P_{BL} = P_0 \left(\frac{V}{V_0} \right)^{k_{pv}} (1 + k_{pf} \Delta f), \quad (2)$$

where k_{pv} is the voltage-dependent parameter of active power and k_{pf} the frequency-dependent parameter. Parameter k_{pv} has been set to zero while $k_{pf} = 1$.

Loss of generation in Fig y. results from a three or single-phase-to ground fault at fault position A or B. Loss of generation is modelled as a 1300 MW constant power load connected to the grid via the circuit breaker.

4.6 Modelling Smart meter connected loads

FCR-D loads are modelled as constant active power loads. Load disconnection is done if the frequency of the measurement reaches the upper limit of the controller. FCR-D load capacity is 200 MW.





4.7 Study cases

Four cases are compared. Three-phase ground fault to ground fault at position A or B. Faults can vary by fault impedance, fault angle, fault duration, fault location and fault type. Faults can also evolve into new faults in some cases.

The fault impedance is selected so that the remaining voltage during fault ranges from 0 pu to 0.8 pu. A series of 80 are run consecutively from remaining voltage at 0 pu to 0.8 pu. Fault location is also varied. Fault sequence results in a loss of generation. Loss of generation is modelled as an increase of 1300 MW of active power.

4.8 Study results

4.8.1 Three-phase-to ground faults

In this paper three-phase faults are considered. The fault impedance is selected so that the remaining voltage during fault ranges from 0 pu to 0.8 pu. Fault location is also varied. Generator frequency after the fault is in Fig K1. Active Power of the generator is in Fig K2. Active power of the FCR-D load reserves is in Fig K3. Input frequency for the FCR-D load reserves is in Fig K4.

It can be seen from Fig K1 that as a result of fault sequence and loss of generation, generator frequency minimum of 49.08 Hz is reached at 9.0 s post fault. Higher remaining voltage during fault decreases the frequency post fault until frequency minimum is reached. Lower remaining voltage causes higher frequency transient than higher remaining voltage during fault.

It can be seen from Fig K2 that as a result of fault sequence and loss of generation, generator power generation fluctuates. The lower the remaining voltage during the fault the bigger the variations are.

In Figure K3 the activation of load reserves can be seen. The higher the remaining voltage during fault the earlier the reserves are activated. All load reserves are gradually switched off by 4 s after the fault.

The input frequency for load reserves is in Fig K4. It can be seen from Fig K4 and K1 that there is both negative and positive error in the frequency estimate during and right after the fault. Measurement error decreases quite fast post fault and thus the Fig K1 and K4 match each other quite well post fault



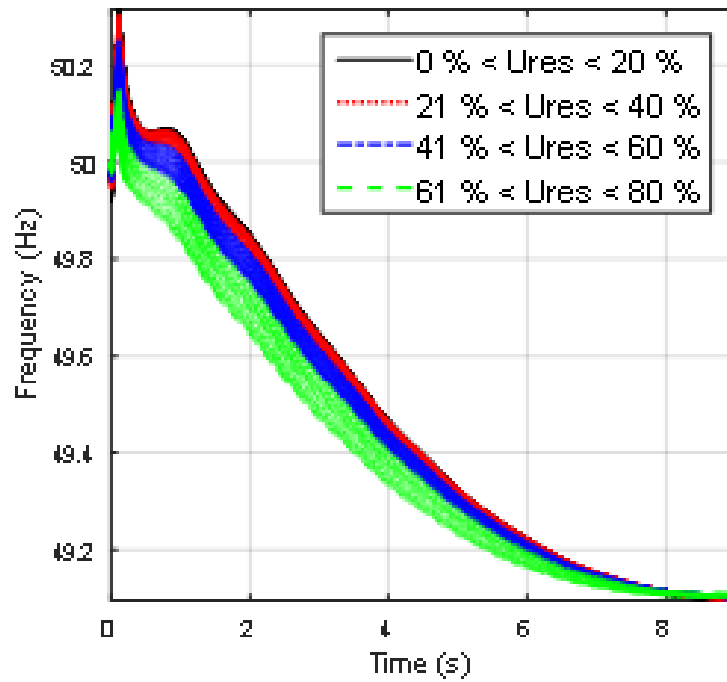


Fig K1. Generator frequency.

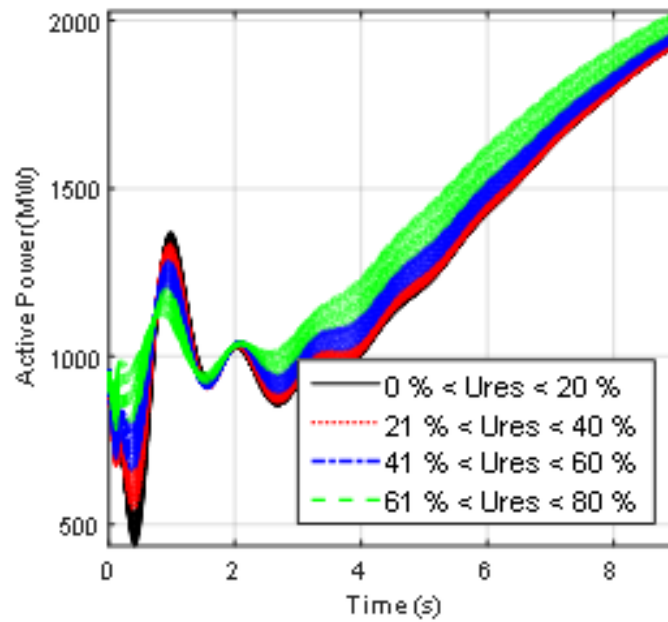


Fig K2. Active Power of Generator with Governor.



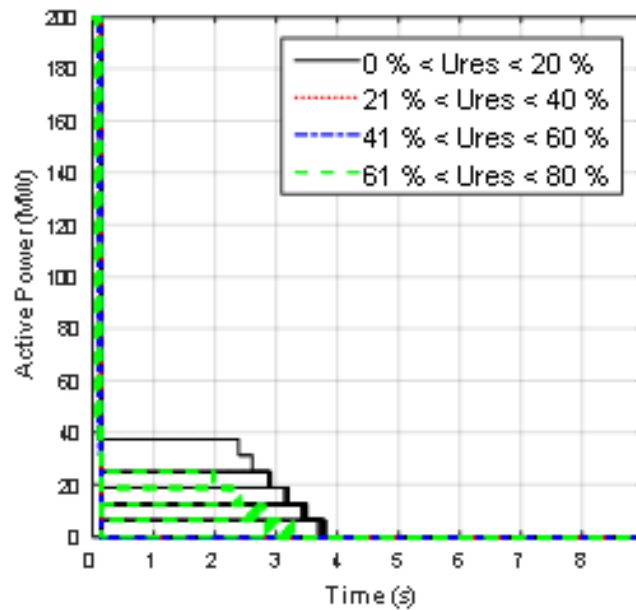


Fig K3. Active power of very fast and fast load.

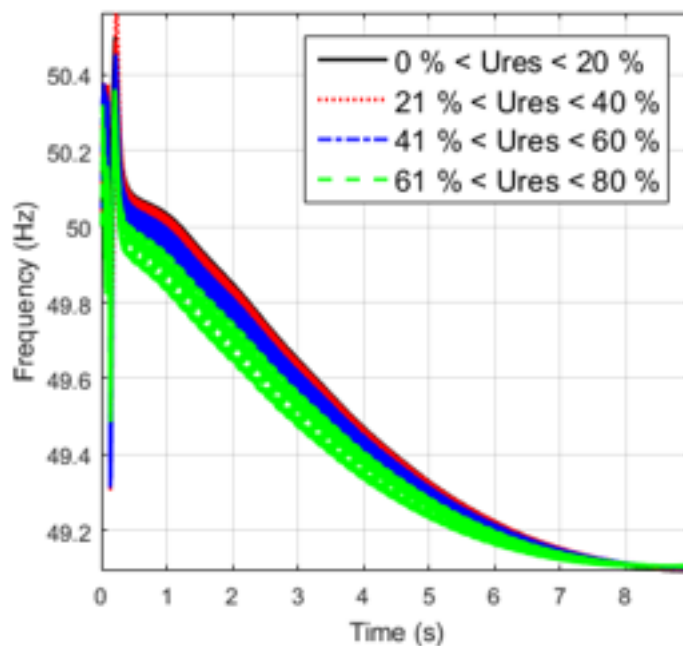


Fig K4. Input frequency for very fast and fast loads.

However, the frequency measurement method plays a major role when exploring the error between the real system frequency and the estimate.

DFT measurement is in Fig x1. Discrete Fourier method used has poor performance overall. In the zero remaining voltage case estimate reaches values less than 45 Hz. Even in cases with higher remaining voltage the estimate drops below 49 Hz. Post fault or at 500 ms the DFT estimate is fairly accurate.





Zero crossing estimate is in Fig x2. Similarly to DFT the method has poor performance during zero remaining voltage fault. Post fault the Zero crossing frequency estimate is fairly accurate.

Phase measurement unit frequency is in Fig x3. PMU unit performs worse when the remaining voltage is lower. As remaining voltage increases, the estimate becomes more accurate. Adding filtering to the PMU estimate would damp the fast frequency transient.



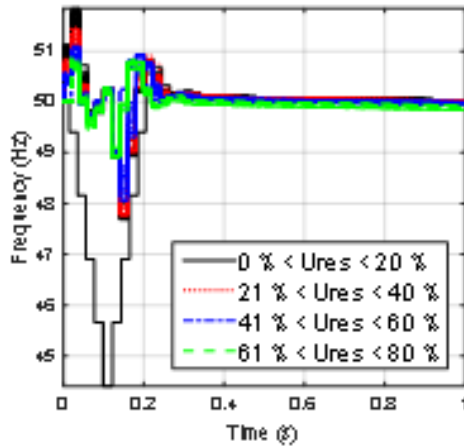


Fig x1. DFT frequency measurement.

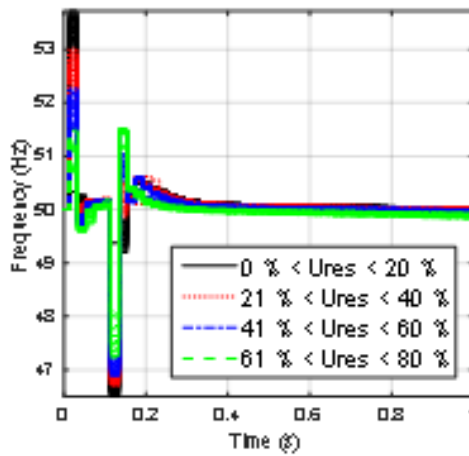


Fig x2. Zero crossing based frequency measurement.

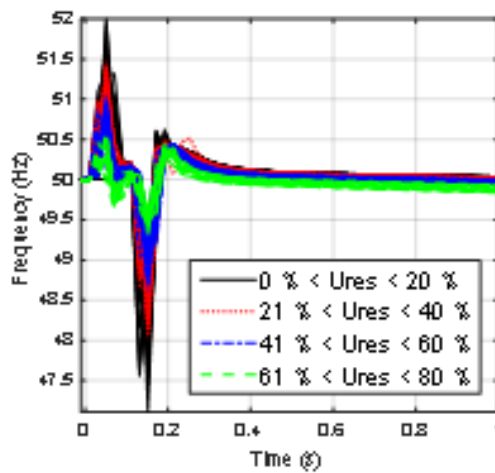


Fig x3. Phase measurement unit frequency measurement.



ELV smart meter frequency estimate is in Fig x4. The smart meter performs worse when the remaining voltage during fault is lower. Frequency stays above 49.4 Hz post fault.

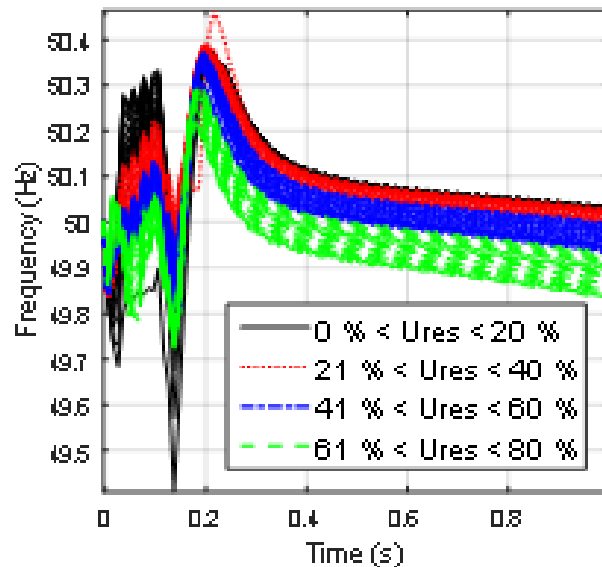


Fig x4. Frequency measurement from an industry product ELV.

In Fig x5 is the input frequency for the load reserves. The performance of this PLL is slightly worse than for the ELV. It can be seen that the upper frequency limit 49.85 Hz for the load switching is reached at 1 s when remaining voltage is 80 %.

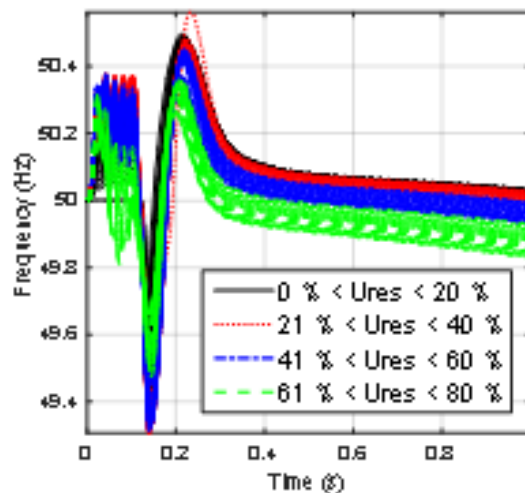


Fig x5. Frequency measurement from SRF-PLL.



4.8.2 Characteristic parameters

Characteristics parameters for the first 40 ms post fault are in Fig x6 to x10. Results from the time based simulations are sorted and maximum values of each run shown. It can be seen again that simple DFT and Zero crossing method for frequency estimation are not adequate during the fault when the remaining



voltage decreases. For zero crossing method the positive error can be as high as 3.7 Hz during fault. DFT method estimate has a positive error of 1.7 Hz.

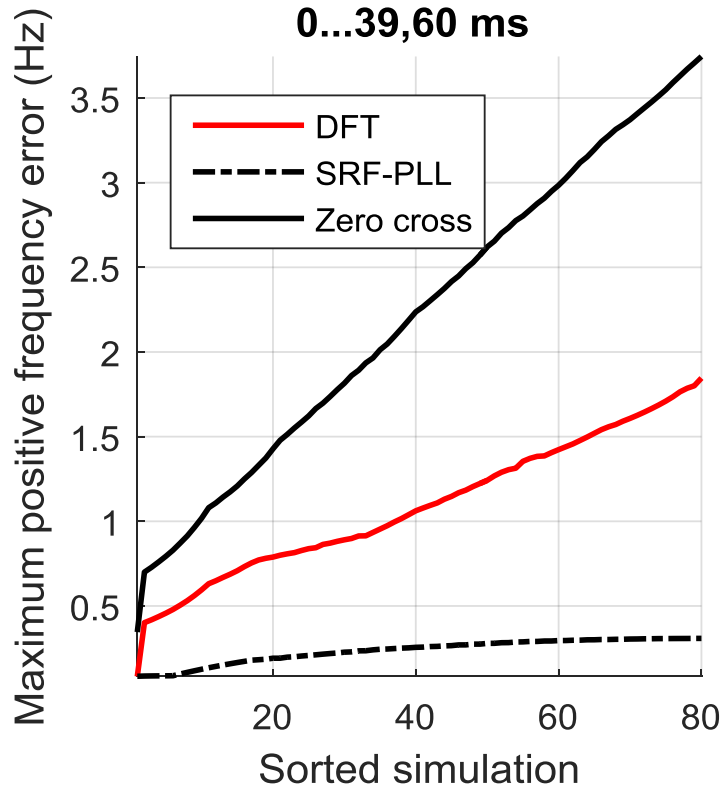


Fig x6. Maximum positive frequency error.

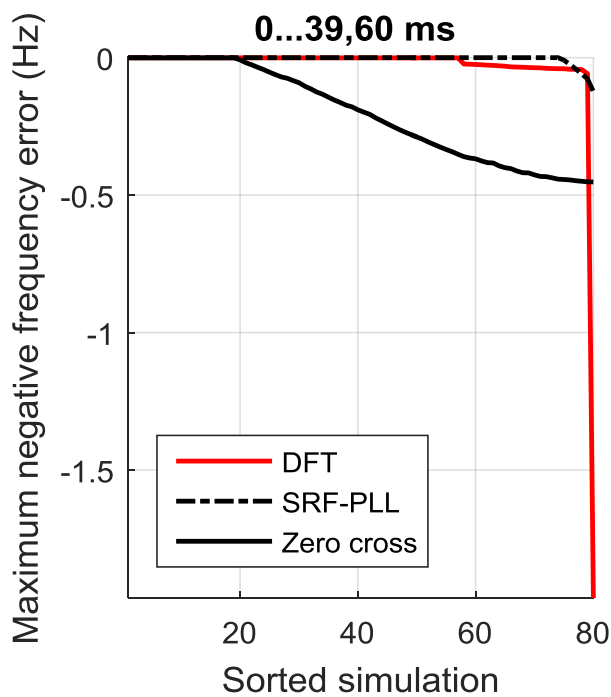


Fig x7. Maximum negative frequency error.



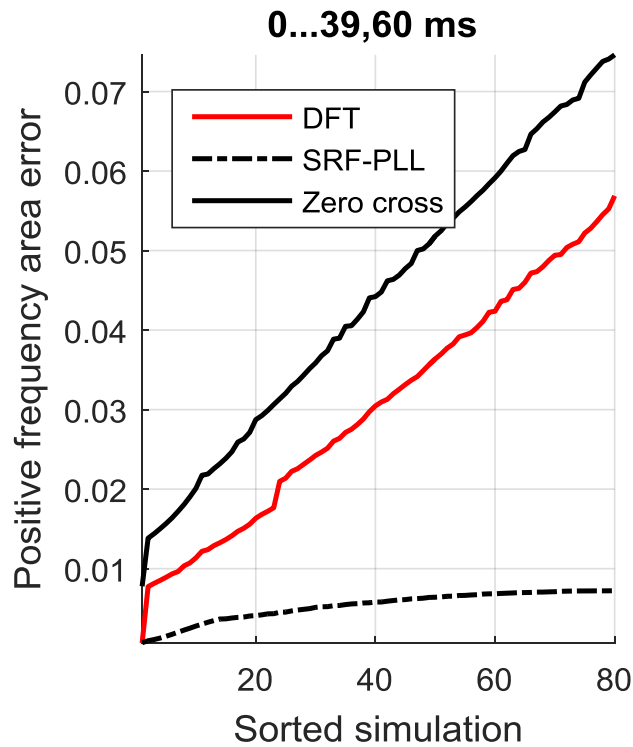


Fig x8. Maximum positive frequency area error.

PLL maximum positive error is below 0.35 Hz and maximum negative error above -0.2 Hz. Positive and negative errors behave similarly to positive and negative area errors in this case. The scale is however different due to time being a variable.

In Fig 10. is the average frequency error. Average frequency error is the sum of errors divided by sample count. It can be seen that the average error of DFT and Zero crossing are affected by the remaining voltage almost linearly.



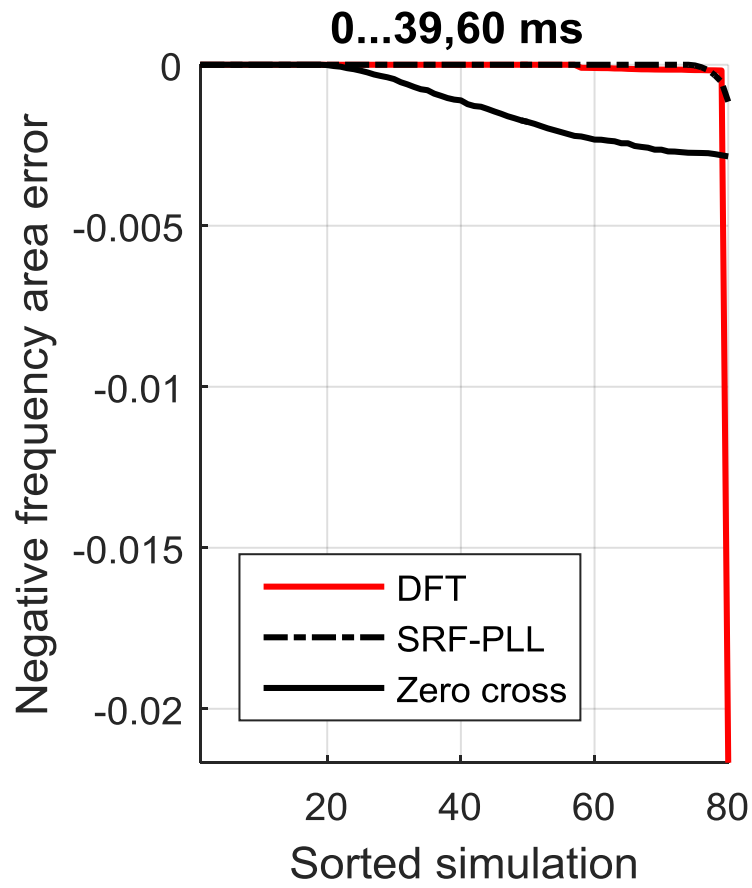


Figure x9. Negative frequency area error.



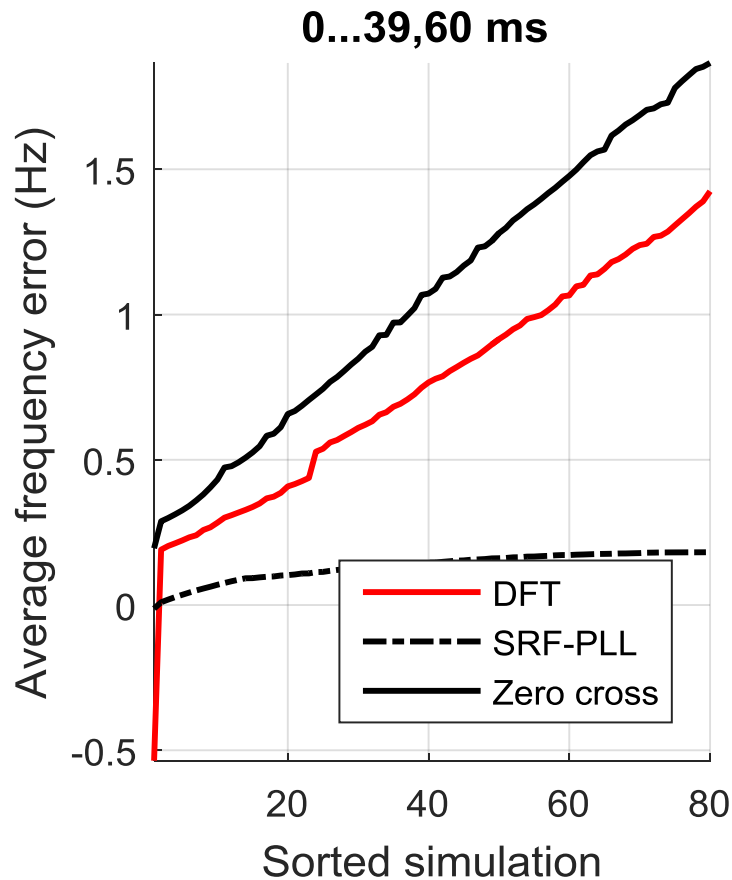


Figure. x10. Average frequency error.

4.8.3 Performance enhancement by adding delay before releasing load switching

Delay of 200 ms is added before releasing load switching. Input frequency for the load switching is in Fig M1. From Fig M1 it can be seen as previously that 49.85 Hz is reached at 1 s. The higher the remaining voltage during fault the faster the estimate and the system reaches the upper frequency limit of FCR-D reserve.

Control of FCR-D load is in Fig M2. Switching is locked during fault and 100 ms post fault. The transient is mostly bypassed.

Activation of reserves can be seen in the estimate in Fig M3. The switching of 137.5 MW load reserves causes a frequency transient of 0.1 Hz. The frequency transient results from a phase angle change at the measurement point nodes. The phase angle change of the voltages results from a change in active power transfer.



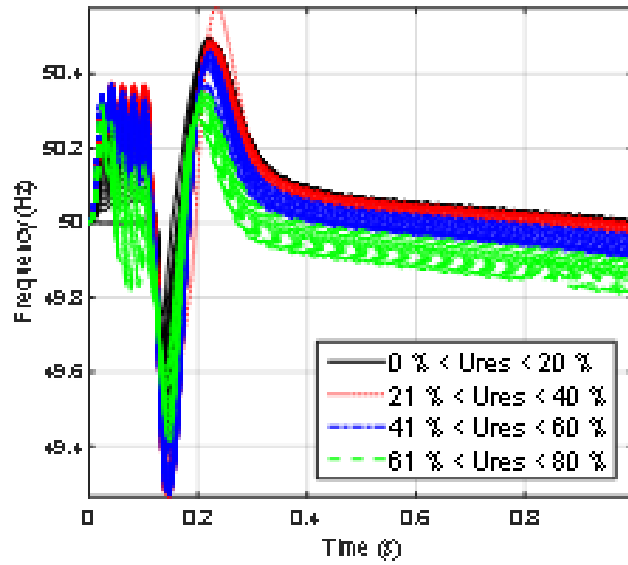


Fig M1. FCR-D input frequency with 200 ms delay.



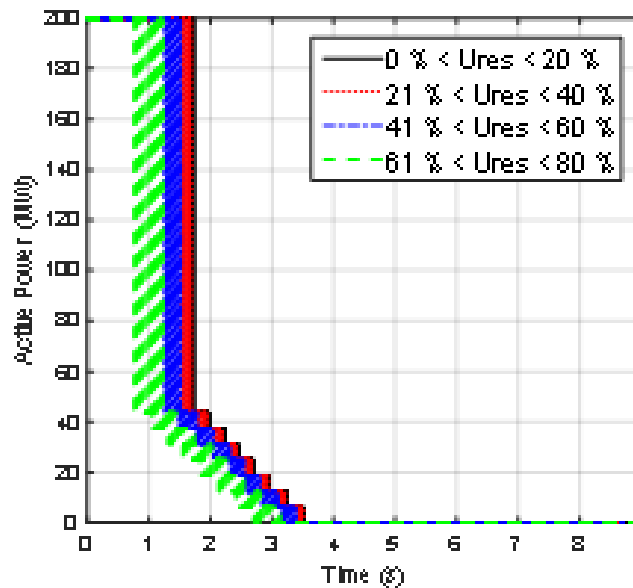


Fig M2. FCR-D Active power of reserve loads.

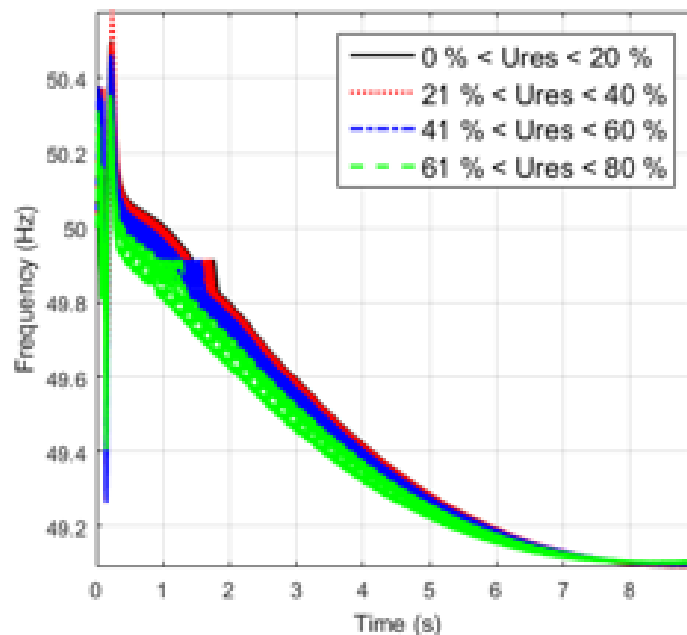


Fig M3. FCR-D input frequency with 200 ms delay.

Table 1. has all the 95% quantiles for all time intervals when there is no delay of reserves. In 95 % of all cases the values are below the 95 % quantile values. Reasonable errors have been marked with blue color and less reasonable errors with red. For all cases the maximum positive error is too high which is more than 0,1 Hz above the reference generator frequency. Maximum negative error is only reasonable within the first time window for DFT and SRF methods. Average error is reasonable for all three methods in the last 100 ms to 500 ms time window. Overall, the three phase fault with a low remaining voltage has a big impact on all the error estimates.





Table 2. has all the errors when there is a 200 ms delay before activation of reserves. The reserves are thus delayed until 1 s after the fault. The results are very similar to Table 1. Table 3 has errors when three phase to ground fault is at position B. When the fault position is at B the errors are much smaller for these estimation methods than in position A. Since fault position is on the medium voltage (B) side there are less fluctuations in the power system variables compared to the high voltage (A).

Table 1. Three phase to ground fault 0 to 0.8 pu residual voltage at position A, 95% quantiles of frequency error with no delay of load reserves.

95 % Time (ms)	Maximum positive error (Hz)			Maximum negative error (Hz)			Positive error area			Negative error area			Average error (Hz)		
	DFT	SRF	Zero cross	DFT	SRF	Zero cross	DFT	SRF	Zero cross	DFT	SRF	Zero cross	DFT	SRF	Zero cross
0 - 39.6	1.750	0.308	3.611	-0.042	-0.033	-0.446	0.053	0.007	0.073	0.000	0.000	-0.003	1.338	0.181	1.813
40 - 99.6	1.232	0.276	0.171	-0.575	-0.206	-0.446	0.007	0.010	0.002	-0.018	-0.007	-0.011	-0.144	0.172	0.016
100 - 500	0.833	0.341	1.438	-2.530	-0.920	-3.770	0.040	0.035	0.052	-0.105	-0.039	-0.096	0.035	0.026	0.018

Table 2. Three phase to ground fault at A, 95% quantiles of frequency error with 200 ms delay of reserves.

95 % Time (ms)	Maximum positive error (Hz)			Maximum negative error (Hz)			Positive error area			Negative error area			Average error (Hz)		
	DFT	SRF	Zero cross	DFT	SRF	Zero cross	DFT	SRF	Zero cross	DFT	SRF	Zero cross	DFT	SRF	Zero cross
0 - 39.6	1.750	0.308	3.609	-0.053	-0.033	-0.446	0.053	0.007	0.072	0.000	0.000	-0.003	1.338	0.181	1.807
40 - 99.6	1.153	0.276	0.171	-0.575	-0.207	-0.446	0.007	0.010	0.002	-0.018	-0.008	-0.012	-0.148	0.172	0.015
100 - 500	0.865	0.354	1.266	-2.529	-0.946	-3.770	0.041	0.034	0.048	-0.105	-0.044	-0.098	0.030	0.019	0.013

Table 3. Three phase to ground fault at position B, 95% quantiles of frequency error with no delay of reserves.

95 % Time (ms)	Maximum positive error (Hz)			Maximum negative error (Hz)			Positive error area			Negative error area			Average error (Hz)		
	DFT	SRF	Zero cross	DFT	SRF	Zero cross	DFT	SRF	Zero cross	DFT	SRF	Zero cross	DFT	SRF	Zero cross
0 - 39.6	1.112	0.066	0.647	-0.016	-0.018	-0.190	0.023	0.002	0.013	0.000	0.000	-0.001	0.567	0.041	0.291
40 - 99.6	0.172	0.048	0.000	-0.650	-0.040	-0.191	0.003	0.001	0.000	-0.026	-0.002	-0.008	-0.069	0.008	-0.047
100 - 500	0.808	0.207	1.149	-1.262	-0.297	-1.739	0.031	0.015	0.037	-0.030	-0.011	-0.034	0.008	0.010	0.008

4.9 Results of analysis of frequency estimation techniques

Two series of cases were compared. The errors for DFT and zero crossing estimates were rather significant. Zero crossing method has the benefit of being simple, however it is not really suited for transient analysis. DFT method requires filtering similarly to zero crossing method to provide reasonable results. PLL and ELV had best performance.

The frequency estimation method has to be accurate and fast enough to keep up with the voltage transient. Adding delay to activation of load reserve switching only had minor impact on the quality of the frequency estimate within the first 500 ms after the fault. This is a possibility if the FCR-D reserves consist of big aggregated loads.





In this paper quality of frequency estimation methods was compared. Zero crossing, DFT, PLL and commercial product frequency estimation methods were compared. From the results it can be seen that fault sequence and especially the remaining voltages during fault affect greatly the error estimate. In future work a more in depth in model for the power system should be considered. Maybe in the future work an aggregated load reserve could be controlled by a smart kWh-meter.





5 Structure of the study and simulation models for analysis of impact on technical performance of transmission network

5.1 Introduction

The alternative sources of the fast frequency reserves are becoming more and more valuable along with the continuously decreasing amount of synchronously connected, rotating generators connected into transmission networks. Their impact on performance of transmission system may be completely different from rotating machines, because it is based on the implementation of the logic applied to connect and disconnect loads from transmission network. This chapter addresses the special case of the smart kWh-meter connected loads which are applied as fast frequency reserves. The chapter presents analysis of the possible impacts of the concept on the dynamic performance of transmission system. For the system study general power system and AMR connected load models has been established and this chapter concentrates to describe the aspects which are most relevant from the perspective of network dynamic.

Although the paper approaches the fast frequency reserved on power system performance from the perspective of smart kWh-meter connected loads, the approach and the results presented by this chapter can be generalized to demonstrate the benefits, challenges and risks related to application of any distributed resource as fast frequency reserve.

5.2 System study need and possible approaches

The concepts identified in Chapter 4, that are most relevant considering the scope of this work, have been implemented as part of simple network equivalent reflecting the frequency response characteristics of Nordic power system. Using this model, the effect of the concepts is studied in order to analyze their impact on system performance in connection of loss of generation or load with and without three phase short circuit. Such assessment is highly interesting considering the one key aspect of feasibility analysis of the concept: under which circumstances the way the concepts have been implemented, may have adverse effect of system technical performance.

5.3 AMR meter connected loads as fast frequency reserves

This chapter provides a short overview of the overall concepts that may be applied for wide scale use of distributed load resources as fast frequency reserves.





5.3.1 Concept for using AMR meter connected load as fast frequency reserves

The use of distributed resources, in this specific case the AMR meter connected loads, is basically very straightforward. The AMR meter switches on or off one or many of the loads depending the load disconnection schemes presented later in the Chapter 5.6. From the perspective of dynamic performance of transmission network, the following key indicators can be identified regarding the response of the frequency to disturbances:

- 1) frequency minimum and time when a frequency minimum is reached
- 2) the amount of rotational reserves that can be replaced by fast reserve loads, and
- 3) damping ratio

5.3.2 Risks related to the concept

The main generally identified risk of switching on or off large amount of distributed resources is continuous uncontrolled connection and disconnection of distributed resources. This has been demonstrated, in different context though, in "what-if" -analysis of the central European system split back in 2006. [ENTSOE 2012]

There are two main approaches to manage this risk. First, a fast frequency measurement with robustness against system transients due to faults, failures and sudden disconnection of network components should be established and ensured. Secondly, the risk should also become manageable if the reduction of load or generation is not sudden, but follows a predetermined gradient or droop allowing linear decrease or increase of power as function of frequency decrease or increase. For smart meter connected loads, the same risk management could be implemented e.g. by introducing same droop by selecting the threshold values for connection and disconnection according to a droop profile for different loads. In section 5.6 and 5.7 these aspects are demonstrated using the models and study approaches presented in chapter 4.

The main measure to manage this risk is a general fundament for all the distributed resources related frequency control applications i.e. establishment of a reliable manner to monitor the availability of the reserves and to validate their response.

5.4 Power system model for analysis of fast frequency reserves

The target of this work was to assess the overall transmission network level impact when large amount, lumped distributed resources are used in frequency restoration. The study was done to illustrate how large penetration of frequency reserves switched on and off based on local frequency measurement may affect the whole system frequency and total response. An equivalent model dedicated





for analysis of the frequency behavior after loss of significant generation or load was established.

The effect of AMR meter connected fast reserves has been studied using a simple model presenting the main characteristics related frequency dynamics of a large synchronous system. The model was built by connecting large lumped generators and loads into the same high voltage bus. Figure 20 illustrates the main components of this model. This model allows testing of the basic concepts and rules as well as risk assessment. The model comprised two synchronous generators, five transformers, one exponential load, one constant power load and two loads are represented as pure resistances.

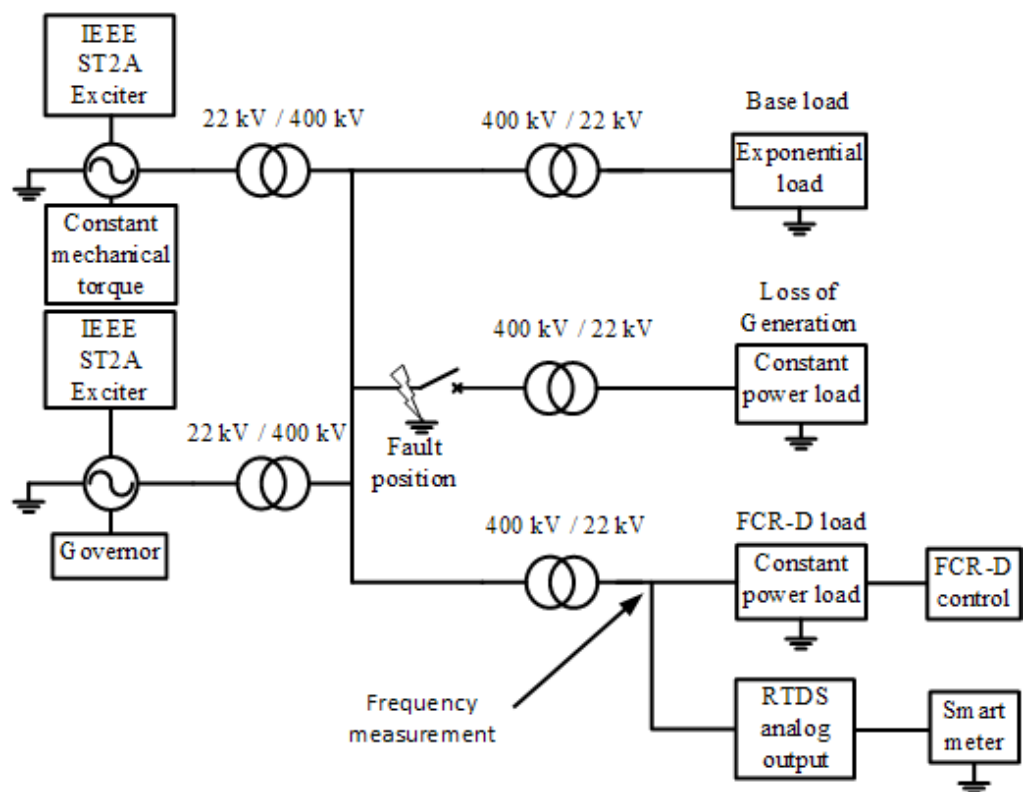


Figure 20. The model used in the simulations.

When the network model had reached steady state in a simulation, the fault was applied to the 400 kV bus, i.e. the position which is demonstrated in Figure 21. After the fault was cleared, in which type and length was variable, change of the total production was made through the straightforward operation of the circuit breaker. After then, the traditionally rotating reserves and fast reserves were controlled in order to reach the new equilibrium.

The parameters of the both generators were taken from [Anderson 1986]. Only the data from one size of generator, measured as apparent power, was selected because the aim was not to study inter-area oscillations. Also the aim was to restrict the number of variables. The selected generator represented typical





hydro power unit in which apparent power is 158 MVA. The upper synchronous generator operated at constant torque mode and it represented all that production which did not participate in frequency control. The lower generator in the Figure 20 was equipped with turbine speed control and hydro turbine and, in contrary to upper generator, represented the amount of available traditional rotational reserves.

Figure 21 illustrate the turbine speed control and turbine of the lower generator. The simple phase lead/lag transfer function models the effects of a penstock.

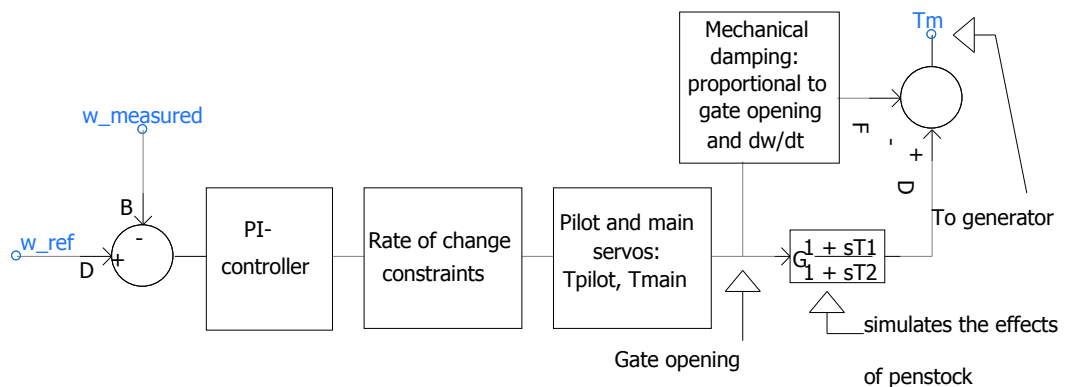


Figure 21. Turbine speed control and turbine of the lower generator.

The proportional and integral terms of the PI-controller block were tuned in order to achieve rapid power response but at the same avoid generating excessive oscillatory movement. The rate of change constraints illustrated in the Figure 21 were 0,16 1/s in both open and close directions in all the simulations. The time constants of pilot and main servo were 0.03 s and 0.2 s, respectively. Water starting time was 2.1 s. The effect of the mechanical damping to maximum frequency deviation was order of 1 %.

Exciter used with both generators was the type of ST2A. ST2A models the static excitation system with slip-rings and with compound source rectifier excitation system. It utilizes terminal voltage, V_t , and terminal current, I_t , to form a model of the exciter power source.

5.5 Modelling smart kWh-meter connected loads

All the three loads, depicted next, consumed only active power. The power system base load, i.e. the upper most load in the Figure 20, is modelled as voltage and frequency dependent exponential load model as in [Chiang 2007] . This base load was permanently connected to the bus. The base load model can be expressed as in (2) in which k_{pv} is the voltage-dependent parameter of active power and k_{pf} the frequency-dependent parameter. Parameter k_{pv} has been set to zero while $k_{pf} = 1$.





The load in the middle, i.e. constant power load represented the power deficit just after the fault. The load model is also polynomial model as in base load but coefficient k_{pf} is also set to zero.

The two lower most loads, lumped in to a one in the Figure 20, acted as a fast frequency reserves. These loads composed of two simple resistance parallel to 22 kV feeder line. The other resistance modelled the very fast reserves and the other resistance modelled fast reserves. The difference between these loads, besides their resistance values, can be found in a way in which the resistance of these loads are controlled as a function of measured frequency in which is depicted in the section 5.6. Both of the two reserve types loads had own control logic.

5.6 Parameterization of the load

The straightforward method is to increase the resistances, i.e. decrease the active power of the load, of the both fast reserves in a case of frequency drop after predetermined thresholds, measured as hertz, was reached. Information of when and how much of fast reserves were shed at certain frequency interval can be found on Table 2 and

Table 3.

All the simulation cases dealt situations in which the frequency dropped after the fault. This meant that the remained production was less than the consumption. That is the reason why load disconnection switching scheme is represented as a only control scheme. There were four different load switching pattern for both distributed reserve types in which are depicted in Figure 22 and Figure 23.





Table 2. Load disconnection logic for very fast reserves.

Combination	f_{start}	f_{end}	Load shedding distribution	Delay (fixed)
1	49.85	49.85	All @ 49.85 Hz	None
2	49.85	49.70	Flat - 1/16 activates for each 10 mHz	None
3	49.85	49.70	Flat - 1/16 activates for each 10 mHz	250 ms
4	49.85	49.70	Linear - ~14% activates @ 49.85 Hz, ~1% remains after 49.70 Hz)	None

Table 3. Load disconnection logic for fast reserves.

Combination	f_{start}	f_{end}	Load shedding distribution	Delay (fixed)
1	49.85	49.50	Flat - 1/8 activates for each 50 mHz	None
2	49.70	49.50	Flat - 1/5 activates for each 50 mHz	None
3	49.85	49.50	Linear - ~20% activates @ 49.85 Hz, ~5% remains after 49.50 Hz	None
4	49.85	49.50	Linear - ~5% activates 49.85 Hz, ~20% remains after 49.50 Hz	None





The operation principle of combination of very fast reserves (1) / fast reserves (1) is depicted in Figure 22.

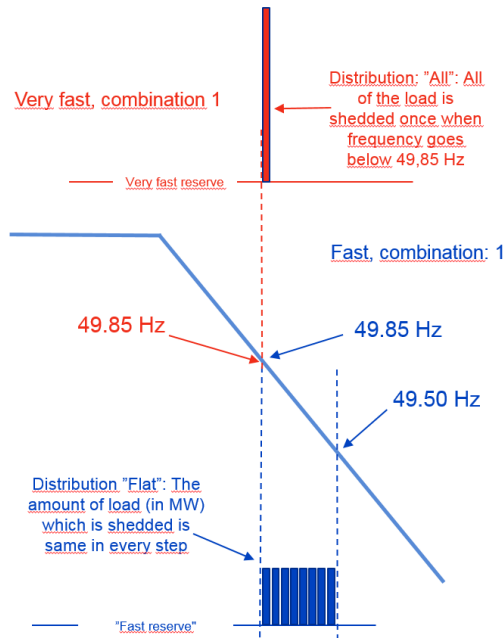


Figure 22. Load disconnection switching scheme for combinations of one and two.

The disconnection switching scheme principle of combination of fast reserves (3) are depicted in the Figure 23. The same method applied also for very fast 3 and fast 4 with different load percentages shares and different thresholds.

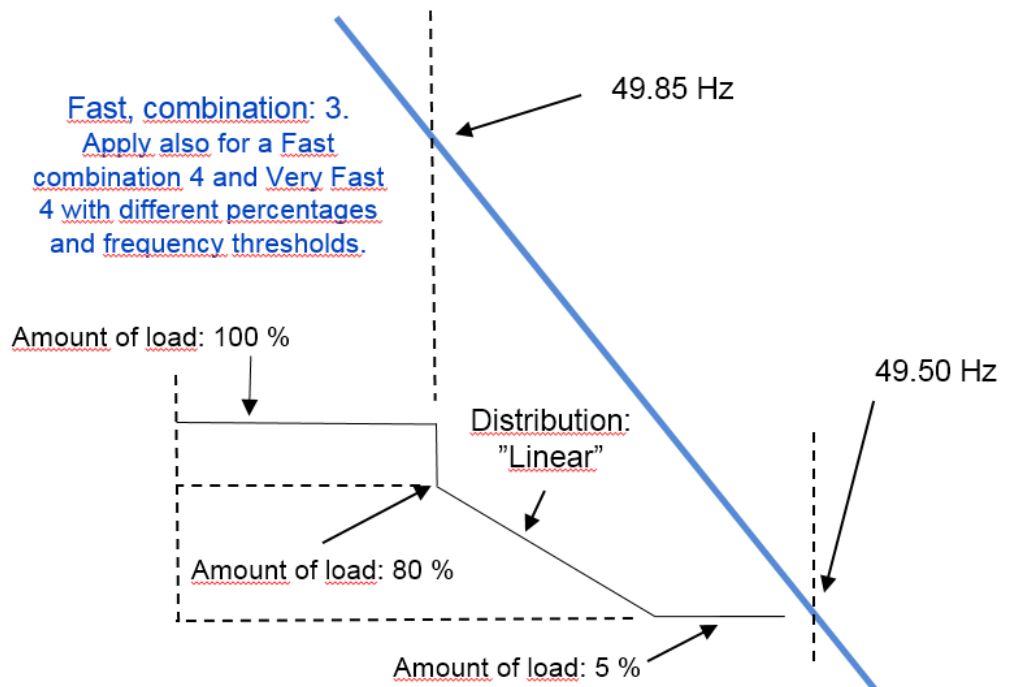


Figure 23. Load disconnection switching scheme for combinations of three and four.



The combinations that were used are summarized in the Table 4. The case numbers, 1-16, in the Table 4 are related to the Figure 24, Figure 25 and Figure 26.

Table 4. Load disconnection combinations.

Case number	Very fast	Fast
1	1	1
2	2	1
3	3	1
4	4	1
5	1	2
6	2	2
7	3	2
8	4	2
9	1	3
10	2	3
11	3	3
12	4	3
13	1	4
14	2	4
15	3	4
16	4	4

The first simulations showed that there exist only minor differences, measured as frequency minimum after the fault and production deficit as a consequence, between the combination 1/1 (Very Fast/Fast) and 3/4 (Very Fast/Fast). All the other combinations gave virtually identical results measured as frequency minimum after the fault. Based on these results, only shedding combination 1/1 was chosen for system study scenarios depicted in the chapter 5.7. This disconnection combination gives fastest response, measured based on the activation of fast reserves as a function of frequency drop, and in consequence, gave the most erroneous results in frequency measurements due to largest sudden change in the voltage angle.





5.7 Results of production loss with the different disconnection switching schemes

In Figure 24 is shown the aforementioned effect of different load disconnection schemes with different amount of fast reserves to frequency minimum. In these cases, the total kinetic energy of rotating masses is 110 GWs and rotational reserves are 1300 MW.

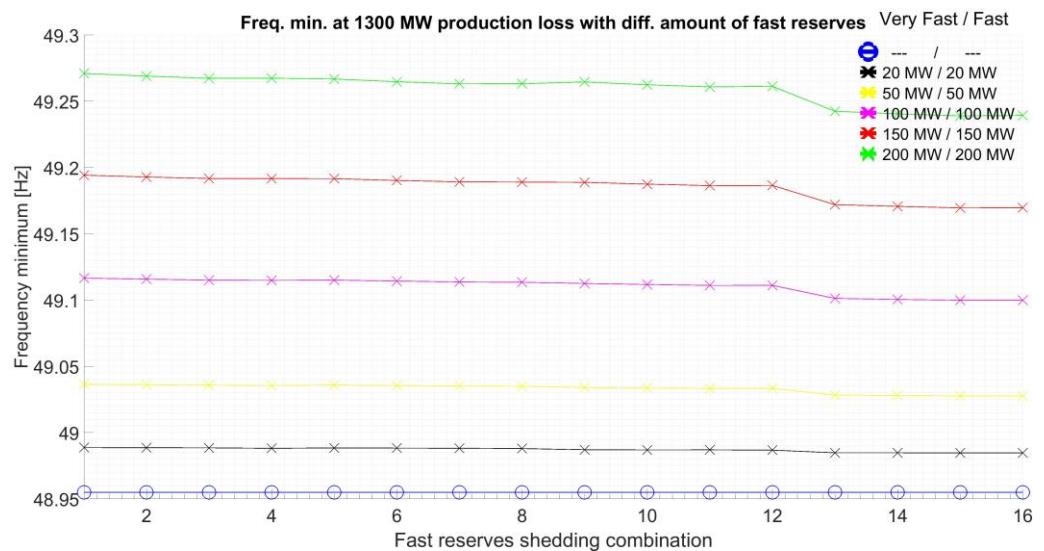


Figure 24. Frequency minimum for each switching combination of distributed fast reserves and for selected combinations of the allocated capacity: cases 20/20-200/200 MW.

Only minor differences in frequency minimum can be seen in a cases in which the load shedding type of fast reserve is at number four, i.e. the cases which numbers are 13-16, compared to all the rest of combinations, i.e. case numbers 1-12.

In Figure 25 only the case 200/200 MW is presented to show the differences more clearly.



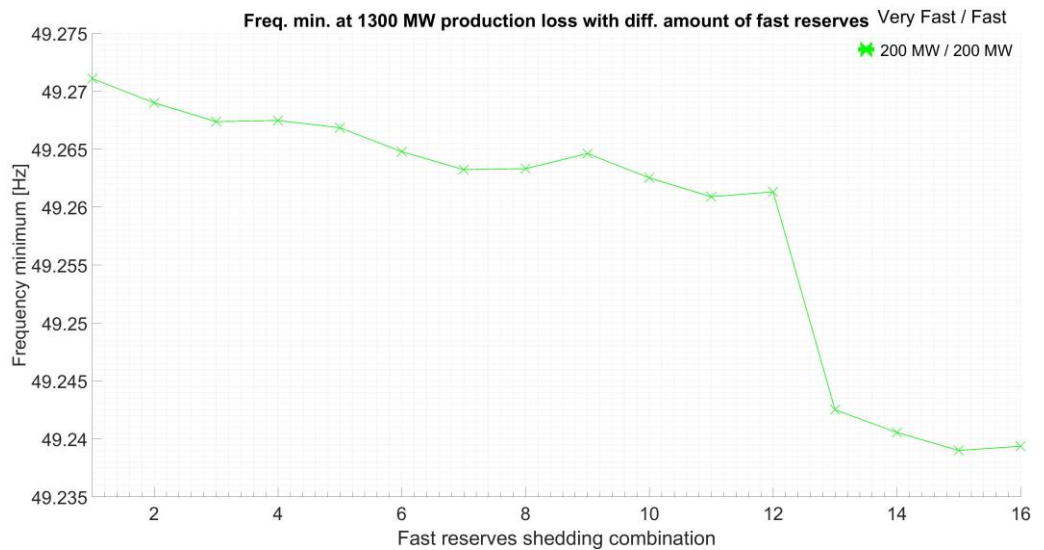


Figure 25. Frequency minimum of the case 200/200 MW from figure 24.

In Figure 26 is shown the differences if only other type of fast reserve is used in frequency restoration.

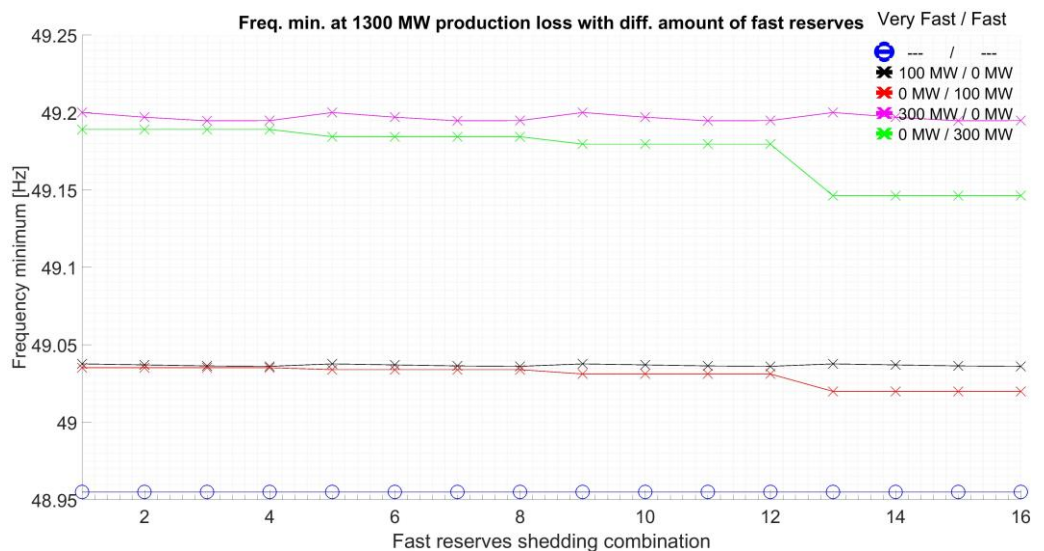


Figure 26. Frequency minimum for each switching combination of distributed fast reserves and for selected combinations of the allocated capacity: cases 100/0-0/300 MW.

5.8 Simulation principle of production loss with different amount of distributed fast reserves and rotational reserves

The length of 50 milliseconds three phase short circuit at the 400 kV bus is applied at the time of 10,1 second. Immediately after the fault is cleared, 1300 MW or 300 MW production is lost. Production lost is modelled by increasing the load by the same amount respectively via straightforward operation of circuit breaker. Frequency restoration process is accomplished together with the operation of rotational reserves and both types of distributed fast reserves all





but in reference cases. In reference cases only the rotational reserves are used in frequency restoration. The studies are performed using following three different allocations of rotating reserves (1300 MW, 750 MW and 450 MW) in order to demonstrate the effect of increasing amount of distributed fast reserves on the response of rotating reserves during frequency disturbances. Total kinetic energy of rotational masses is 110 GWs.

The frequency measurement is located at the 22 kV feeder at the same node in which both fast reserves are located. The frequency measurement method is PLL srf and based on these results the distributed fast reserves are controlled.

The rule how fast reserves could react based on PLL srf frequency measurement, measured as a time span from the beginning of fault, was 200 ms. Before that, the control of both fast reserves were locked and after the 200 ms interval, the fast reserves could react based on the frequency measurement and aforementioned load shedding rules. This “lock rule” is presented in the graphs as “Lock: 200 ms”. The control of the fast reserves were implemented in a way that when the reserves were activated at the low frequency threshold, their reconnection was prevented for the rest of the simulation.

5.8.1 110 GWs, fast reserve control based on PLL srf method – production loss 1300 MW

Total kinetic energy of the rotational masses is 110 GWs and remaining voltage is varied linearly (0-80 %) in a one simulation set (100 runs). In the first set, the production loss is set to 1300 MW in order to study underfrequency situations.

First set is the reference case (no fast reserves) and after that the following combinations of distribute very fast / fast – rotational reserves as is shown in set two to seven:

1. – MW / -- MW – 1300 MW
2. 150 MW / 50 MW – 1300 MW
3. 50 MW / 150 MW – 1300 MW
4. 450 MW / 150 MW – 750 MW
5. 150 MW / 450 MW – 750 MW
6. 750 MW / 250 MW – 450 MW
7. 250 MW / 750 MW – 450 MW





5.8.2 110 GWs, fast reserve control based on PLL srf method – production loss 300 MW

These studies are similar in all parts expect for amount of the production loss. The production loss was set to a level of 300 MW in order to study possible overfrequency situations. Also, the combinations of 150 MW / 50 MW and 50 MW / 150 MW are left out because the main interest was to study situations in which overfrequencies are at the maximum.

5.9 Results of production loss with different amount of distributed fast reserves and rotational reserves

The next chapters are labeled by the key parameters of each case. First parameter is the kinetic energy of all rotational masses. Second is the amount of rotational reserves measured as active power. Third and fourth are the amounts of very fast and fast reserves and the last one is the parameter in which change within the case. In the first set is shown remaining voltage as a function of all the runs. After that the next four figures are labeled. The four figures in the other sets after the first set have similar figures and in same order so the labels here are omitted.

In Figure 27 is shown how the remaining voltage change from the first run to the last as in previous cases. The remaining voltage varies in a same manner in reference case and the study cases two to seven.

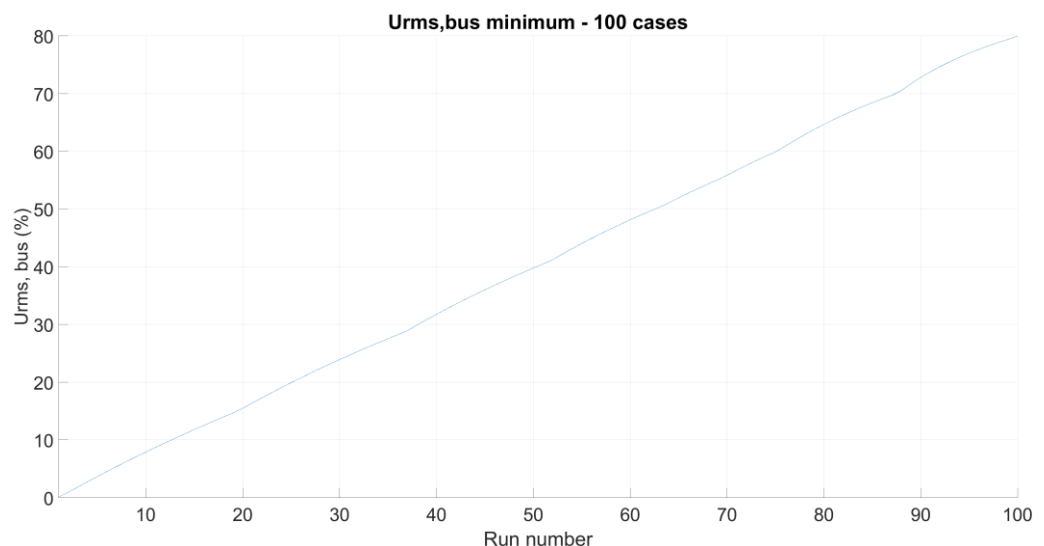


Figure 27. Remaining voltage of the cases depicted from 5.9.1 to 5.9.7.

5.9.1 Reference case – 110 GWs, 1300 MW, no fast reserves

In Figure 28 is shown the frequency minimum measured by PLL srf without any fast reserves as the function of the time. Remaining voltage is as a parameter.



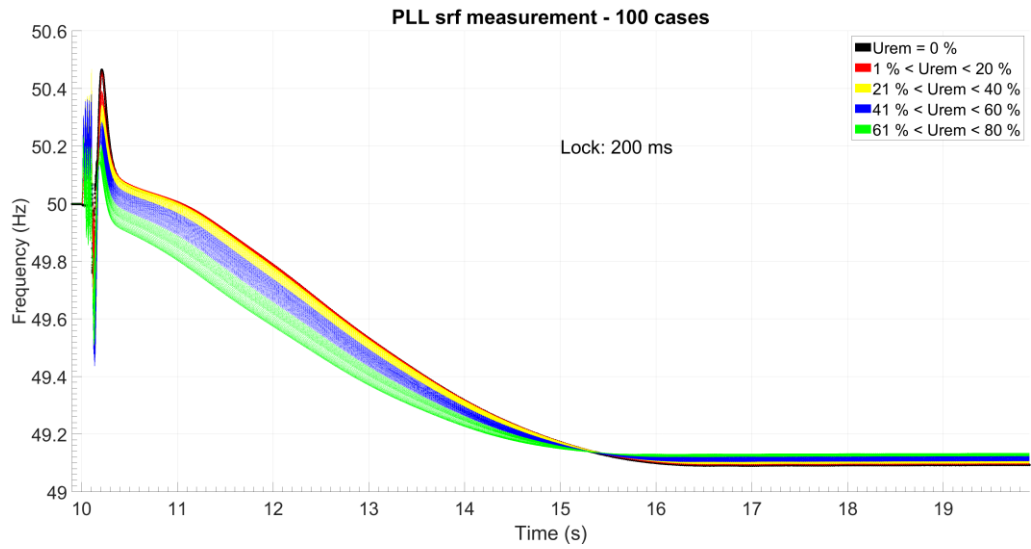


Figure 28. Frequency minimum measured by PLL srf without any distributed fast reserves and 1300 MW rotational reserves.

In Figure 29 is shown the load disconnection pattern of the distributed fast reserves as a function of time. In the reference case the fast reserves are both zero.

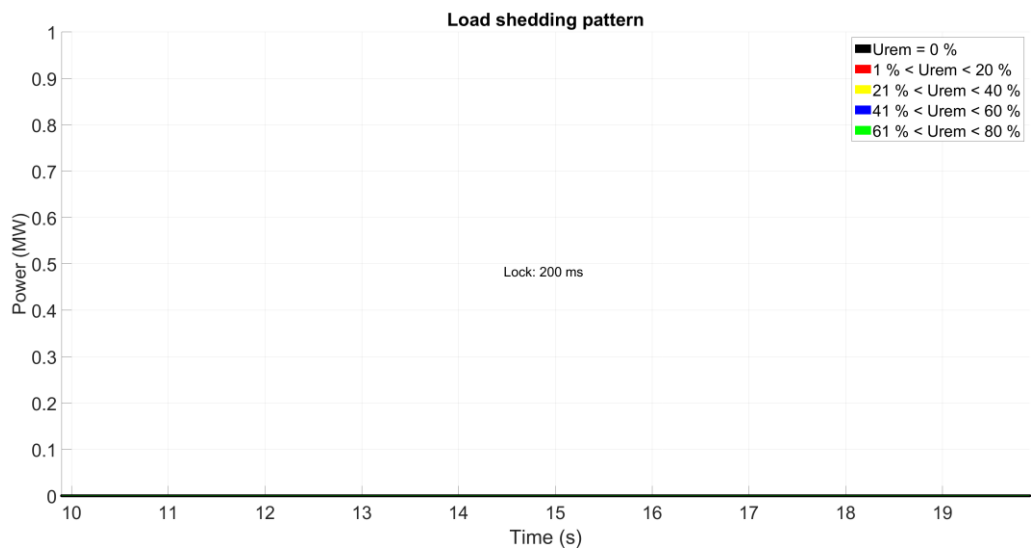


Figure 29. Load disconnection pattern of distributed fast reserves.

In Figure 30 is shown the system frequency derived directly from the rotational speed of the biggest generator.



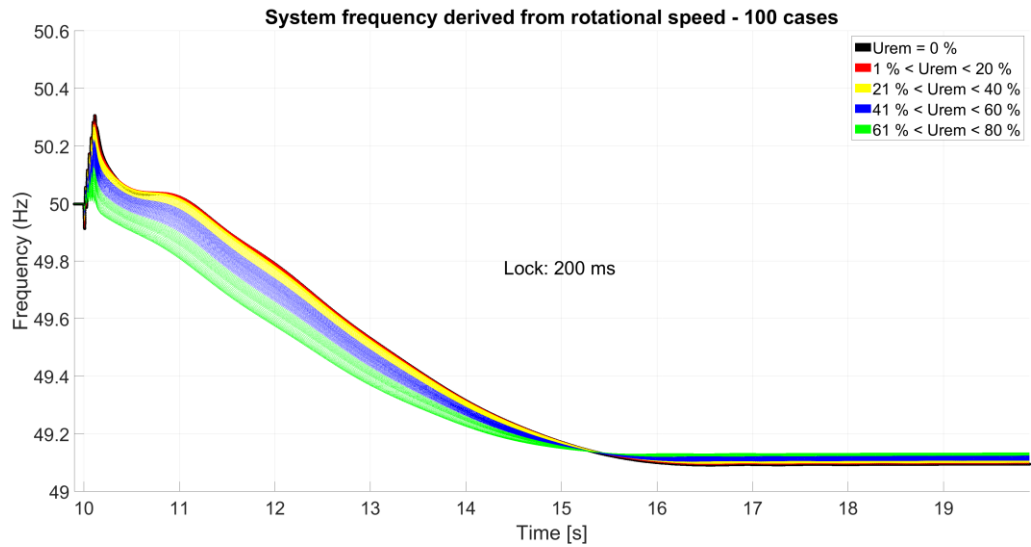


Figure 30. System frequency derived directly from the rotational speed of the biggest generator.

In Figure 31 is shown the output power of the generator equipped with turbine speed control.

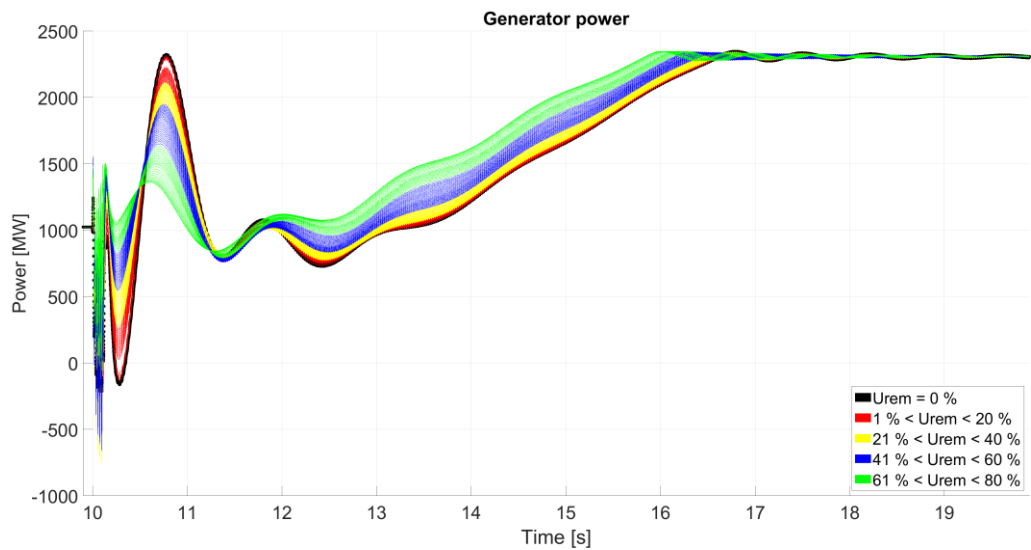


Figure 31. Output power of the generator equipped with turbine speed control.

5.9.2 110 GWs, 1300 MW, 150 MW / 50 MW

Figure 32, Figure 33, Figure 34 and Figure 35 show frequency minimum measured by PLL srf, load disconnection pattern of the distributed fast reserves, system frequency derived directly from the rotational speed of the biggest generator and output power of the generator equipped with turbine speed control respectively.



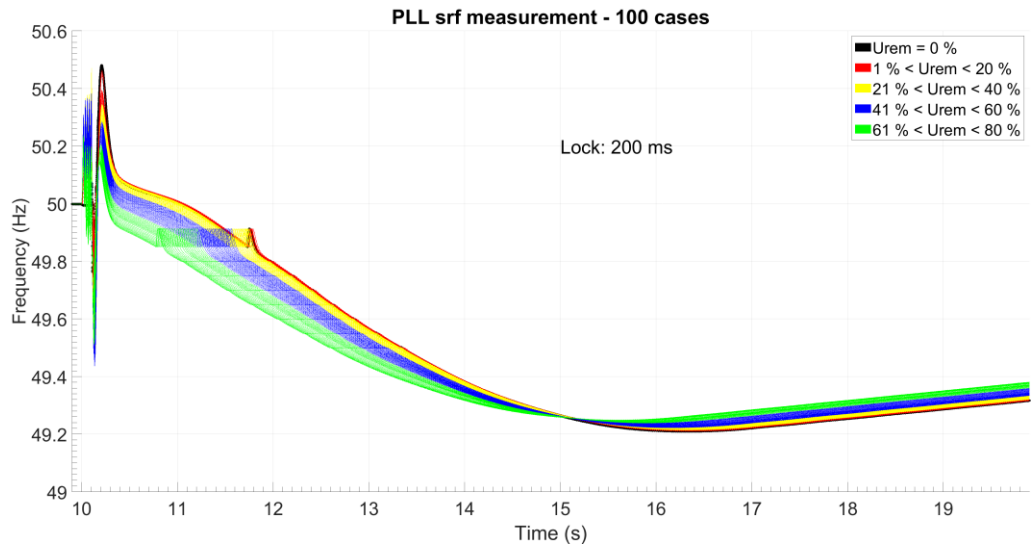


Figure 32. Frequency minimum measured by PLL srf with 150 MW / 50 MW distributed fast reserves and 1300 MW rotational reserves.

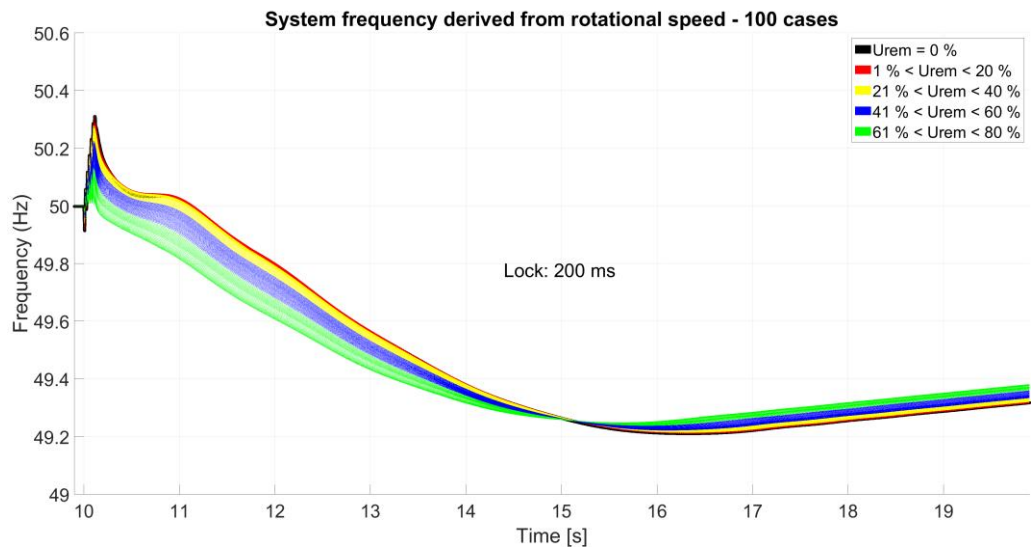


Figure 33. System frequency derived directly from the rotational speed of the biggest generator.



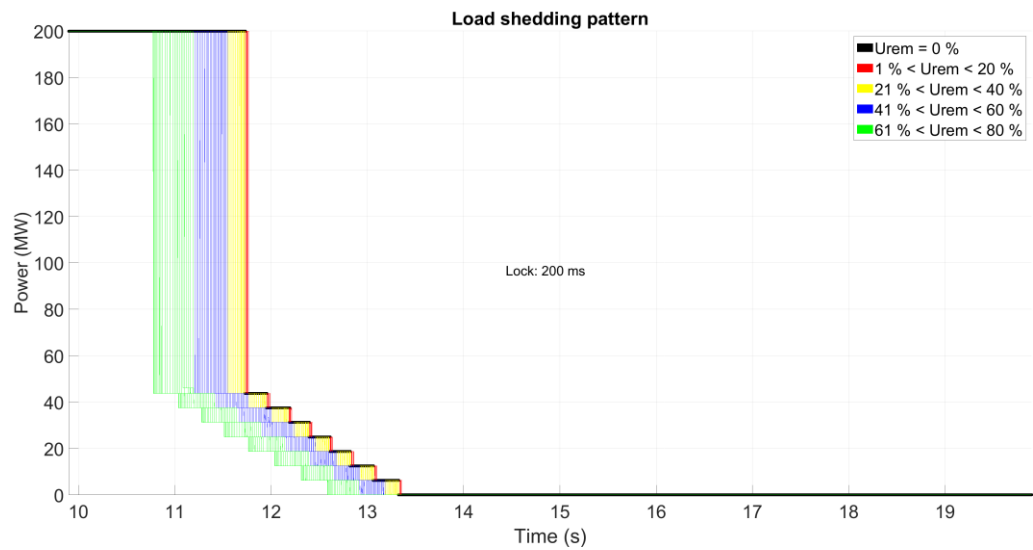


Figure 34. Load disconnection pattern of distributed fast reserves.

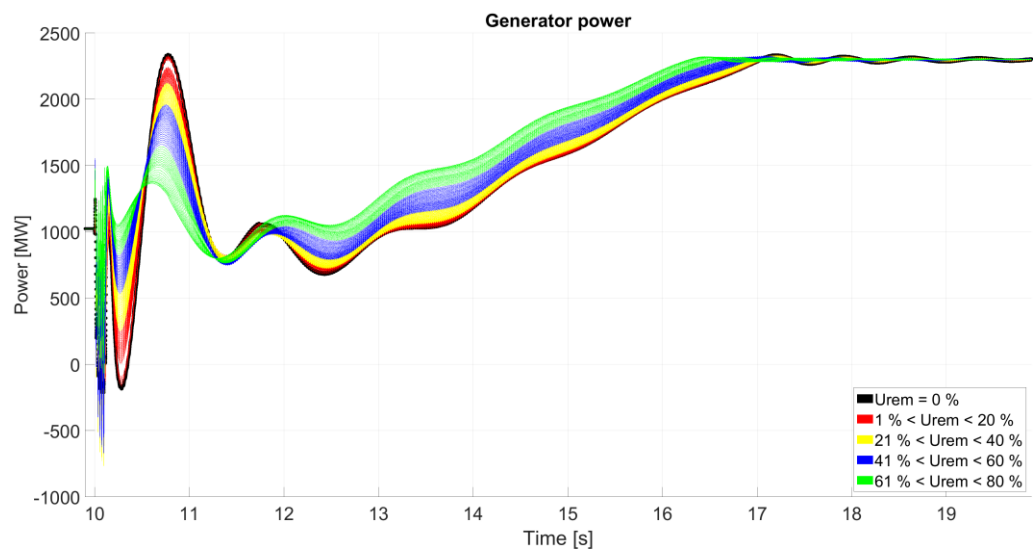


Figure 35. Output power of the generator equipped with turbine speed control.

5.9.3 110 GWs, 1300 MW, 50 MW / 150 MW

Figure 36, Figure 37, Figure 38 and Figure 39 show frequency minimum measured by PLL srf, load disconnection pattern of the distributed fast reserves, system frequency derived directly from the rotational speed of the biggest generator and output power of the generator equipped with turbine speed control respectively.



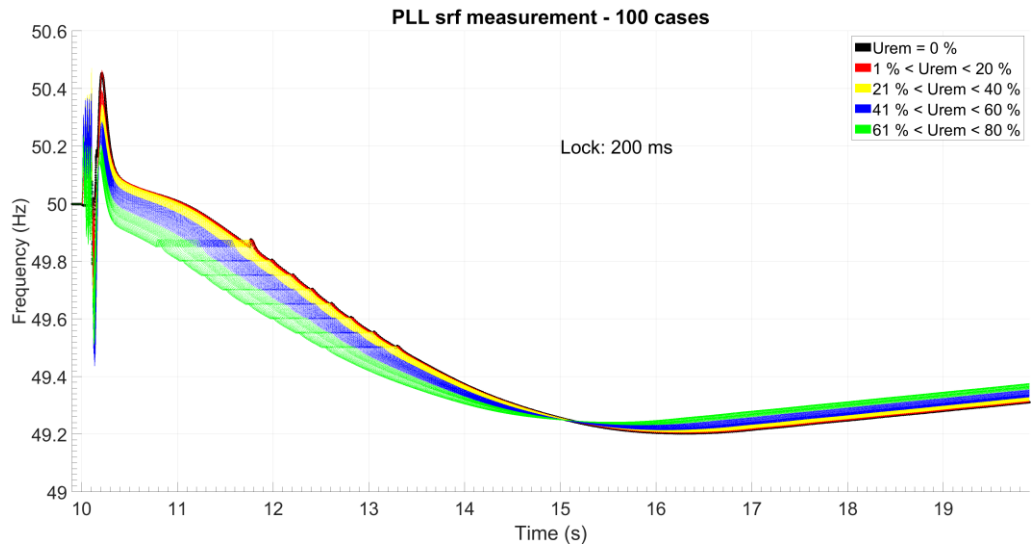


Figure 36. Frequency minimum measured by PLL srf with 50 MW / 150 MW distributed fast reserves and 1300 MW rotational reserves.

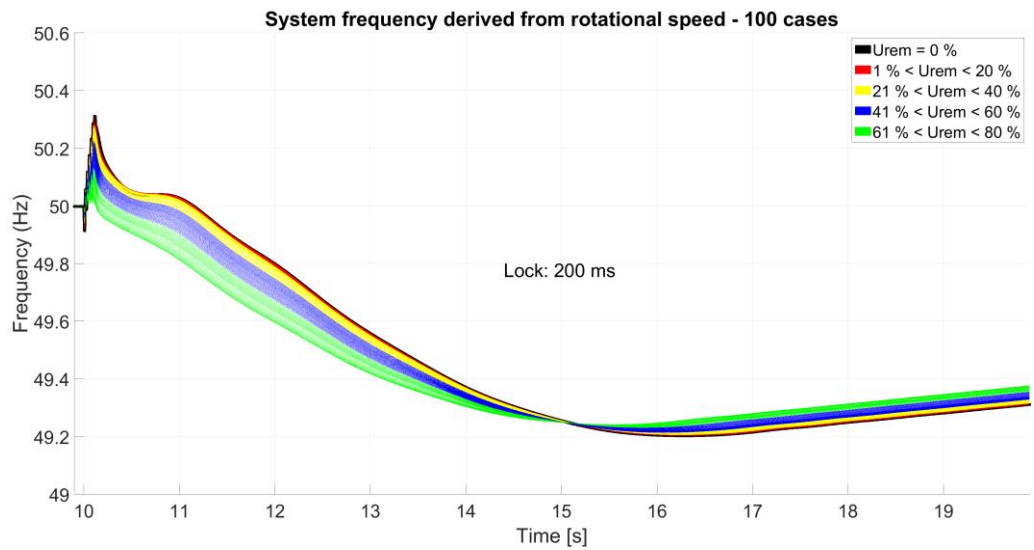


Figure 37. System frequency derived directly from the rotational speed of the biggest generator.



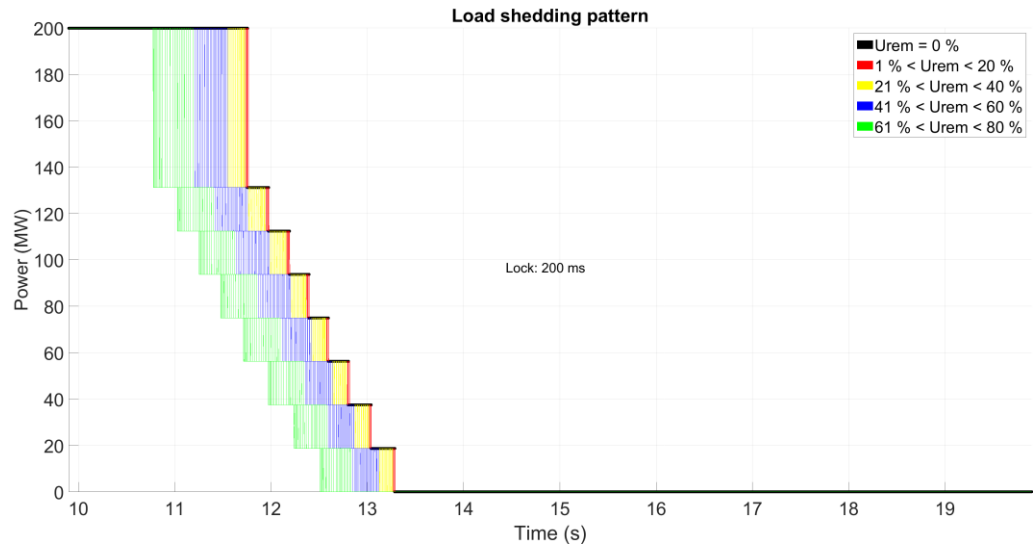


Figure 38. Load disconnection pattern of distributed fast reserves.

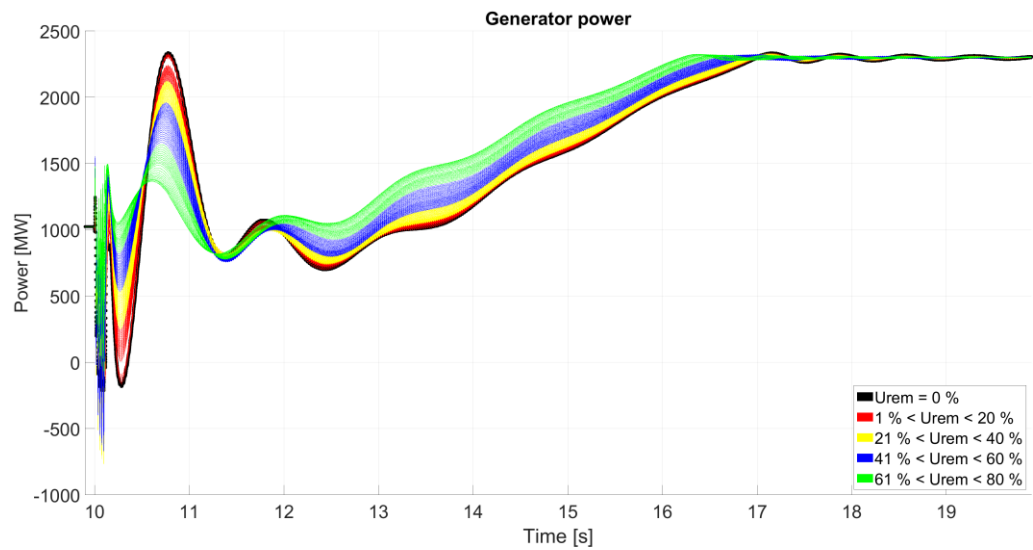


Figure 39. Output power of the generator equipped with turbine speed control.

5.9.4 110 GWs, 750 MW, 450 MW / 150 MW

Figure 40, Figure 41, Figure 42 and Figure 43 show frequency minimum measured by PLL srf, load disconnection pattern of the distributed fast reserves, system frequency derived directly from the rotational speed of the biggest generator and output power of the generator equipped with turbine speed control respectively.



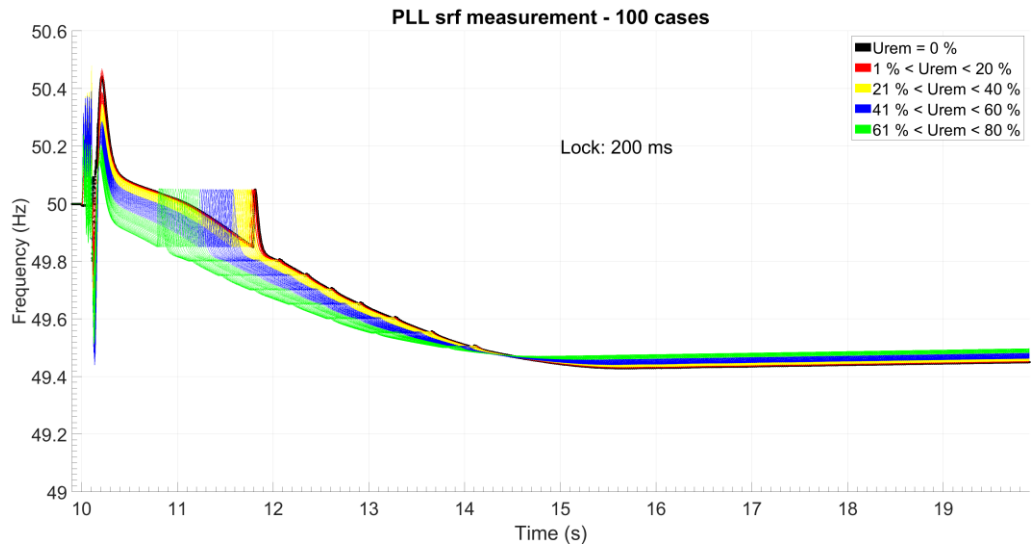


Figure 40. Frequency minimum measured by PLL srf with 450 MW / 150 MW distributed fast reserves and 750 MW rotational reserves.

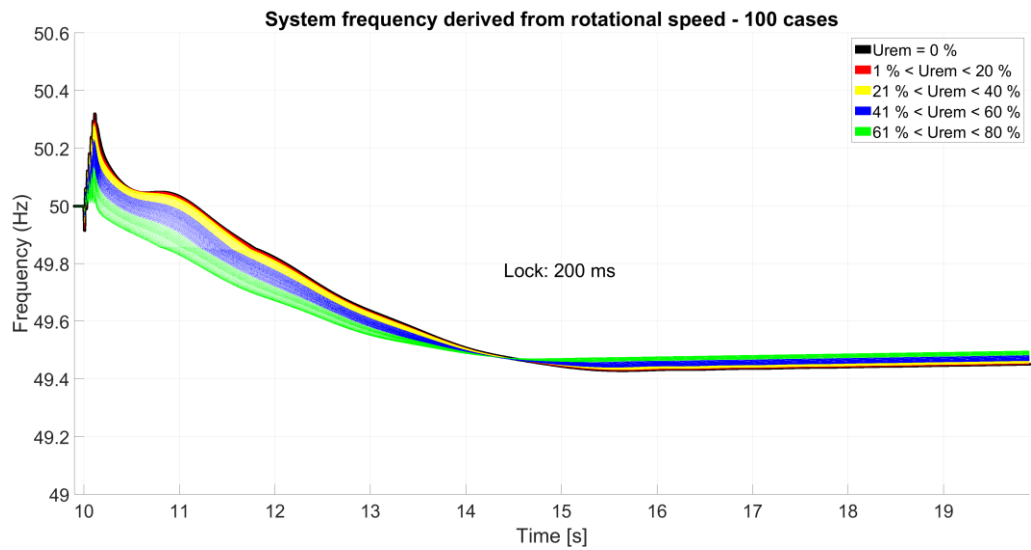


Figure 41. System frequency derived directly from the rotational speed of the biggest generator.



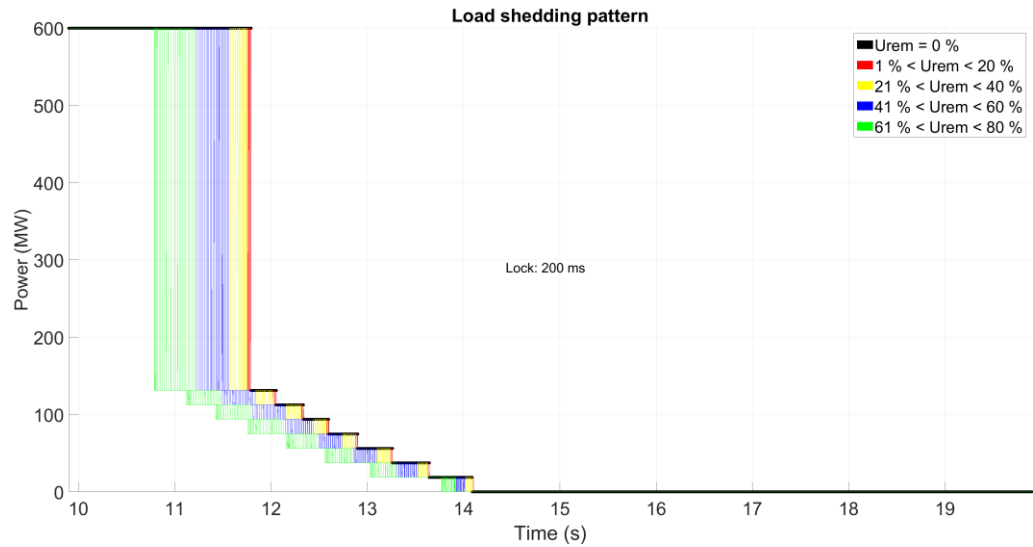


Figure 42. Load disconnection pattern of distributed fast reserves.

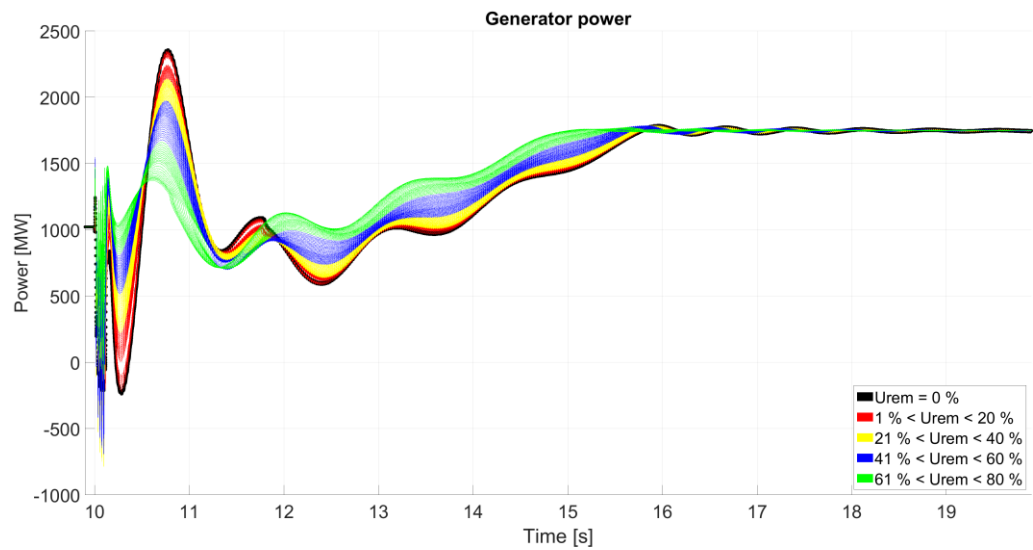


Figure 43. Output power of the generator equipped with turbine speed control.

5.9.5 110 GWs, 750 MW, 150 MW / 450 MW

Figure 44, Figure 45, Figure 46 and Figure 47 show frequency minimum measured by PLL srf, load disconnection pattern of the distributed fast reserves, system frequency derived directly from the rotational speed of the biggest generator and output power of the generator equipped with turbine speed control respectively.



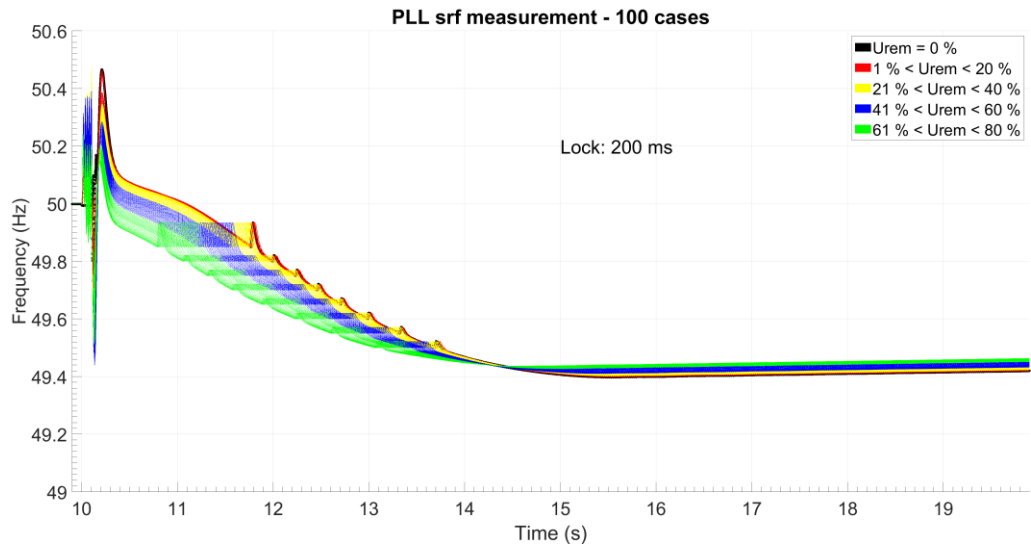


Figure 44. Frequency minimum measured by PLL srf with 150 MW / 450 MW distributed fast reserves and 750 MW rotational reserves.

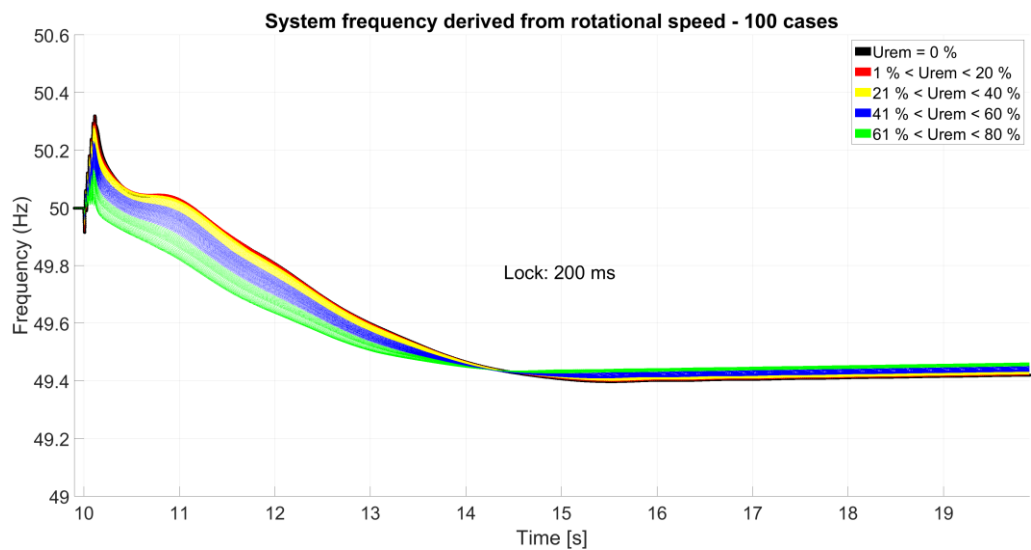


Figure 45. System frequency derived directly from the rotational speed of the biggest generator.



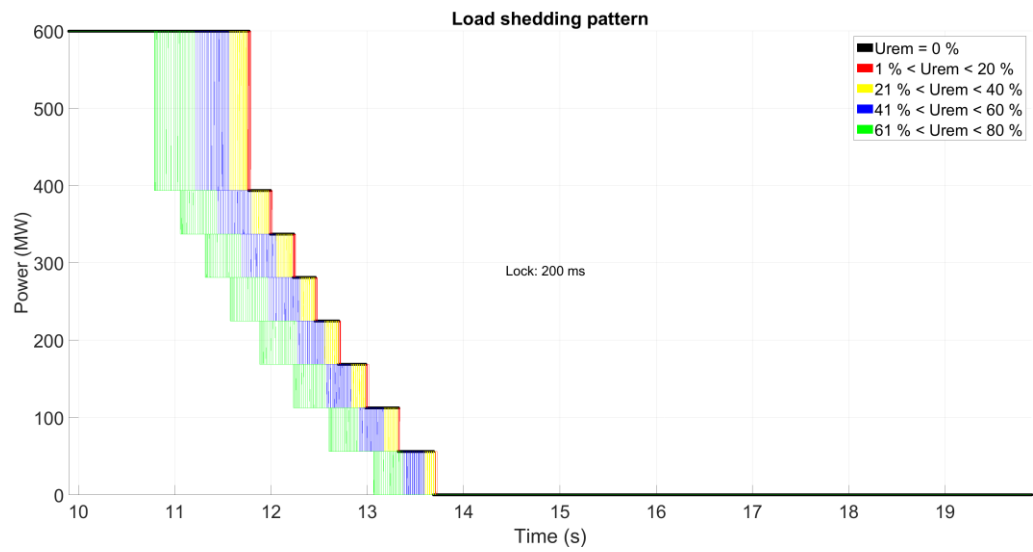


Figure 46. Load disconnection pattern of distributed fast reserves.

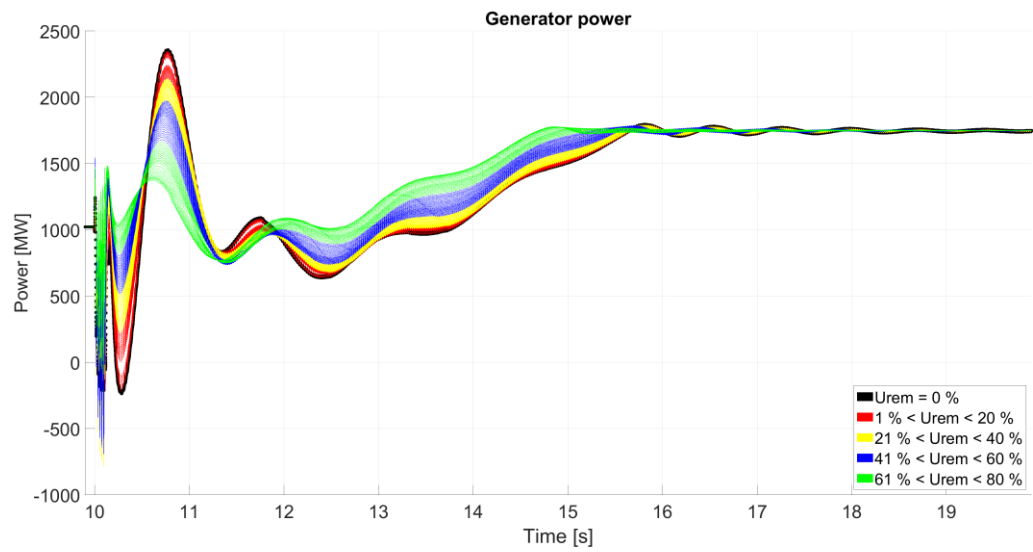


Figure 47. Output power of the generator equipped with turbine speed control.





5.9.6 110 GWs, 450 MW, 750 MW / 250 MW

Figure 48, Figure 49, Figure 50 and Figure 51 show frequency minimum measured by PLL srf, load disconnection pattern of the distributed fast reserves, system frequency derived directly from the rotational speed of the biggest generator and output power of the generator equipped with turbine speed control respectively.

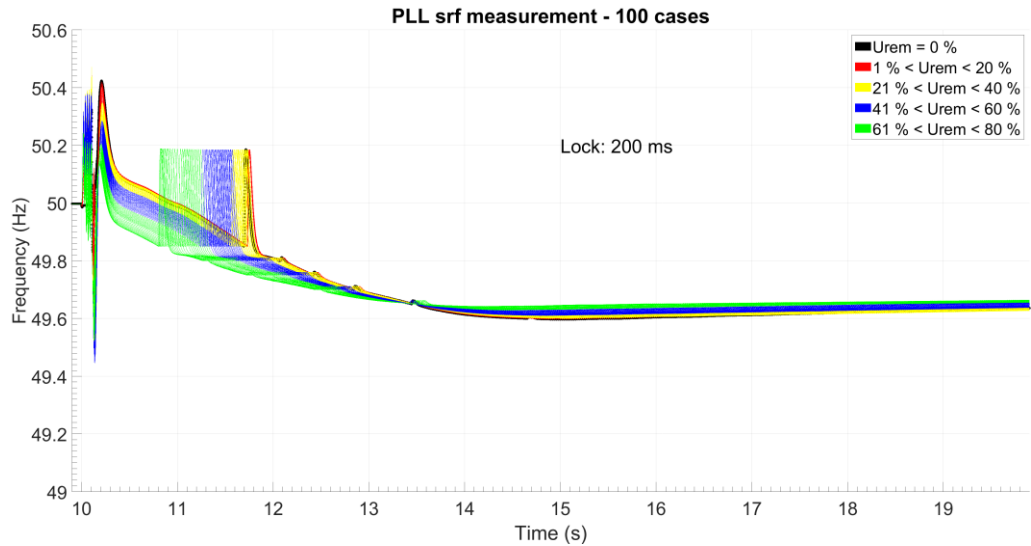


Figure 48. Frequency minimum measured by PLL srf with 750 MW / 250 MW distributed fast reserves and 450 MW rotational reserves.

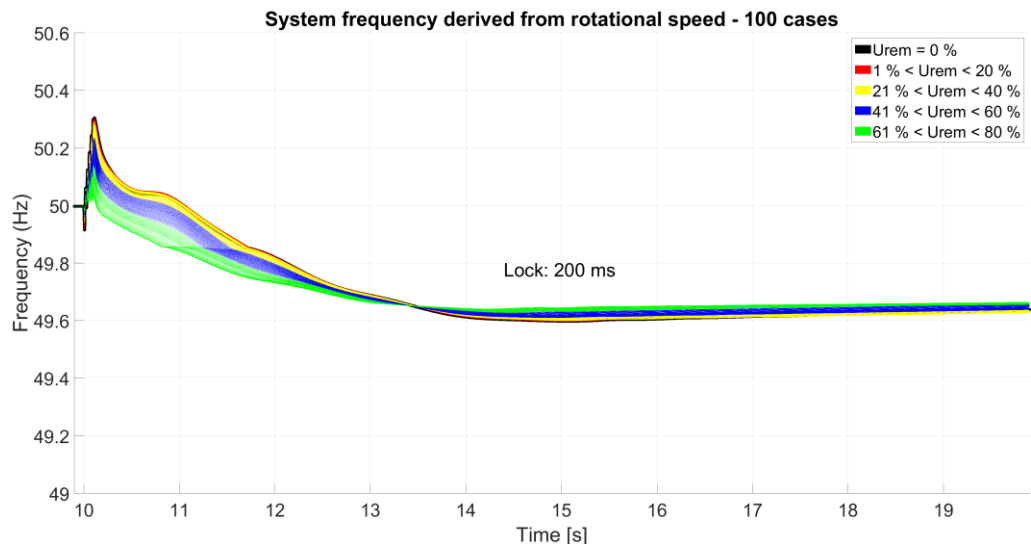


Figure 49. System frequency derived directly from the rotational speed of the biggest generator.



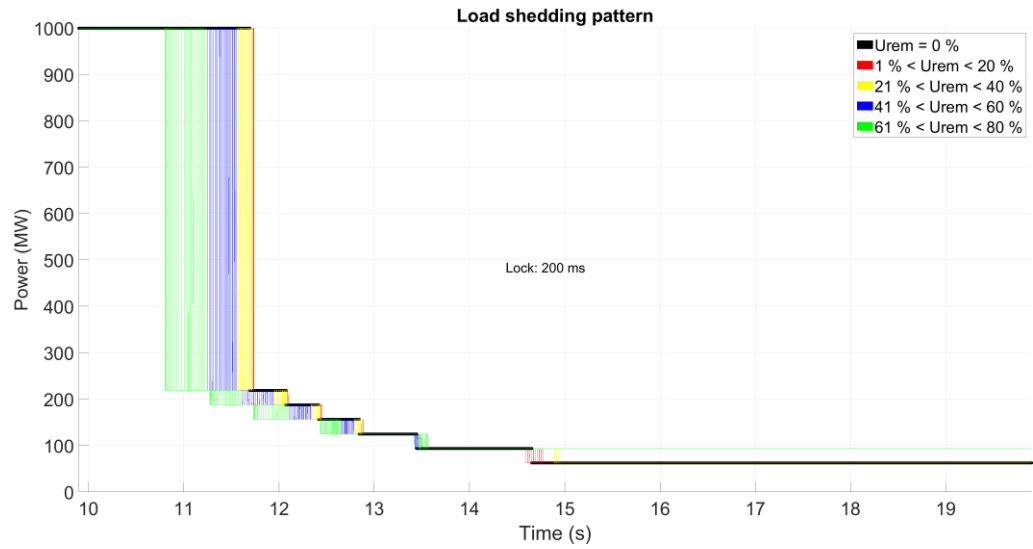


Figure 50. Load disconnection pattern of distributed fast reserves.

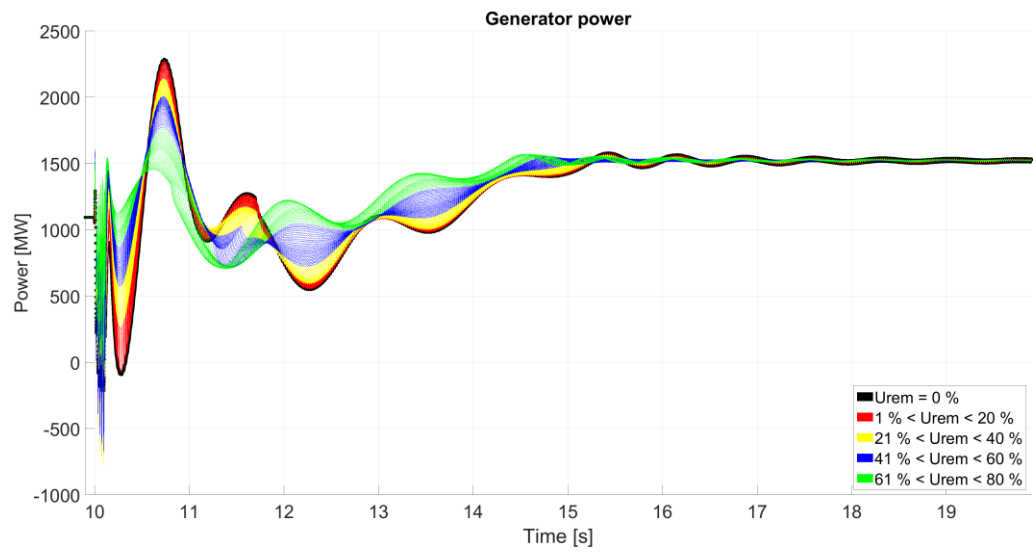


Figure 51. Output power of the generator equipped with turbine speed control.





5.9.7 110 GWs, 450 MW, 250 MW / 750 MW

Figure 52, Figure 53, Figure 54 and Figure 55 show frequency minimum measured by PLL srf, load disconnection pattern of the distributed fast reserves, system frequency derived directly from the rotational speed of the biggest generator and output power of the generator equipped with turbine speed control respectively.

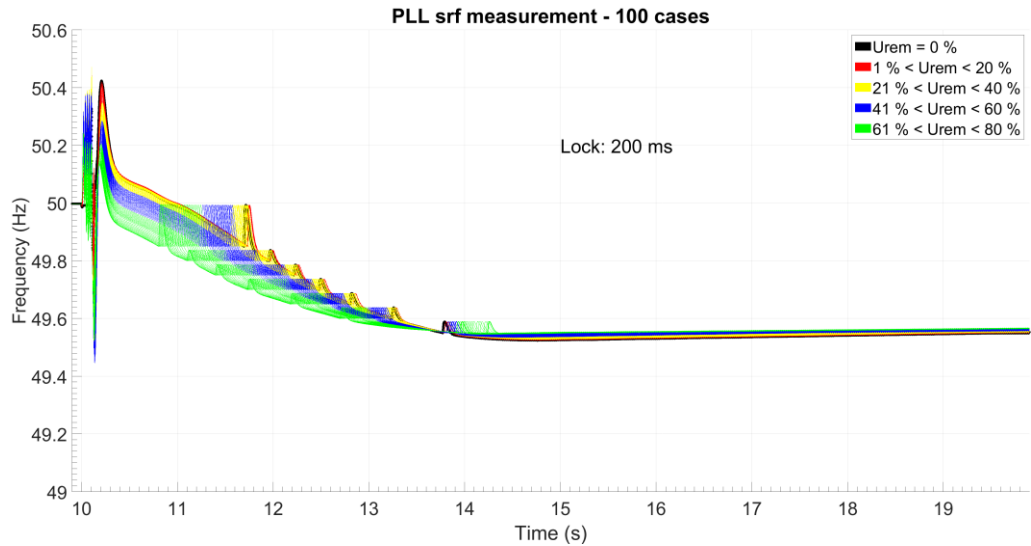


Figure 52. Frequency minimum measured by PLL srf with 250 MW / 750 MW distributed fast reserves and 450 MW rotational reserves.

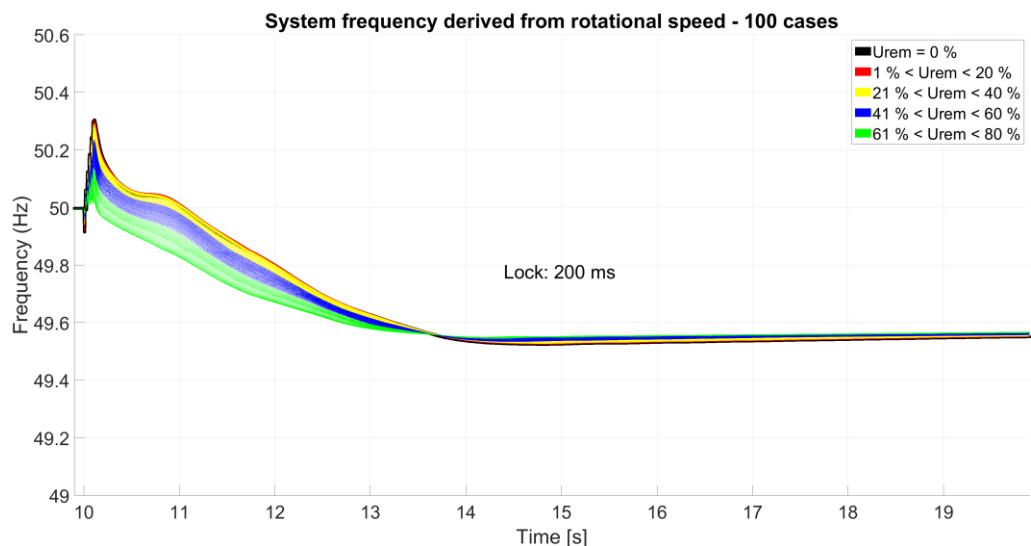


Figure 53. System frequency derived directly from the rotational speed of the biggest generator.



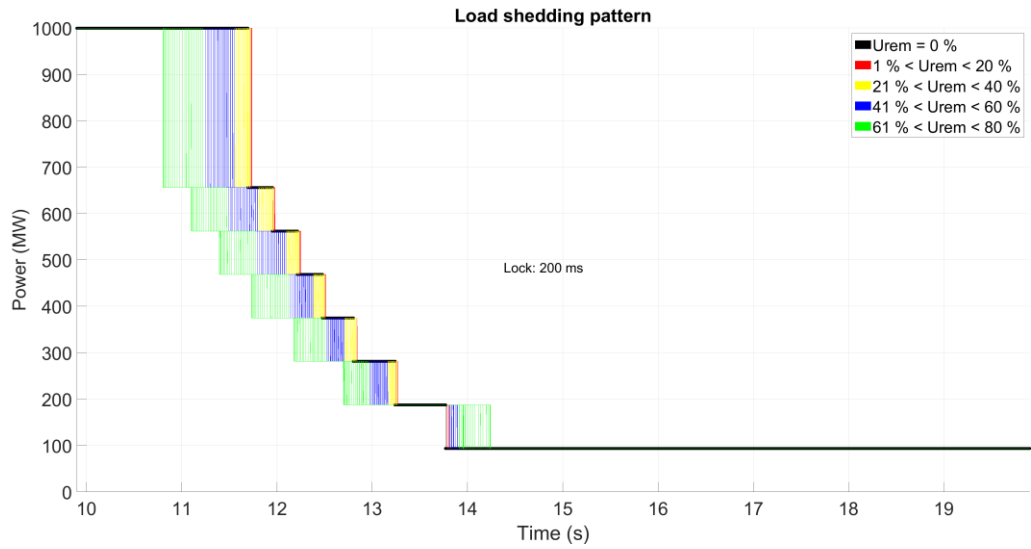


Figure 54. Load disconnection pattern of distributed fast reserves.

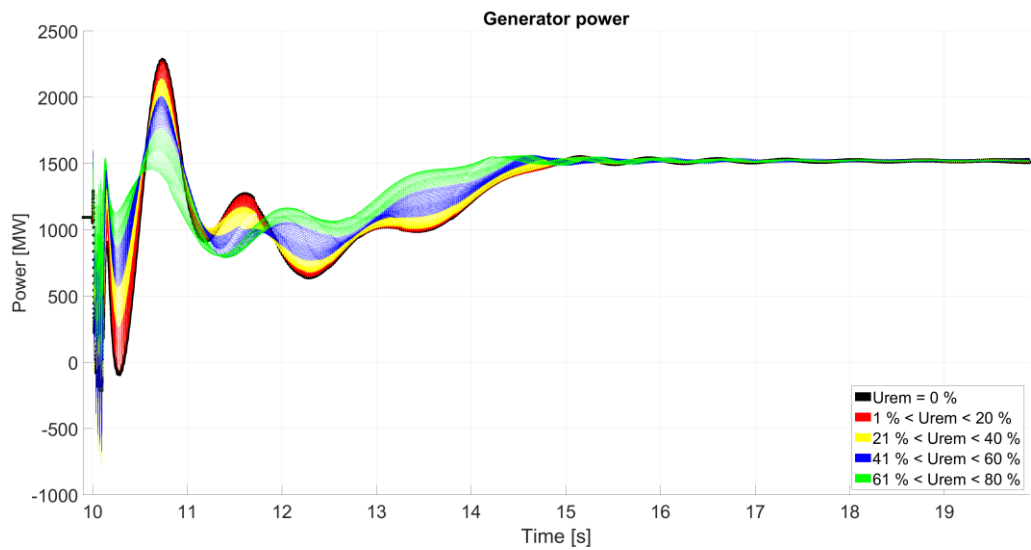


Figure 55. Output power of the generator equipped with turbine speed control.





5.9.7.1 Summarizing graphs of 1300 MW production loss

In Figure 56 and Figure 57 frequency minimum and the time when frequency minimum is reached, are summarized.

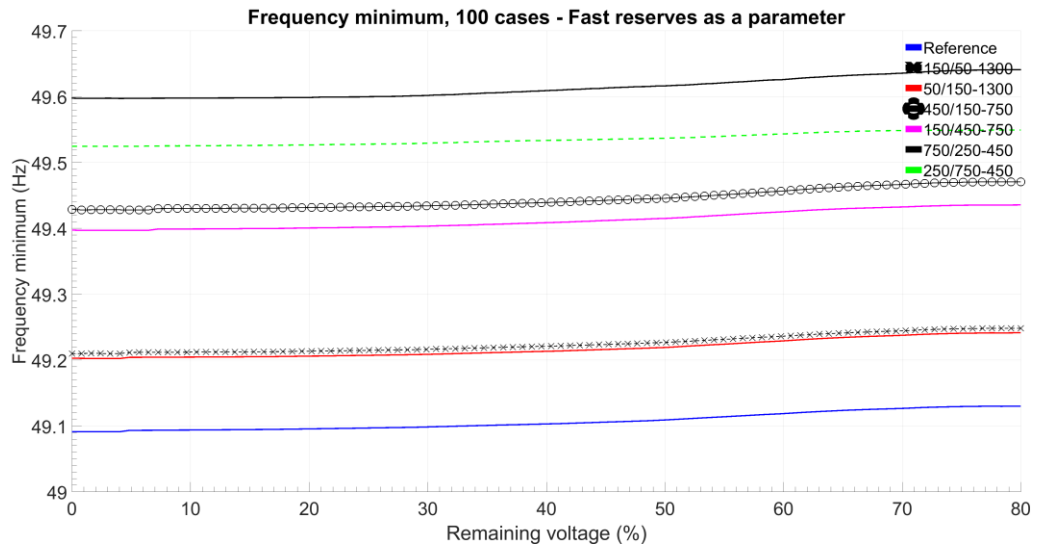


Figure 56. Frequency minimum of different amount of distributed fast reserves with a production loss of 1300 MW.

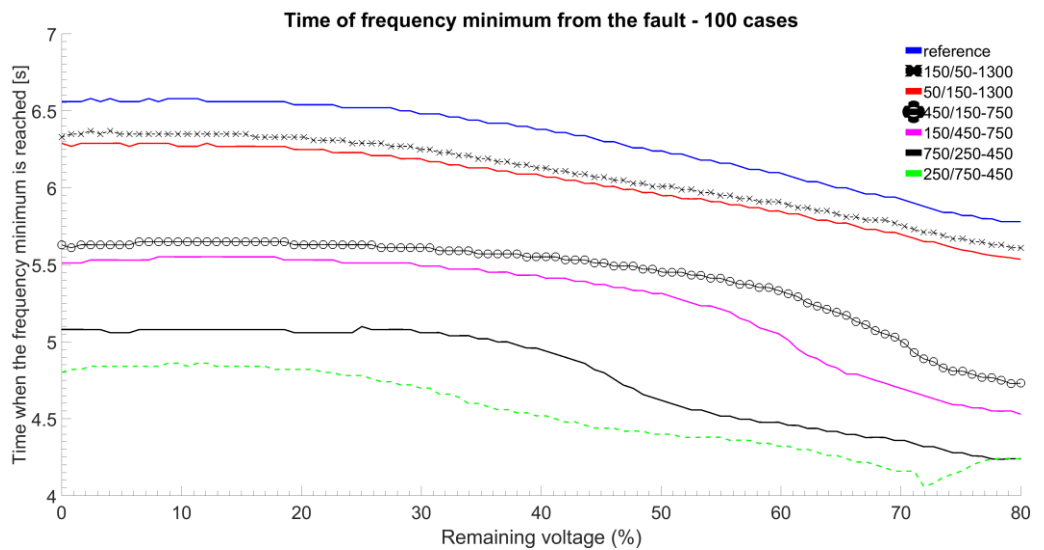


Figure 57. Time of frequency minimum of different amount of distributed fast reserves with a production loss of 1300 MW.





5.9.8 Reference case - 110 GWs, 300 MW, no fast reserves

Figure 58, Figure 59, Figure 60 and Figure 61 show frequency minimum measured by PLL srf, load disconnection pattern of the distributed fast reserves, system frequency derived directly from the rotational speed of the biggest generator and output power of the generator equipped with turbine speed control respectively.

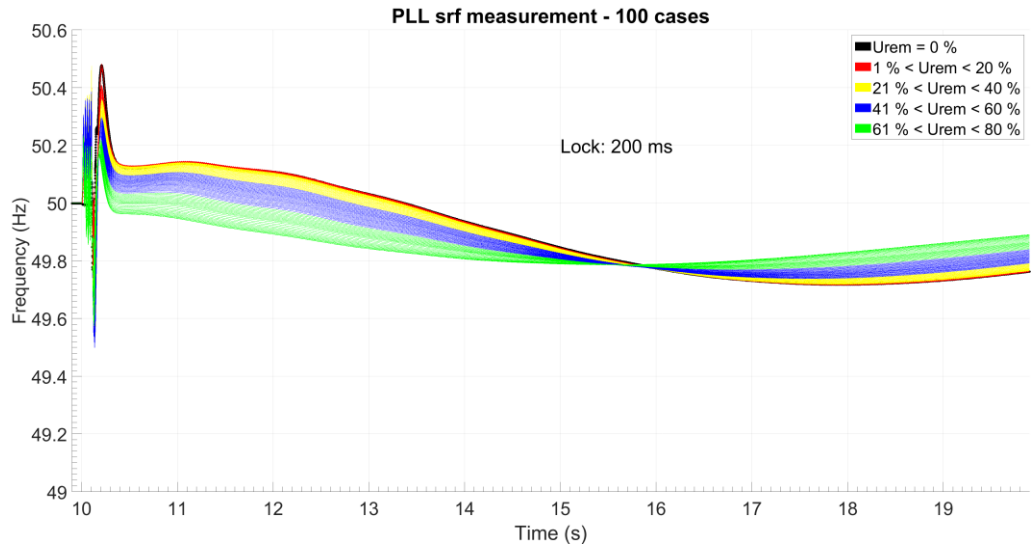


Figure 58. Frequency minimum measured by PLL srf without any distributed fast reserves and 300 MW rotational reserves.

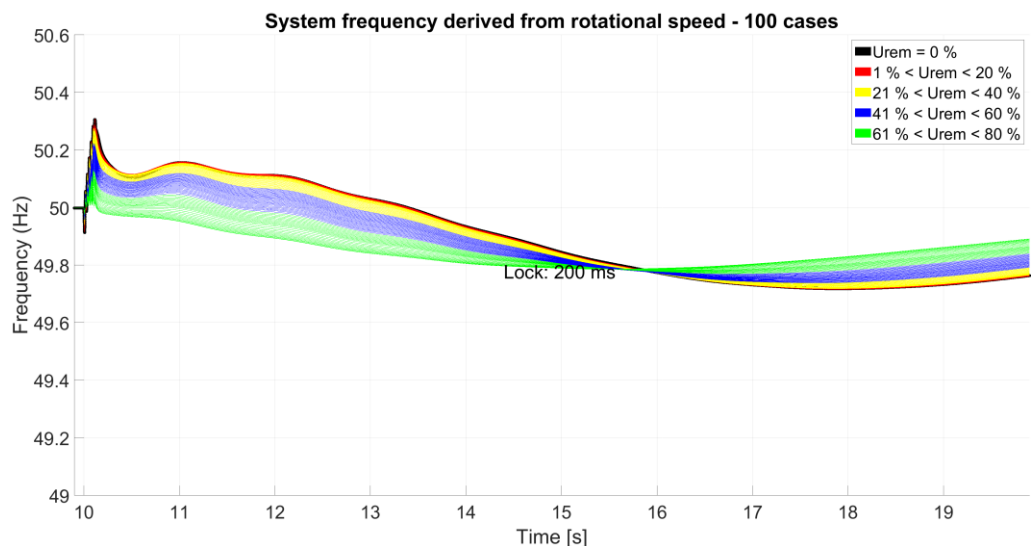


Figure 59. System frequency derived directly from the rotational speed of the biggest generator.



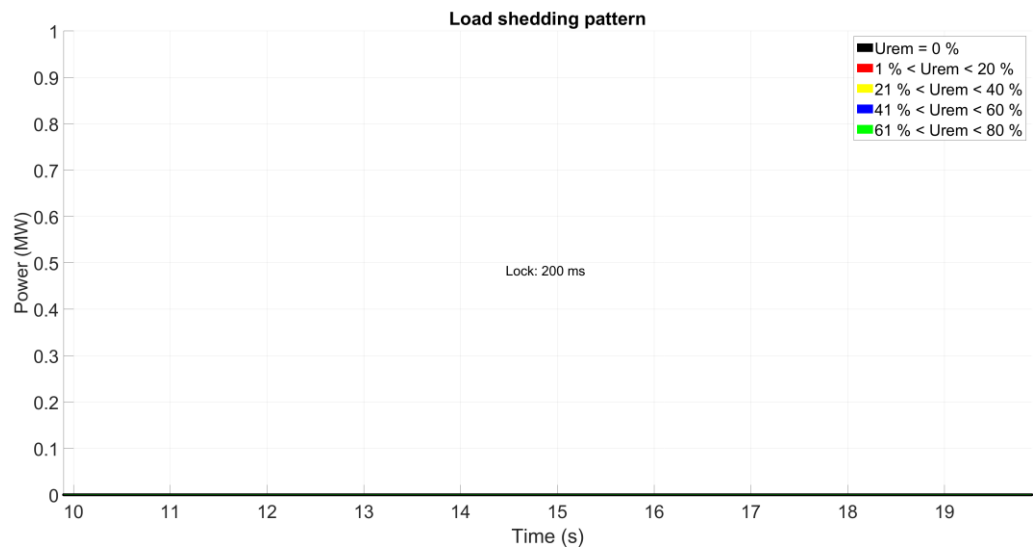


Figure 60. Load disconnection pattern of distributed fast reserves.

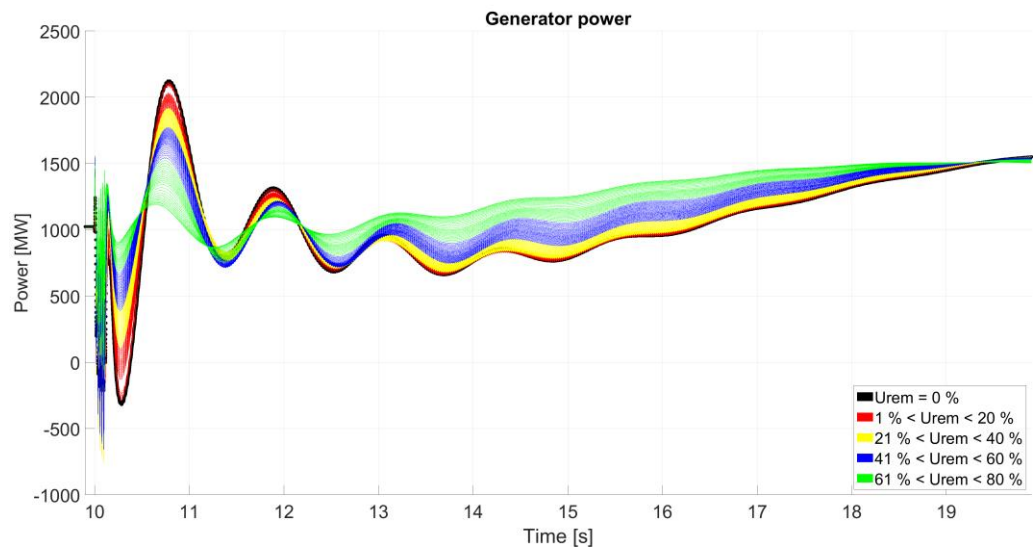


Figure 61. Output power of the generator equipped with turbine speed control.





5.9.9 110 GWs, 300 MW, 450 MW / 150 MW

Figure 62, Figure 63, Figure 64 and Figure 65 show frequency minimum measured by PLL srf, load disconnection pattern of the distributed fast reserves, system frequency derived directly from the rotational speed of the biggest generator and output power of the generator equipped with turbine speed control respectively.

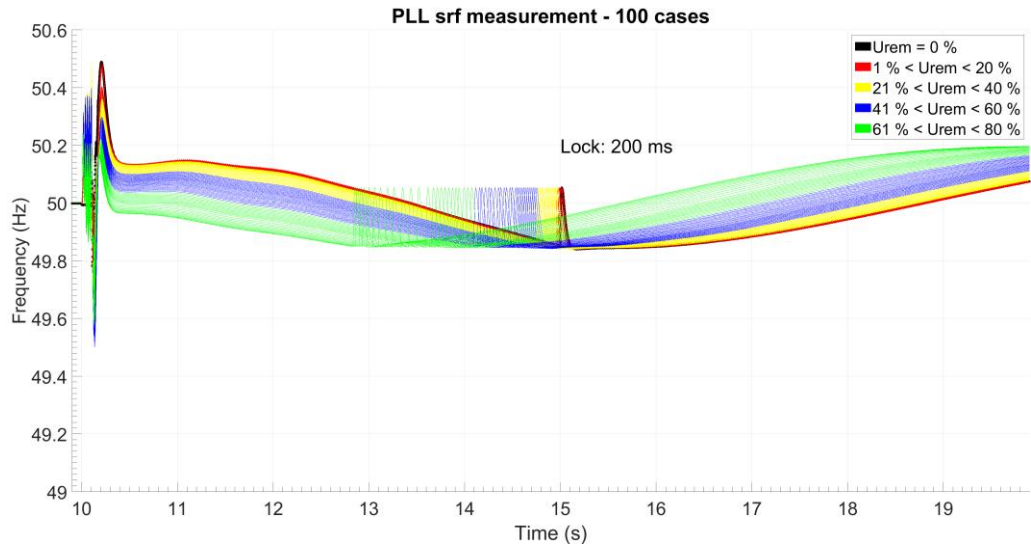


Figure 62. Frequency minimum measured by PLL srf with 450 MW / 150 MW distributed fast reserves and 300 MW rotational reserves.

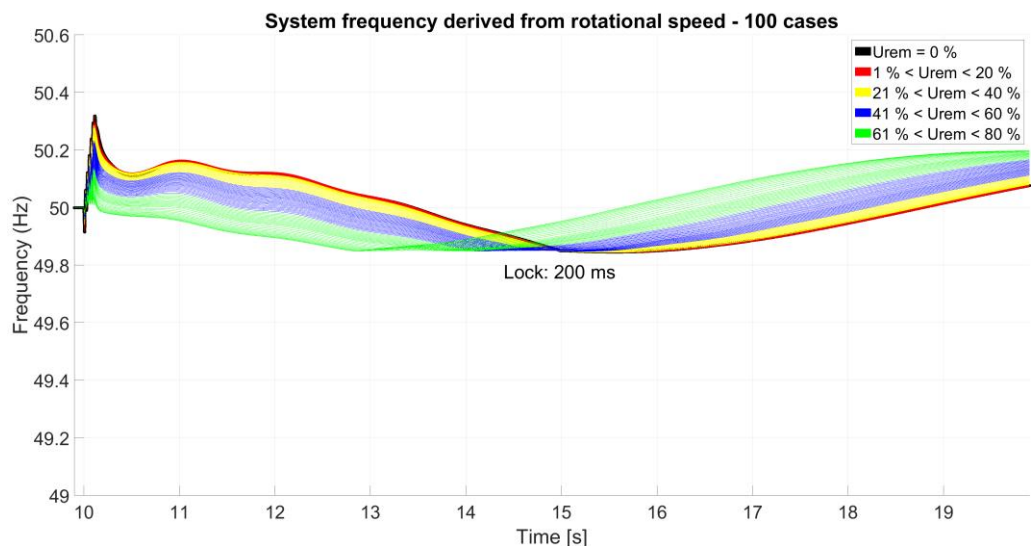


Figure 63. System frequency derived directly from the rotational speed of the biggest generator.



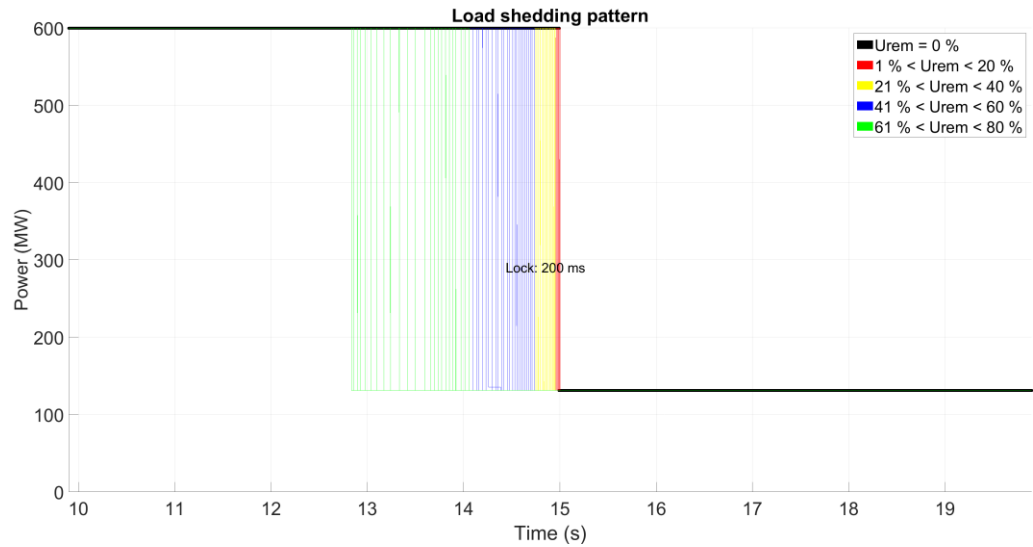


Figure 64. Load disconnection pattern of distributed fast reserves.

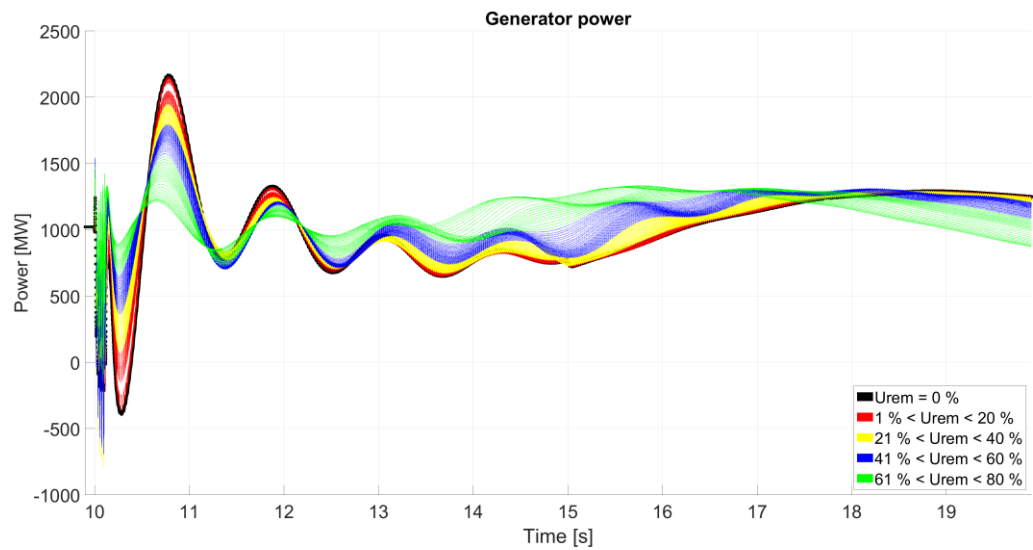


Figure 65. Output power of the generator equipped with turbine speed control.

5.9.10 110 GWs, 300 MW, 150 MW / 450 MW

Figure 66, Figure 67, Figure 68, Figure 69 show frequency minimum measured by PLL srf, load disconnection pattern of the distributed fast reserves, system frequency derived directly from the rotational speed of the biggest generator and output power of the generator equipped with turbine speed control respectively.



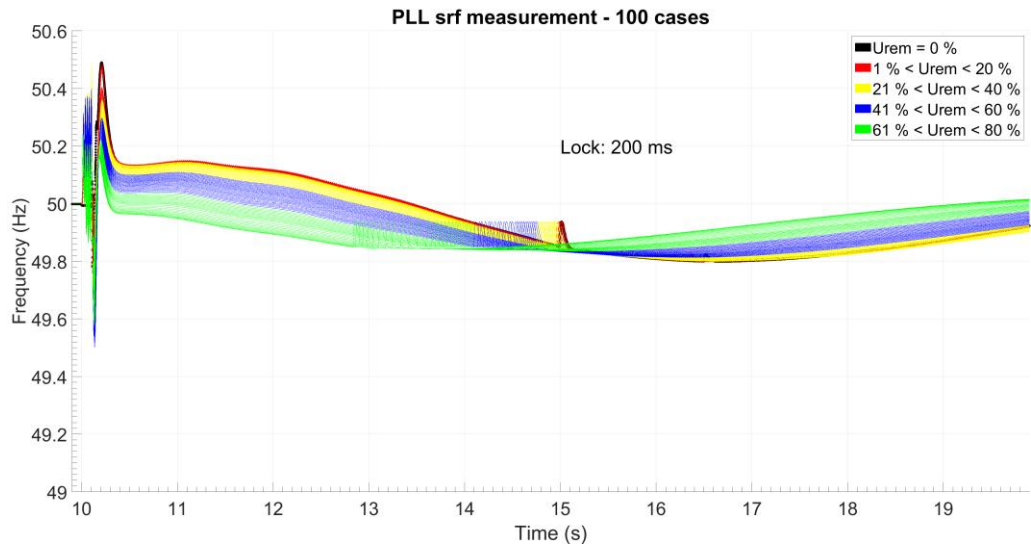


Figure 66. Frequency minimum measured by PLL srf with 150 MW / 450 MW distributed fast reserves and 300 MW rotational reserves.

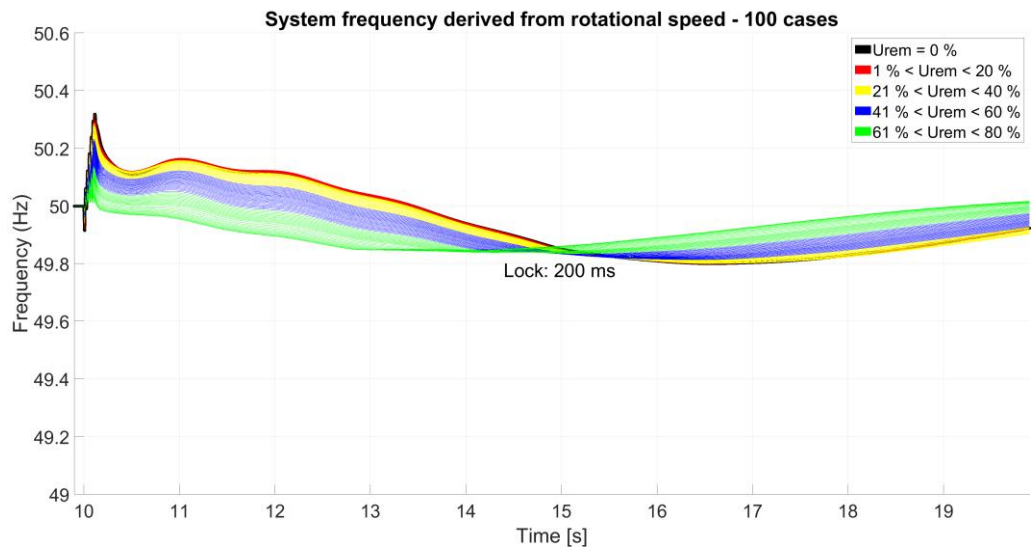


Figure 67. System frequency derived directly from the rotational speed of the biggest generator.



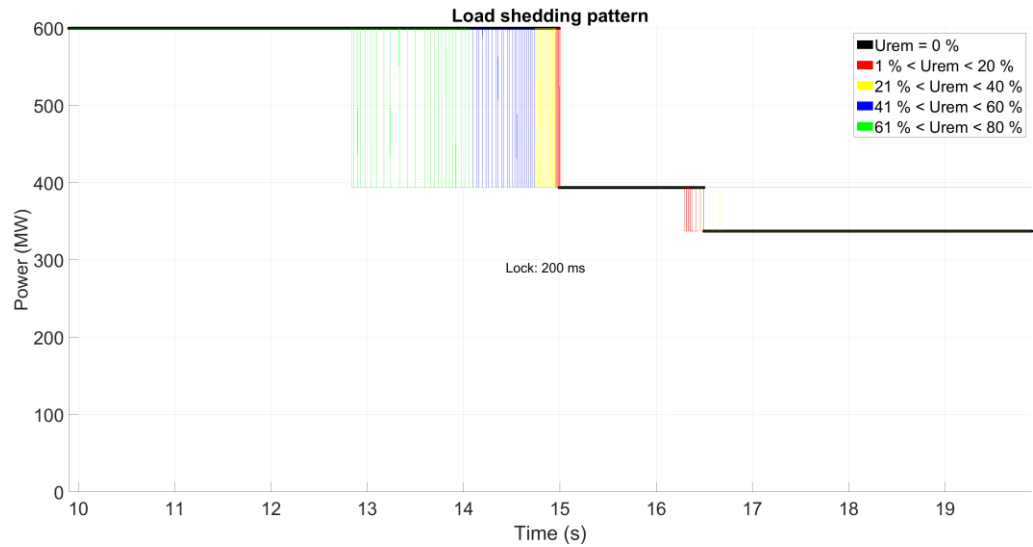


Figure 68. Load disconnection pattern of distributed fast reserves.

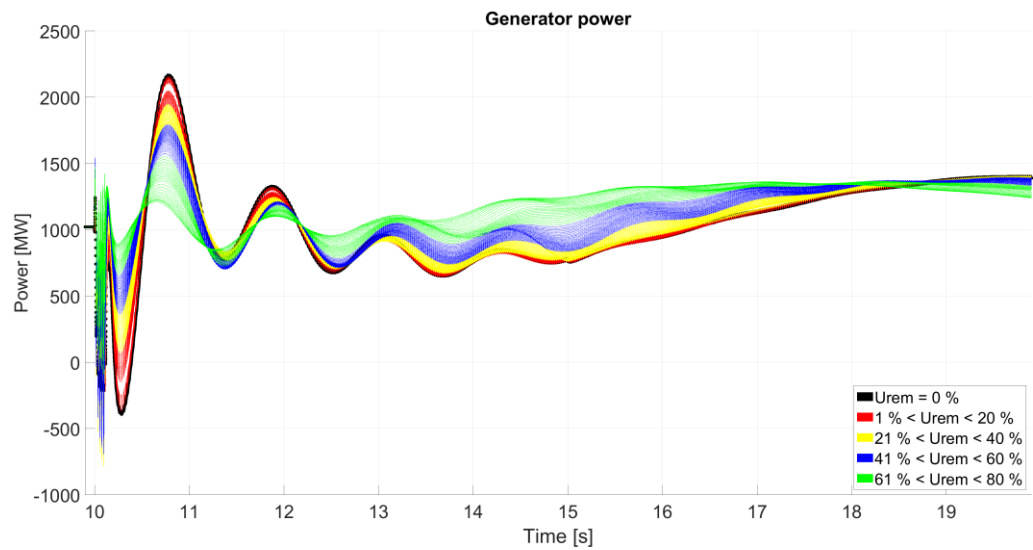


Figure 69. Output power of the generator equipped with turbine speed control.

5.9.11 110 GWs, 300 MW, 750 MW / 250 MW

Figure 70, Figure 71, Figure 72 and Figure 73 show frequency minimum measured by PLL srf, load disconnection pattern of the distributed fast reserves, system frequency derived directly from the rotational speed of the biggest generator and output power of the generator equipped with turbine speed control respectively.



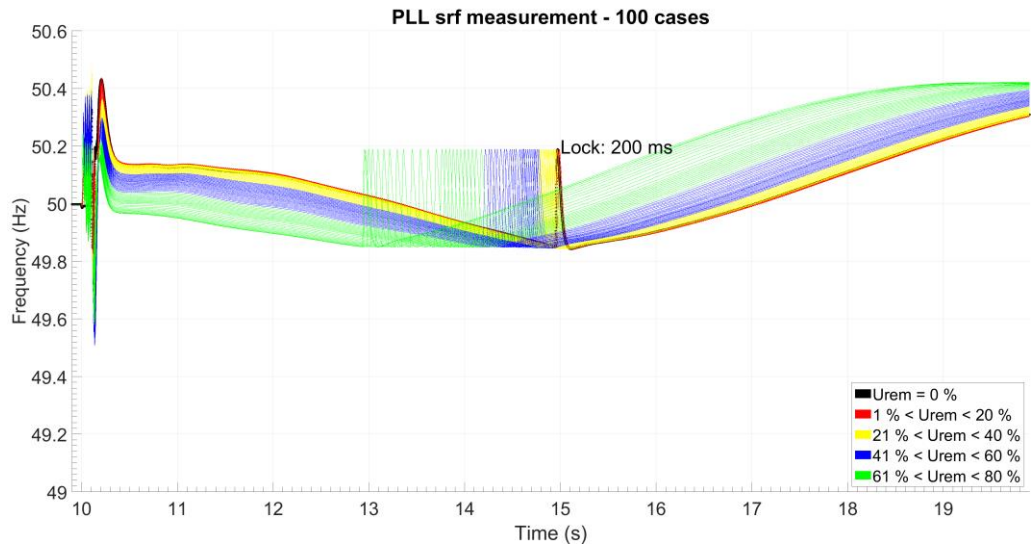


Figure 70. Frequency minimum measured by PLL srf with 750 MW / 250 MW distributed fast reserves and 300 MW rotational reserves

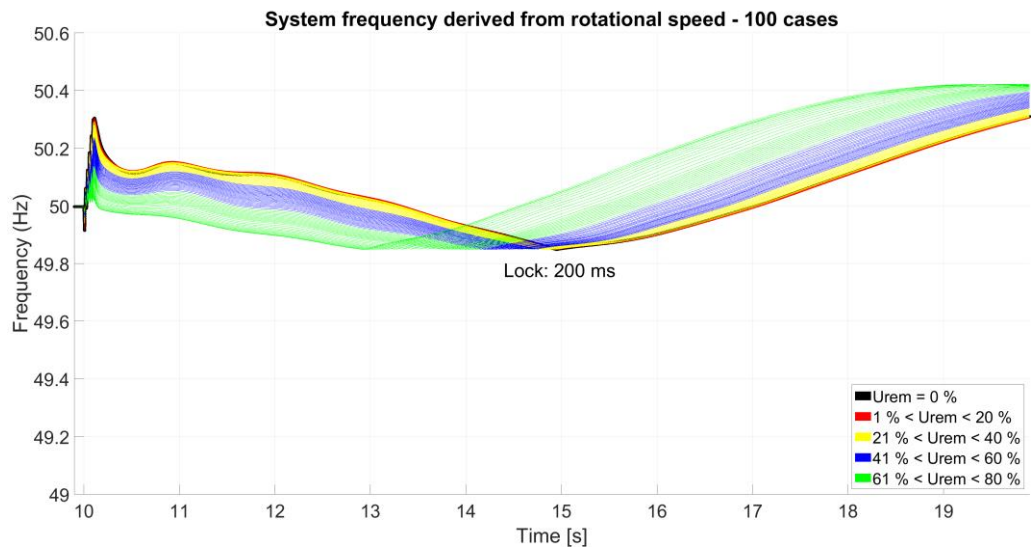


Figure 71. System frequency derived directly from the rotational speed of the biggest generator.



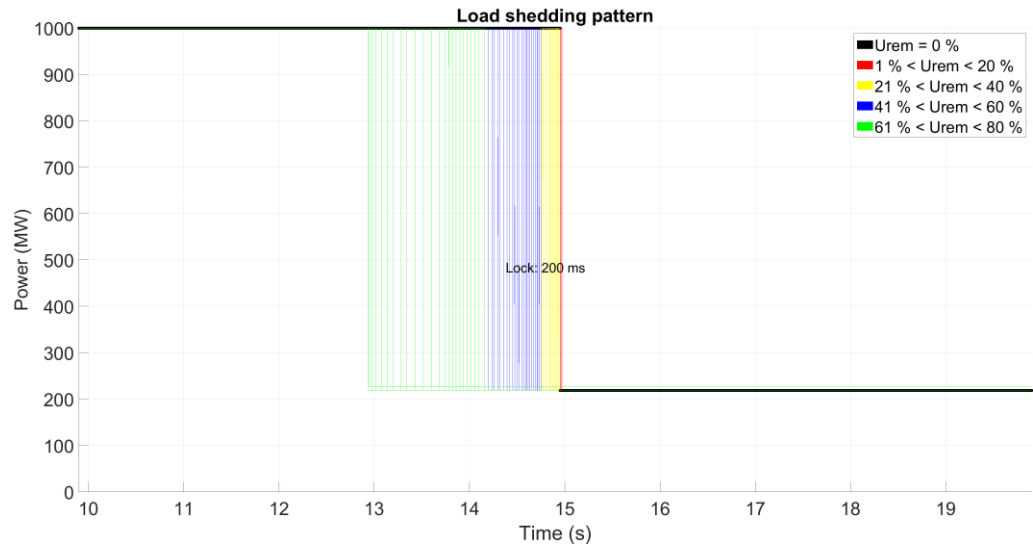


Figure 72. Load disconnection pattern of distributed fast reserves.

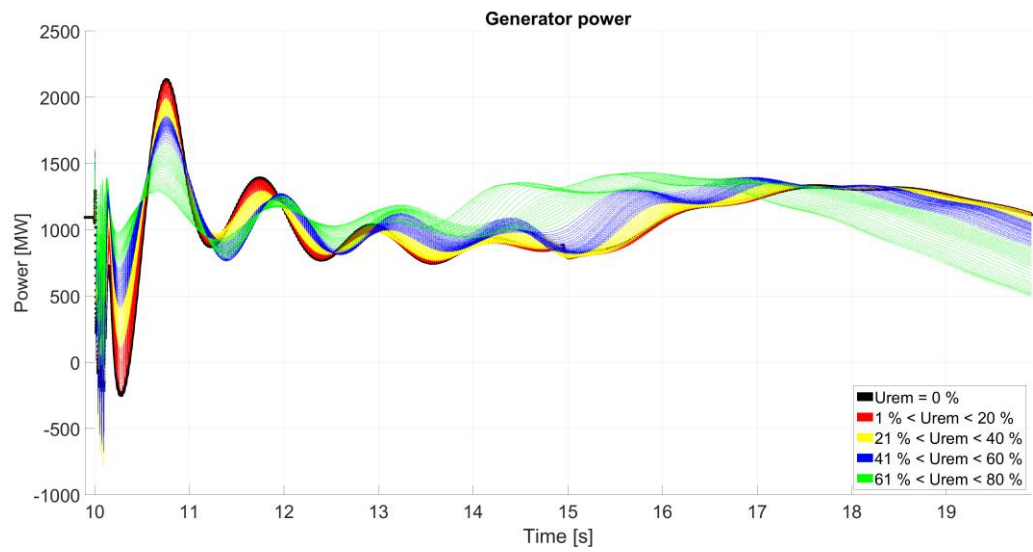


Figure 73. Output power of the generator equipped with turbine speed control.





5.9.12 110 GWs, 300 MW, 250 MW / 750 MW

Figure 74, Figure 75, Figure 76 and Figure 77 show frequency minimum measured by PLL srf, load disconnection pattern of the distributed fast reserves, system frequency derived directly from the rotational speed of the biggest generator and output power of the generator equipped with turbine speed control respectively.

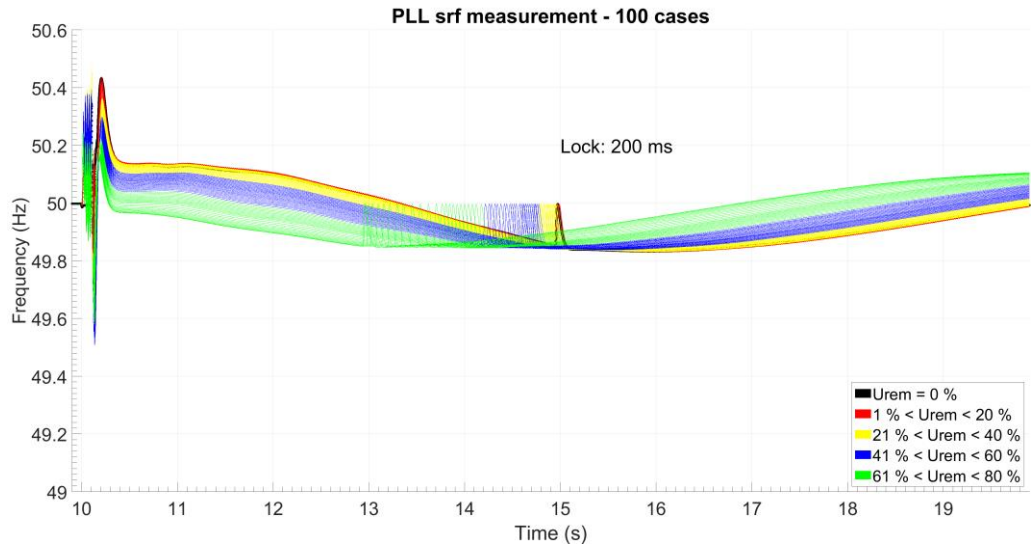


Figure 74. Frequency minimum measured by PLL srf with 250 MW / 750 MW distributed fast reserves and 300 MW rotational reserves

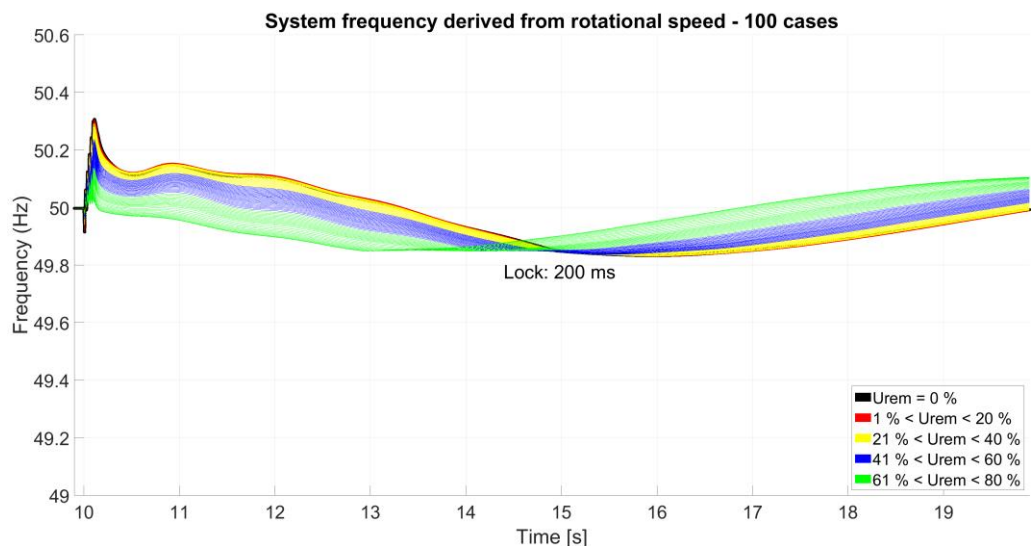


Figure 75. System frequency derived directly from the rotational speed of the biggest generator.



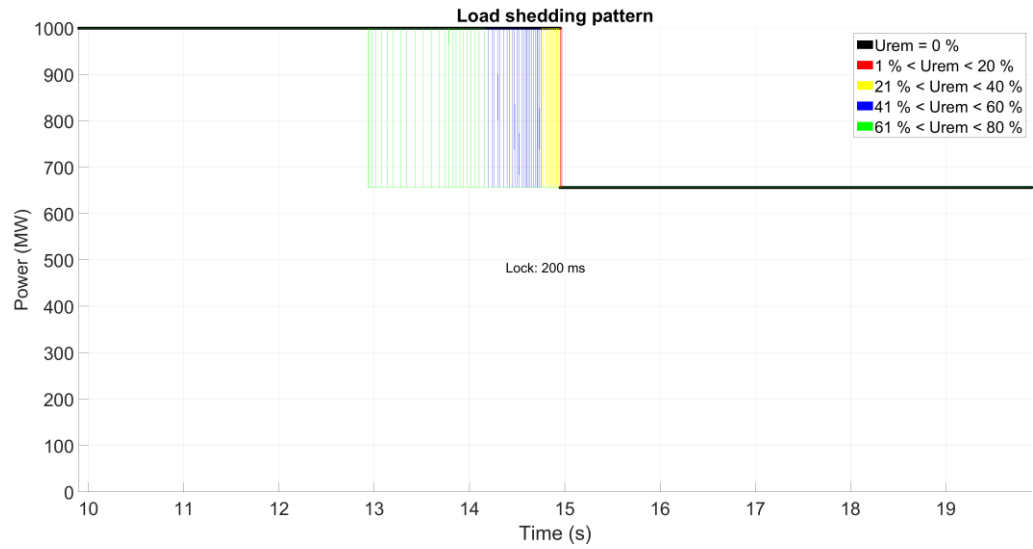


Figure 76. Load disconnection pattern of distributed fast reserves.

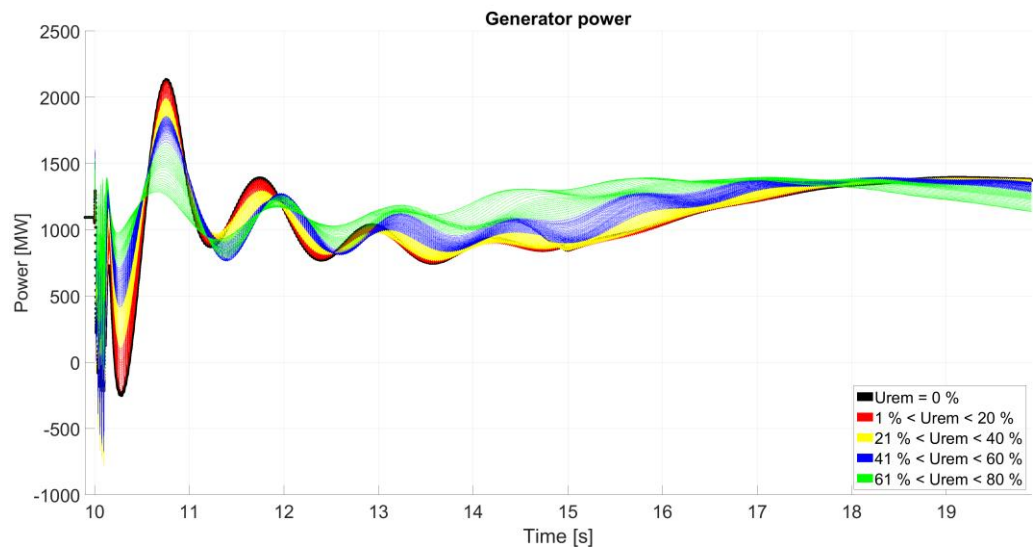


Figure 77. Output power of the generator equipped with turbine speed control.





5.9.13 Summarizing graphs of 300 MW production loss

In Figure 78 and Figure 79 the frequency minimum and the time when frequency minimum is reached, are summarized.

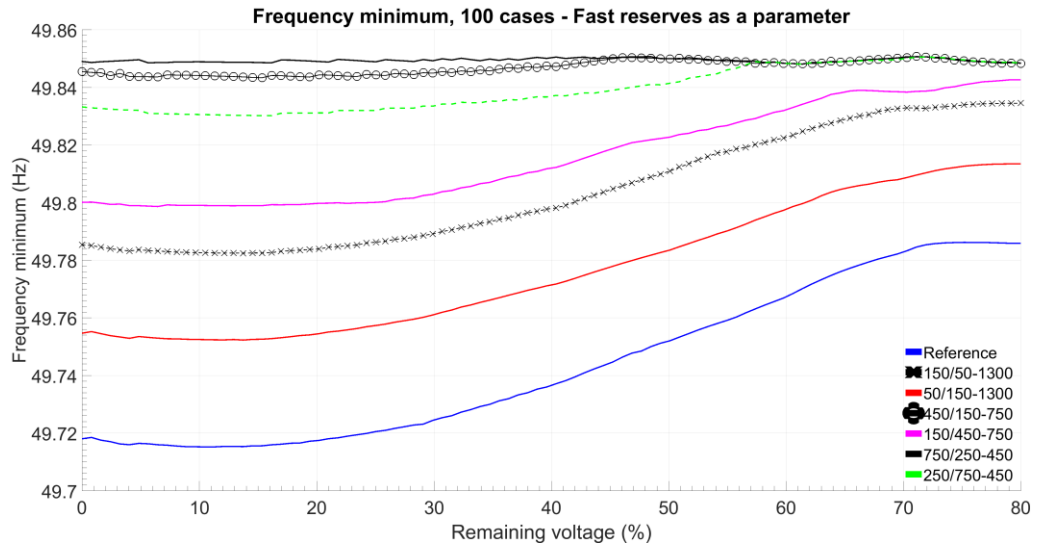


Figure 78. Frequency minimum of different amount of distributed fast reserves with a production loss of 300 MW.

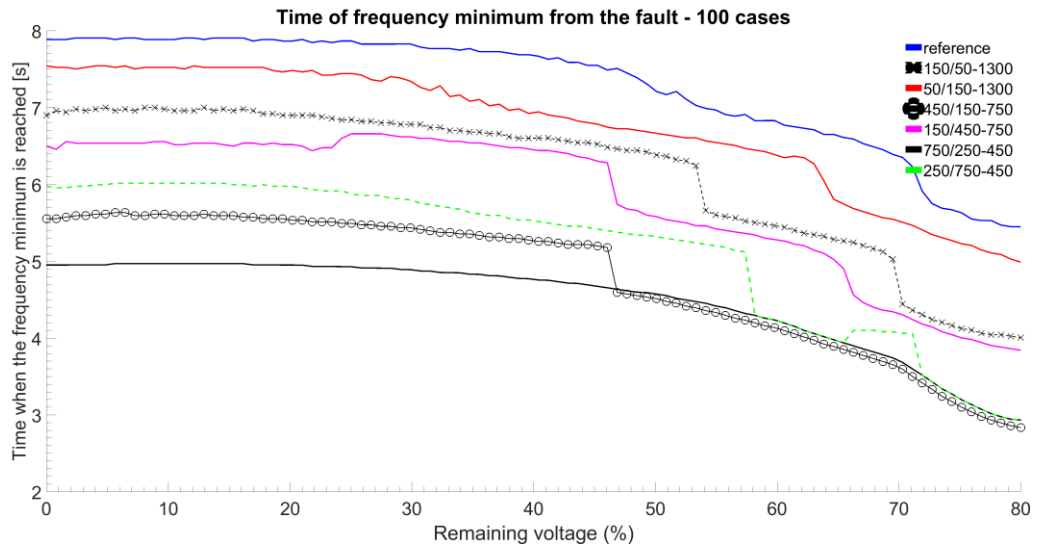


Figure 79. Time of frequency minimum of different amount of distributed fast reserves with a production loss of 300 MW.





5.10 Results of analysis of impact on technical performance of transmission network)

Simulations with different load shedding schemes showed that there exists only minor differences between the schemes. Based on this results only the fastest shedding combination logic was used in the system simulations.

It was noted that with the used frequency measurement method, the PLL srf gave the most accurate results in three phase short circuits and because of that, this method was used in system simulation studies.

In the cases with 1300 MW production loss, the frequency minimum of the reference case was ~49,1 Hz. With the fast reserves combination of 750 MW and 250 MW, the frequency minimum could be raised circa 0,5 Hz so that the new frequency minimum was 49,6 Hz.

In the cases with 300 MW production loss, the frequency minimum of the reference case was ~49,72 Hz. The worst overfrequencies commenced in the case in which fast reserves were 750 MW and 250 MW. In these cases the maximum frequency was order of 50,4 Hz.





6 Conclusions and contributions

Feasibility of small distributed demand response resources as fast frequency reserves was assessed in general. The research focused especially on smart meter based implementation issues.

A compact power system simulation model based on the structure and data provided by Fingrid Oyj was developed in the project for PSCAD and RTDS (real time digital simulator) transient simulation softwares, and was applied to analysis of frequency measurement techniques and effect of switching patterns of distributed fast reserves on power system performance.

Various frequency measurement techniques presented in literature were studied and compared by simulations and with real measurement devices in real time digital simulator (RTDS) laboratory environment. Robust frequency measurement method was developed in the project and implemented in a prototype smart meter by MX Electrix Oy. The measurement performance of the smart meter was verified in the RTDS environment and compared with PMU and the simulated measurement techniques. The impact of different fault types and locations in the power system were varied (e.g. remaining voltage, fault inception angle) on frequency measurement located at the customer connection point in the distribution network was studied in the above comparison of frequency measurement techniques.

Large scale use of small distributed resources as fast frequency reserves was assessed in system performance studies by varying amount of reserve loads and their response time (i.e. fast and very fast) with different rotational kinetic reserves of power generation participating in frequency control.





7 References

[Beil 2016] I. Beil, I. Hiskens, S. Backhaus, Frequency Regulation From Commercial Building HVAC Demand Response, Proceedings of the IEEE, Vol. 104, No. 4, April 2016, pp. 745-757.
<http://web.eecs.umich.edu/~hiskens/publications/07407597.pdf>

[Donnelly 2012] M. Donnelly, S. Mattix, D. Trudnowski, J.E. Dagle, Autonomous Demand Response for Primary Frequency Regulation. Prepared for the U.S. Department of Energy under Contract DE-AC05-76RL01830. Pacific Northwest National Laboratory, PNNL-21152, January 2012, 69 p.
http://www.pnnl.gov/main/publications/external/technical_reports/PNNL-21152.pdf

[ENTSO-E 2013] Network Code on Load-Frequency Control and Reserves, ENTSO-E, 28 June 2013. 68 p.

[Fingrid 2016] Frequency containment reserves, Available:
<http://www.fingrid.fi/en/electricity-market/reserves/reservetypes/containment/Pages/default.aspx>.

[Järventausta 2015] Järventausta, P., Repo, S., Trygg, P., Rautiainen, A., Mutanen, A., Lummi, K., ... Belonogova, N. (2015). Kysynnän jousto - Suomeen soveltuvat käytännön ratkaisut ja vaikutukset verkkoyhtiöille (DR pooli): Loppuraportti. Tampere: Tampereen teknillinen yliopisto.

[Ma 2013] O. Ma, N. Alkadi, P. Cappers, P. Denholm, J. Dudley, S. Goli, M. Hummon, S. Kiliccote, J. MacDonald, N. Matson, D. Olsen, C. Rose, M. Sohn, M. Starke, B. Kirby, and M. O'Malley, Demand Response for Ancillary Services, IEEE Transactions on Smart Grid, 2013.

[Karimi-Ghartemani 2004] M. Karimi-Ghartemani and M.R. Iravani, "Estimation of Frequency and its Rate of Change for Applications in Power Systems", IEEE TRANSACTIONS ON POWER DELIVERY, VOL. 19, NO. 2, APRIL 2004.

[Koponen 1994] Pekka Koponen, Seppo Vehviläinen, Juha Rantanen; Additional functions of remote read kWh-meters. Proceedings of DA/DSM'94 Europe Conference, September 27-29, 1994, Paris, France, vol I, pp. 267 – 277.

[Koponen 1996] Pekka Koponen, Reino Seesvuori, Ralf Böstman; Adding power quality monitoring to a smart kWh meter. Power Engineering Journal (IEE), August 1996, 10, (4), pp. 159-163.

[Koponen 2001] Pekka Koponen, Seppo Vehviläinen; Improved power quality monitoring kWh-meter, proceedings of the 6th International Conference on Power Quality and Utilisation, EPQU'01, September 19-21, 2001, Cracow, Poland, pp. 217-224.





[Koponen 2002] Pekka Koponen; Sparse Sampling Methods for Power Quality Monitoring. Thesis for the degree of Doctor of Technology. Tampere University of Technology, Publications 379, Tampere 2002.

[Kuisti 2015] H. Kuisti, M. Lahtinen, M. Nilsson, K. Eketorp, E. Örum, D. Whitney, A. Slotsvik and A. Jansson, NAG Frequency quality report, version 3.0. ENTSO-E, 12 June 2015, 84 p.

[Landau 1979] Y. Landau, Adaptive control, the model reference approach, Marcel Decker, 1979, pp. 97-198 and 325-331.

[Liao 2011] Yizheng Liao, Phase and Frequency Estimation: High-Accuracy and Low-Complexity Techniques. A Master of Science Thesis, Worcester Polytechnic Institute, May 2011, 118 p.

[NAG 2015] NAG Frequency Quality Report v.3.0, 12 June 2015)

[Ni 2011] Min Ni, An Optimized Software-Defined-Radio Implementation of Time-Slotted Carrier Synchronization for Distributed Beamforming. A Master of Science Thesis, Worcester Polytechnic Institute, Feb. 2011, 133 p.

[Reza 2012] Md. S. Reza, M. Ciobotary, V. G. Agelidis; Frequency Adaptive Instantaneous Power Quality Analysis Using Frequency Locked Loop Based Kalman Filter Technique. 3rd IEEE International Symposium on Power Electronics and Distributed Generation Systems (PEDG) 2012, pp. 767-774.

[Reza 2015] Md. S. Reza, M. Ciobotary, V. G. Agelidis; Power System Frequency Estimation by Using a Newton-Type Technique for Smart Meters, IEEE Transactions on Instrumentation and Measurement, Vol 64, No 3. March 2015, pp. 615-624.

[SmartNet 2016] www.SmartNet-Project.eu.

[Terzija 1994] V. Terzija, M. Duric, Adaptive Algorithm for Estimation of Voltage Phasor, Frequency and Rate of Change of Frequency. ETEP Vol,4 No.3, May/June 1994, ss. 243 – 249.

[Zhou 2011] L. Zhou and J. Höglund, New Indices for Frequency Quality, STRI Report R11-799, STRI Ludvika Sweden 19 Dec. 2011, 55 p (The report is owned by Svenska Kraftnät and to my knowledge it is not publicly published.)

[Anderson 1986] Anderson, P. Fouad, A. (1986). Power System Control And Stability. Fourth edition. Ephrata. p. 438.

[Chiang 2007] Y. Li, H. d. Chiang, B. k. Choi, Y. t. Chen, D. h. Huang and M. G. Lauby. (2007, May). "Representative static load models for transient stability analysis: development and examination," in *IET Generation, Transmission & Distribution*, vol. 1, no. 3, pp. 422-431.





[Radhakrishna 2001] C. Radhakrishna, M. Eshwardas and G. Chebiyam. (2001). "Impact of voltage sags in practical power system networks," *Transmission and Distribution Conference and Exposition, 2001 IEEE/PES*, Atlanta, GA, pp. 567-572 vol.1.

[Koponen 1996] P. Koponen, R. Seesvuori and R. Bostman. (1996 Aug.). Adding power quality monitoring to a smart kWh meter. *Power Engineering Journal*, vol. 10, no. 4, pp. 159-163.

[ENTSOE 2012] https://www.entsoe.eu/publications/system-operations-reports/Documents/120530_Assessment_of_the_System_security_with_respect_to_disconnection_rules_of_PV_Panels.pdf



